# Hyperosmotic Stress and the Impact on Metabolite Formation and Redox Balance in *Saccharomyces cerevisiae* and *Saccharomyces bayanus* strains

Caitlin Heit, B.Sc. Hon.

Biotechnology

Submitted to the Centre for Biotechnology in partial fulfillment
of the requirements for the degree of Master of Science

Faculty of Mathematics and Science, Brock University
St. Catharines, Ontario
December 2013

**Abstract**

Wine produced using an appassimento-type process represents a new and exciting innovation for the Ontario wine industry. This process involves drying grapes that have already been picked from the vine, which increases the sugar content due to dehydration and induces a variety of changes both within and on the surface of the grapes. Increasing sugar contents in musts subject wine yeast to conditions of high osmolarity during alcoholic fermentations. Under these conditions, yeast growth can be inhibited, target alcohol levels may not be attained and metabolic by-products of the hyperosmotic stress response, including glycerol and acetic acid, may impact wine composition. The further metabolism of acetic acid to acetylCoA by yeast facilitates the synthesis of ethyl acetate, a volatile compound that can also impact wine quality if present in sufficiently high concentrations.

The first objective of this project was to understand the effect of yeast strain and sugar concentration on fermentation kinetics and metabolite formation, notably acetic acid and ethyl acetate, during fermentation in appassimento-type must. Our working hypotheses were that (1) the natural isolate *Saccharomyces bayanus* would produce less acetic acid and ethyl acetate compared to *Saccharomyces cerevisiae* strain EC-1118 fermenting the high and low sugar juices; (2) the wine produced using the appassimento process would contain higher levels of acetic acid and lower levels of ethyl acetate compared to table wine; (3) and the strains would be similar in the kinetic behavior of their fermentation performances in the high sugar must.

This study determined that the *S. bayanus* strain produced significantly less acetic acid and ethyl acetate in the appassimento wine and table wine fermentations. Differences in acetic acid and ethyl acetate production were also observed within strains fermenting the two sugar conditions. Acetic acid production was higher in table wine fermented by *S.*

*bayanus* as no acetic acid was produced in appassimento-style wine, and 1.4-times higher in appassimento wine fermented by EC-1118 over that found in table wine. Ethyl acetate production was 27.6-times higher in table wine fermented by *S. bayanus*, and 5.2-times higher by EC-1118, compared to that in appassimento wine. Sugar utilization and ethanol production were comparable between strains as no significant differences were determined.

The second objective of this project was to bring a method in-house for measuring the concentration of pyridine nucleotides, $NAD^+$, $NADP^+$, NADH and NADPH, in yeast cytosolic extract. Development of this method is of applicative interest for our lab group as it will enable the redox balance of the $NAD^+$/ NADH and $NADP^+$/ NADPH systems to be assessed during high sugar fermentations to determine their respective roles as metabolic triggers for acetic acid production. Two methods were evaluated in this study including a UV-endpoint method using a set of enzymatic assay protocols outlined in Bergmeyer (1974) and a colorimetric enzyme cycling method developed by Sigma-Aldrich® using commercial kits. The former was determined to be limited by its low sensitivity following application to yeast extract and subsequent coenzyme analyses, while the latter was shown to exhibit greater sensitivity. The results obtained from the kits indicated high linearity, accuracy and precision of the analytical method for measuring NADH and NADPH, and that it was sensitive enough to measure the low coenzyme concentrations present in yeast extract samples. $NAD_{total}$ and $NADP_{total}$ concentrations were determined to be above the lower limit of quantification and within the range of the respective calibration curves, making this method suitable for our research purposes.

**Acknowledgments**

I would like to express my appreciation to my supervisor, Dr. Inglis, for giving me the opportunity to pursue my thesis project under her advisement. Throughout my research, you provided good teaching, sound advice and support, all of which I am incredibly grateful for. Your guidance and encouragement allowed me to develop my laboratory, problem-solving and communication skills, and perhaps more importantly, have confidence in my own research abilities. Special thanks to Dr. Atkinson, Dr. van der Merwe and Dr. Liang for your time, participation and guidance. It was all very much appreciated.

To everyone in the IH210 lab group (Candace, Fei, Ian, Lisa, Cristina, Matilda, Tony and Jen) and Mary, you are a wonderful collection of bright minds and souls, all of whom are exceptionally kind, funny, warm-hearted, understanding and best of all, supportive. It was a pleasure to work with each and every one of you. I am especially indebted to Fei and Candace for their constant support and encouragement during my time in the lab. To both of you, your assistance was truly invaluable and your friendship even more so. I would also like to extend my gratitude to Ian for his unconditional support over these two years. Your wit, intellect and kindness are truly astounding, and it has been a privilege to know you. Special thanks to Linda Tremblay, Lynda van Zuiden and Fred Di Profio for your assistance. I was lucky to have help from people like you.

Lastly, I would like to thank my family. My mom, dad and sisters always made sure I felt their encouragement and love a distance away, and I am forever grateful for their support. And a loving thanks to you, Kristy for being a wonderful friend. Knowing you has been an absolute pleasure. Accordingly, I dedicate this thesis to all of you.

## Table of Contents

# List of Tables

## List of Illustrations

### Chapter 1



### Chapter 2



### Chapter 3

**Chapter 4**

## List of Abbreviations

ACH: acetylCoA hydrolase

ACS: acetylCoA synthetase

ADH: alcohol dehydrogenase

ALD: aldehyde dehydrogenase

ANOVA: analysis of variance

ATF: alcohol acetyltransferase

ATP: adenine triphosphate

AWRI: Australian Wine Research Institute

BSA: bovine serum albumin

CCOVI: Cool Climate Oenology and Viticulture Institute

CDC: cell division cycle

CFU: colony forming unit

CoA: coenzyme A

CV: coefficient of variation

C6: carbon-six

DAP: diammonium phosphate

DHAP: dihydroxyacetone phosphate

DNA: deoxyribonucleic acid

DTT: dithiolthreitol

EDTA: ethylendiaminetetraacetic acid

EGTA: ethyleneglycoltetraacetic acid

FID: flame ionization detector

GC: gas chromatography

GDP: glycerol-3-phosphate dehydrogenase

GlDH: glutamate dehydrogenase

GPDH: glucose-6-phosphate dehydrogenase

GPP: glycerol-3-phosphatase

GTP: guanosine-5'-triphosphate

Gly-3-P: glycerol-3-phosphate

Glyceraldehyde-3-P: glyceraldehyde-3-phosphate

G6P-DH: glucose-6-phosphate dehydrogenase

HCl: hydrochloric acid

HEPES: 4-(2-hydroxyethyl)-1-piperazineethanesulfonic acid

HOG: high osmolarity glycerol

KCl: potassium chloride

KOH: potassium hydroxide

LiCl: lithium chloride

LLOQ: lower limit of quantification

Lg: lager-type genome

LSD: least significant difference

MAPK: mitogen activated protein kinase

MAPKK: mitogen activated protein kinase kinase

MAPKK: mitogen activated protein kinase kinase kinase

MWCO: molecular weight cut-off

$NAD^+$: nicotinamide adenine dinucleotide

NADH: nicotinamide adenine dinucleotide, reduced

$NADP^+$: nicotinamide adenine dinucleotide phosphate

NADPH: nicotinamide adenine dinucleotide phosphate, reduced

NaCl: sodium chloride

NaOH: sodium hydroxide

N: nitrogen

PAN: primary amino nitrogen

PBS: polymyxin B resistance

PDC: pyruvate decarboxylase

PDH: pyruvate dehydrogenase

PMSF: phenylmethylsulfonylfluoride

PPP: pentose phosphate pathway

OD: optical density

RH: relative humidity

RNA: ribonucleic acid

SD: standard deviation

SLN: snythetic lethal of N-end rule

STE: sterile (α motif)

SSK: suppressor of sensor kinase

TA: titratable acidity

Tris: tris(hydroxymethyl)aminomethane

ULOQ: upper limit of quantification

UV: ultraviolet

VA: volatile acidity

Vis: visible

VQA: Vintners Quality Alliance

YANC: yeast assimilable nitrogen content

YPD: yeast peptone dextrose

YPD: tyrosine (y) phosphatase dependent

# 1. Introduction and Literature Review

## 1.1. Responding to Hyperosmotic Stress and Osmoadaptation in *S. cerevisiae*

### 1.1.1. Hyperosmotic stress: cellular effects, consequences and responses

Yeast live in a continually changing environment where the intracellular water activity can fluctuate considerably over the lifetime of the cell due to changes in the extracellular water activity. When yeast cells are exposed to conditions of high osmolarity, the immediate effect is the loss of cytosolic water by osmosis. This process is driven by the osmotic pressure difference across the cell membrane (Logothetis *et al*. 2007), and eventually leads to changes in cell volume and shape, loss of turgor pressure and cell polarity, compression of the cytoplasm and changes in metabolism (Blomberg and Adler 1992; Varela and Mager 1996; Billi and Potts 2002; Tamás and Hohmann 2003). For these reasons, maintaining a constant internal environment under high osmolarity growth conditions is important for cell function and survival.

Yeast have evolved specialized biochemical pathways to adapt to stressful, often changing environments. Within the cell, specialized sets of sensing and signalling proteins form modules that function to monitor the environmental conditions of the cell (Miermont *et al*. 2011), and to mediate appropriate stress responses including altered gene expression, metabolism, secretion, proliferation and apoptosis (Furukawa and Hohmann 2013). Osmoadaptation is a cellular survival mechanism used by yeast to adjust to changes in fluctuations in external osmotic pressure by re-establishing the osmotic gradient across the plasma membrane (Martin *et al*. 1999). This response is associated with the increased intracellular accumulation of compatible solutes to counteract dehydration caused by water efflux, thereby restoring cell shape and turgor pressure, and to ensure the proteins within

the cellular environment remain hydrated (Mollapour and Piper 2006). During this response, biomass production is also reduced to help cells in diverting the carbon flux away from growth and metabolism and towards combating the osmotic stress (Parmar *et al*. 2011).

In addition to the aforementioned physiological effects, exposure to sudden changes in environmental tonicity alters the internal concentrations of compounds, possibly shifting the equilibrium of ongoing biochemical reactions occurring within the cell (Petelenz-Kuedziel *et al*. 2011). This consequence can be detrimental for overall cellular function, making it essential that yeast possess an active defense mechanism to mitigate the negative effects of water loss. Glycerol plays an essential role in osmo-adaptation and osmoregulation (reviewed in Nevoigt and Stahl 1997), and is the main osmolyte produced by *S. cerevisiae* under hyperosmotic stress.

Adaptation to increased osmolarity is an active process dependent on sensing osmotic changes and activating appropriate cellular responses to protect cells against physiological stress (reviewed in Hohmann 2002). The principal cellular response in yeast is the activation of the high osmolarity glycerol (HOG) pathway (Brewster *et al*. 1993). The HOG pathway is a mitogen-activated protein kinase (MAPK) cascade that, when stimulated, results in both transcriptional and non-transcriptional responses to allow cells to cope with changes in the extracellular environment (Hohmann 2002). In addition to the HOG response, yeast also possess a general stress response which has an important role in stress adaptation and survival, allowing cells to cope with stresses under a range of conditions including exposure to hyperosmolarity.

### 1.1.2. Overview of the HOG response: signalling

Adaptation to high osmotic stress in *S. cerevisiae* is controlled, in part, by an osmosensing and signalling network called the HOG (High Osmolarity Glycerol) MAPK pathway. MAPK pathways are well conserved among eukaryotes and are involved in many cellular processes such as stress response, the regulation of differentiation and proliferation (Miermont *et al*. 2011). In addition to the HOG pathway, the genome of *S. cerevisiae* encodes four other distinct MAPK signal transduction pathways, each of which is catalyzed by a specific MAP kinase possessing distinguishing features of this enzyme class (Chen and Thorner 2007). These include: (i) the mating pheromone response pathway (MAP kinase Fus2p); (ii) the pseudohyphal development pathway (Kss1p); (iii) the protein kinase C or cell wall integrity pathway (Slt2/ Mpk1p); (iv) and the spore wall assembly pathway (Smk1p) (Hohmann 2002).

The core of the HOG pathway is the Hog1 cascade. This cascade contains a three-component signal relay based on the successive phosphorylation of the enzymes MAP kinase kinase kinase (MAPKKK), MAP kinase kinase (MAPKK), and MAP kinase (MAPK). To initiate MAPK cascades, the MAPKKK must first be activated in response to a stimulus, typically by interactions with a small GTPase or other activator proteins and/ or phosphorylation by protein kinases downstream from cell surface receptors, depending on the pathway (Cuevas *et al*. 2007). Upon stimulation, the MAPKKK activates the MAPKK, a dual-specific protein kinase, by directly phosphorylating the two serine and threonine residues residing in the activation loop of the MAPKK catalytic domain. The activated MAPKK in turn phosphorylates a threonine or serine residue and a tyrosine residue located within the activation segment of its target MAPK. Dual phosphorylation of

the tripeptide motif is required for MAP kinase activation, where it is subsequently translocated from the cytosol into the nucleus to mount a response to the stimulus. In the case of the HOG pathway and hyperosmotic environments, this response includes the induction or repression of the expression of various genes, regulation of protein translation and glycerol synthesis (reviewed in Hohmann 2002; Saito and Tatebayashi 2004). Once osmotic balance is restored, either through intracellular changes due to osmolyte accumulation or from alternations in the external environment, cascade activity terminates, and Hog1p nuclear enrichment is reduced (Mettetal *et al*. 2008).

### 1.1.3. Overview of the HOG response: sensing osmotic stress

Within the HOG MAPK pathway of *S. cerevisiae*, the MAP kinases appear to be activated via two distinct transmembrane proteins, Sln1p (Ostrander and Gorman 1999) and Sho1p (Reiser *et al*. 2000), both initiating two independently operating branches which provide two signals as inputs to the pathway (Thorne *et al*. 2011). These proteins, or osmosensors, have been implicated in detecting osmotic stress and in regulating the activity of the Hog1 MAPK (Hohmann 2009). Mutations in the genes encoding for Sln1p (Maeda *et al*. 1994) and Sho1p (Posas and Saito 1997) were determined to affect the activity of the HOG pathway as both proteins are localized in the plasma membrane, thereby placing the sensors upstream of all the other pathway components. Although the molecular details of the mechanism for activating Sln1p and Sho1p are not fully understood, the sensors appear to be stimulated by osmotic shock, specifically in response to turgor-induced stress of the cell membrane resulting from high extracellular osmolarity (reviewed in Hohmann 2002; Tamas *et al*. 2000).

However, both branches of the HOG pathway were reported to be differently activated in response to varying degrees of osmotic stress, specifically when induced by salt (KCl). Using transcriptional profiling, O'Rourke and Herskowitz (2004) showed no redundancy in the Sln1 and Sho1 branches for regulating gene induction at lower osmolarity to exist as the transcription of genes associated with only the S1n1-branch were induced in yeast exposed to solute concentrations <0.125 M KCl. In contrast, redundancy between the Sln1 and Sho1 branches exposed to moderately high osmolarity (>0.5 M KCl) was determined as genes associated with both pathways were induced under higher solute conditions. At higher osmolarities, both branches of the HOG pathway as well as the general stress response were involved in the response to osmotic stress. However, blocking either branch of the pathway still permits phosphorylation and activation of Hog1p upon exposure to high osmolarity (Maeda *et al*. 1995).

In general, the Sln1p and Sho1p branches function in regulating the HOG pathway and activating the MAPK Hog1p, MAPKK Pbs2p, and MAPKKK Ssk2p (Fig. 1.1). Both the Sln1 and Sho1 branches are located upstream from Pbs2p and Hog1p, and link the HOG cascade through Pbs2p. Of the two branches, the first is initiated by the Sho1p adaptor protein, while the second is initiated by Sln1p, a histidine kinase receptor (Boisnard *et al*. 2008). Activation of the HOG pathway via the Sho1p branch commences with the formation of a transient multi-protein complex at the cell surface in response to osmotic shock, which ultimately interacts with a proline-rich region on Pbs2p (Cheetham *et al*. 2007). Under these conditions, signal transduction from the osmosensor to Pbs2p requires Cdc42p, Ste20p and Ste50p to activate Ste11p (Posas and Saito 1997; O'Rourke and Herskowitz 2004; Posas *et al*. 1998; Raitt *et al*. 2000; Reiser *et al*. 2000). Of these branch

components, Cdc42p is a GTPase that binds and activates Ste20p, a p21-activated protein kinase homologue, which, in turn, phosphorylates and activates the MAPKKK Ste11p (Reiser *et al*. 2000; reviewed in O'Rourke *et al*. 2002). Ste11p is putively associated with the SAM-domain containing protein Ste50p (Posas *et al*. 1998; Jansen *et al*. 2001), and once activated, it subsequently phosphorylates the MAPKK Pbs2p.

Differently from Sho1p, Sln1p relays a signal to Pbs2p via the proteins Ypd1p, Ssk1p and Ssk2p/ Ssk22p. While Sho1p positively regulates the HOG response, Sln1p, along with Ypd1p, negatively regulate this pathway. These differences have been discerned through deletion experiments of *SLN1*and *YPD1*, where disruption of the respective genes encoding for these proteins resulted in lethal phenotypes, notably in abnormal and deleterious osmoregulatory responses, due to the constitutive expression of the MAPK cascade (Maeda *et al*. 1994). Furthermore, Sln1p also functions differently under low and high osmolarity conditions. Under low osmotic stress, the histidine kinase domain of Sln1p is activated, allowing the protein to phosphorylate itself and subsequently phosphorylate Ypd1p and Ssk1p (reviewed in Posas *et al*. 1996). Phosphorylation of these proteins inactivates Ssk1p, causing the HOG pathway to cease as the protein is unable to bind and activate the final MAPKKKs in the cascade, Ssk2p and Ssk22p (Posas and Saito 1998).

However, when cells are osmotically stressed the histidine kinase domain of Sln1p is inactivated, which allows the Sln1p-Ypd1p-Ssk1p phosphorelay to continue as phosphotransfer of Ssk1p is diminished. As a consequence, unphosphorylated Ssk1p accumulates within the cell, where it is able to bind and activate Ssk2p/ Ssk22p. Activation of these MAPKKKs enables the pathway to be maintained as the subsequent phosphorylation of Pbs2p MAPKK leads to the nuclear translocation of Hog1p (Ferrigno

*et al*. 1998). Within the nucleus, dually phosphorylated Hog1p regulates the transcription of osmo-induced genes, including those which encode enzymes involved in glycerol production (Rep *et al*. 1999; 2000). The up-regulation of glycerol-3-phosphate dehydrogenase (*GDP1/2*) and glycerol-3-phosphatase (*GPP1/2*) alters the metabolic state of *S. cerevisiae*, allowing the osmotic stress to be counteracted through the synthesis and accumulation of glycerol as a compatible solute, and regulation of the internal osmotic pressure. Based on this coordinated response involving the activation of a signalling pathway, gene regulation, and alterations in cellular metabolism, yeast are able to survive upon increased osmolarity in the medium (Parmar *et al*. 2011). The overall osmo-adaptation process is illustrated schematically in Figure 1.1.

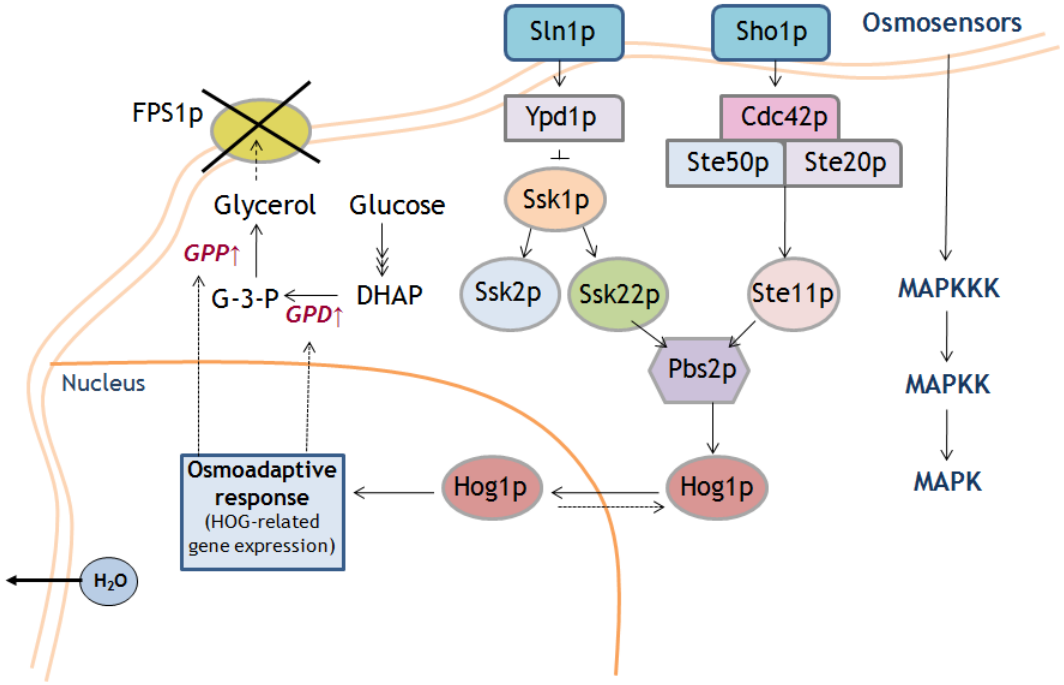


**Figure 1.1: Schematic diagram of the HOG pathway and its components in *S. cerevisiae*. Under conditions of high osmolarity, a series of phosphorylation events lead to the activation of Pbs2p (MAPKK). Once activated, Pbs2p activates the Hog1p MAPK, which induces glycerol synthesis and other osmoregulatory responses. Adapted from Nadal *et al*. (2002).**

### 1.1.4. Overview of the HOG response: glycerol production and redox implications

Intracellular accumulation of glycerol, the major compatible solute in yeast, is essential for cell survival when yeast are subjected to hyperosmotic stress under high osmolarity conditions (Blomberg and Alder 1989; Blomberg 2000). In *S. cerevisiae*, glycerol is synthesized from dihydroxyacetone phosphate (DHAP), a glycolytic intermediate, in two enzymatic reactions. The first reaction, and also the rate-limiting step in glycerol synthesis, requires the reduction of DHAP to glycerol-3-phosphate, along with the oxidation of NADH to $NAD^+$. This step is catalyzed by a $NAD^+$-dependent glycerol-3-phosphate dehydrogenase encoded by two isogenes, *GPD1* and *GPD2*. In the second and final reaction, glycerol-3-phosphate is dephosphorylated to glycerol via glycerol-3-phosphatases, encoded by *GPP1* and *GPP2* (Påhlman *et al.* 2001).

The genes encoding for the isoforms of glycerol-3-phosphate dehydrogenase and glycerol-3-phosphatase are differentially expressed under conditions of osmotic and anaerobic stress, allowing yeast cells to adapt to altered growth conditions (Påhlman *et al*. 2001). In response to hyperosmotic stress, increased glycerol production has been shown to be mainly due to enhanced *GPD1* and *GPP2* expression (Tamás and Hohmann 2003). Of the isogenes, *GPD1* has been demonstrated to be majorly responsible for glycerol formation under high osmolarity conditions as its expression was up-regulated in response to hyperosmotic stress (Larsson *et al*. 1993; Albertyn *et al*. 1994). In comparison, *GPD2* has been determined to have no role in the osmoregulatory response (Eriksson *et al*. 1995), as it is slightly repressed under hyperosmotic conditions, and to be up-regulated in the absence of oxygen (Ansell *et al*. 1997). Under anaerobic conditions, expression of *GPD2*

is to maintain intracellular redox balance between reducing equivalents, $NAD^+$ and NADH (Påhlman *et al*. 2001).

Under different conditions of sugar-induced osmotic stress, the expression of these genes has been measured. During fermentation in chaptalized Riesling grape juice (400 g $l^{-1}$ sugar), both *GPD1* and *GPP2* were shown to respond to sugar-induced osmotic stress, although strain differences in the expression of *GPD1* existed (Erasmus *et al*. 2003). During fermentation in Icewine juice (400 g $l^{-1}$ sugar), Pigeau and Inglis (2005) showed an increase in the expression of only *GPD1*, which corresponded to an increase in glycerol production by the wine yeast. Subsequent to this study, Pigeau and Inglis (2007) determined the expression of *GPD2* to be unaffected by changes in osmolarity as the gene was not differentially expressed in high and low sugar conditions. Thus, only *GPD1* was found to have a role in osmotically-induced glycerol biosynthesis during Icewine fermentation. In contrast to the *GPD* isoforms, both *GPP1* and *GPP2* are involved in the osmoregulatory glycerol response (Påhlman *et al*. 2001). Although these genes are up-regulated in response to osmotic shock, *GPP2* expression is more strongly induced than *GPP1* under conditions of high osmolarity (Hirayarna *et al*. 1995; Norbeck *et al*. 1996). However, when transferred to anaerobic conditions, *GPP1* expression is transiently up-regulated, while *GPP2* expression remains unaffected (Påhlman *et al*. 2001).

Glycolysis with subsequent alcoholic fermentation represents a redox-neutral metabolic sequence whereby the NADH generated during glycolysis is re-oxidized during alcoholic fermentation, thereby allowing glycolysis to continue (Kukec *et al*. 2003). (Fig. 1.2). Glycerol biosynthesis, however, is not a redox-neutral process, so a potential imbalance in the $NAD^+$/ NADH coenzyme system is established as osmotically-stressed

wine yeast ferment sugar into alcohol. For osmotic adjustment to occur within cells, glycerol production requires the oxidation of NADH to $NAD^+$, as DHAP is reduced to glycerol-3-phosphate, which results in the production of high $NAD^+$ levels as NADH consumption continues (van Dijken and Scheffers 1986).

Yeast cells lack the transhydrogenase activity to convert reducing equivalents between coenzyme systems (van Dijken and Scheffers 1986) and depend on metabolite formation to balance the $NAD^+$ formed in glycerol biosynthesis. Production of many yeast metabolites, including organic acids, esters, volatile fatty acids and higher alcohols, is thought to impact or be impacted by the ratio of $NAD^+$/ NADH, and therefore may contribute to maintaining intracellular redox balance (van Dijken and Scheffers1986; Schoondermark-Stolk *et al*. 2005; Jain *et al*. 2012). Of these metabolites, acetic acid biosynthesis has been suggested as a mechanism that yeast can use to balance excess $NAD^+$ produced in response to hyperosmotic stress and glycerol overproduction by regenerating NADH (Blomberg and Alder 1989). The NADH consumed during DHAP reduction could be provided by the $NAD^+$-dependent oxidation of acetaldehyde to acetic acid by an aldehyde dehydrogenase, which results in the concomitant reduction of $NAD^+$ to NADH (Pigeau and Inglis 2007). In addition to this redox sink, there is also a direct correlation between the sugar concentration in juice and the amount of glycerol and acetic acid produced by yeast (Erasmus *et al*. 2004; Pigeau *et al*. 2007).

### 1.1.5. Acetic acid formation and redox balance

Within the *S. cerevisiae* genome, there are five genes which encode aldehyde dehydrogenases that are capable of catalyzing this reaction: *ALD2*, *ALD3* and *ALD6* correspond to the cytoplasmic isoforms, and *ALD4* and *ALD5* correspond to the

mitochondrial isoforms (Navarro-Avino *et al.* 1999). Of the cytoplasmic isoforms, *ALD2* and *ALD3* encode $NAD^+$-dependent isoforms and *ALD6* encodes a $NADP^+$-dependent isoform, while the coenzyme requirements for the mitochondrial isoforms are $NAD^+$/ $NADP^+$ for *ALD4* and $NADP^+$ for *ALD5*. Based on the coenzyme dependency of each isoform, only *ALD2*, *ALD3* and *ALD4*, all of which are specific to $NAD^+$, may solve a redox imbalance issue resulting from glycerol production, although only *ALD2* and *ALD3* encode for enzymes localized in the cytosol, the site of glycerol biosynthesis.

Yeast cells respond to increases in extracellular osmolarity by activating the HOG pathway and increasing glycerol synthesis and $NAD^+$ formation (Posas *et al*. 1998). If it is correct that acetic acid is formed under conditions of osmotic stress as a mechanism to maintain intracellular redox potential balance within the $NAD^+$/NADH coenzyme system, then cytosolic Ald2p and/or Ald3p are assumed to be the main enzymes responsible for its biosynthesis as both are dependent on $NAD^+$ for catalysis (Pigeau and Inglis 2005; 2007). However, the $NADP^+$-dependent Ald6p was determined to be the main aldehyde dehydrogenase responsible for acetic acid production in laboratory *S. cerevisiae* strains fermenting glucose media (Remize *et al*. 1999; Eglinton *et al*. 2002), while Ald5p has also been found to contribute to acetate formation from acetaldehyde during glucose fermentation, as determined through single and double deletion mutant experiments using lab and wine yeast-derived strains of *S. cerevisiae* (Saint-Prix *et al.* 2004).

In this study, the deletion of *ALD5* decreased acetic acid formation in both strains examined, while the additional deletion of *ALD5* slightly reduced acetate formation in the *ald4*Δ mutant and delayed growth in the *ald6*Δ*ald4*Δ mutant. Of the two isoforms, only *ALD6* was up-regulated under salt stress, and its induction required activation of the HOG

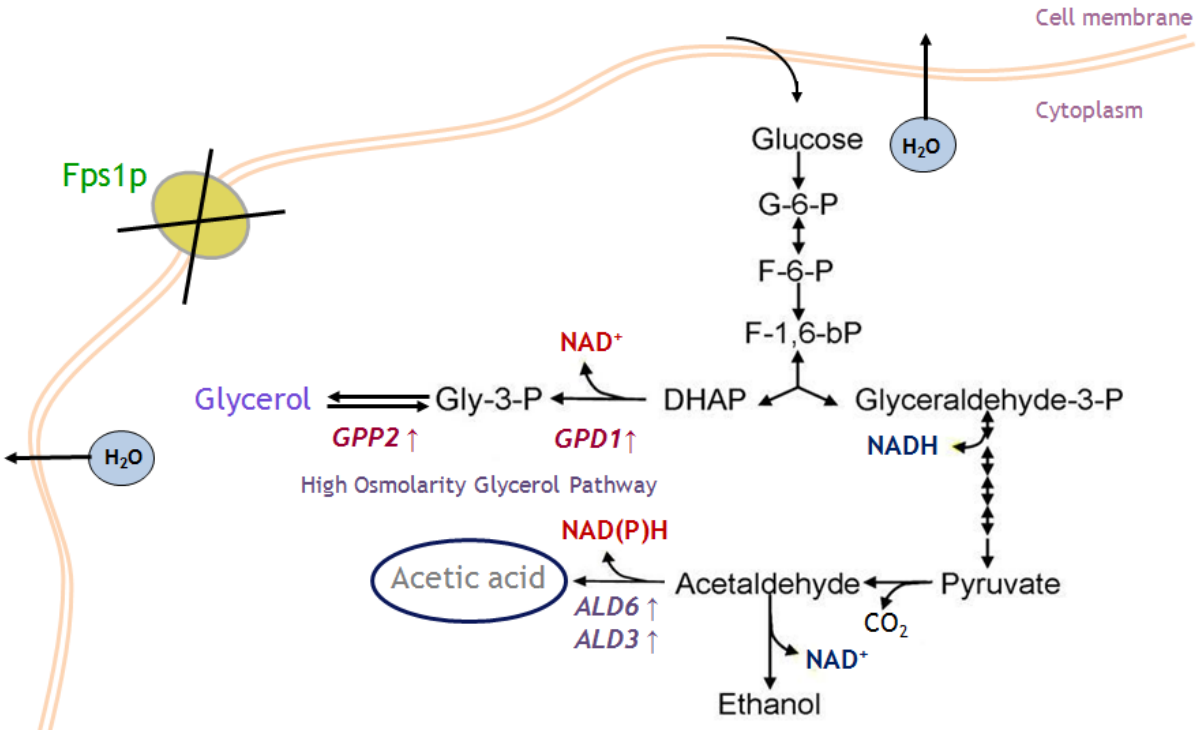


**Figure 1.2: Osmo-induced glycerol formation in *S. cerevisiae* during Icewine fermentation and its relationship to acetic acid production.**

MAPK pathway (Akhtar *et al*. 1997; Rep *et al*. 2000). Furthermore, deletion of *ALD6* in synthetic medium simulating a standard grape juice containing 20% glucose resulted in a decrease in acetic acid formation compared to the wild-type strain and a marked increase in glycerol concentration, along with compounds such as 2,3-butanediol and succinate. Although the major findings from these studies suggest a role for Ald6p in acetic acid biosynthesis during fermentation, its involvement in resolving cytosolic redox imbalance during osmo-induced glycerol biosynthesis remains unclear due to its $NADP^+$-specificity.

Furthermore, the precise roles for the homologous *ALD2* and *ALD3* are also unknown to date. Of the isoforms, *ALD3*, encoding a cytosolic $NAD^+$-dependent isoform, was found up-regulated under salt stress (Norbeck and Blomberg 2000). Within the strains examined, all exhibited induced expression of *ALD3*, and at the transcript level, during

growth under osmotic stress, while the *ALD2* transcript appeared to be unaffected by osmotic stress. Based on these results, *ALD3* was determined to be the osmoregulated form of the two isogenes. However, Navarro-Avino *et al*. (1999) determined the expression of both *ALD2* and *ALD3* to be induced by salt stress, and the regulation of these genes to be mediated by a Hog1-independent pathway. Under normal growth conditions, no expression of *ALD2* and *ALD3* was determined in wild-type and *ald2*Δ*ald3*Δ mutant cells, while Ald2p and Ald3p activity levels increased in wild-type cells exposed to salt-induced osmotic stress, but remained unchanged in the double null mutant.

To differentiate the specific roles of these isoforms in this study, *ALD2-lacZ* and *ALD3-lacZ* reporter fusions were used, and the expression of β-galactosidase driven by the *ALD2* and *ALD3* promoters was induced by osmotic stress through various solutes, including KCl, NaCl and sorbitol (Navarro-Avino *et al*. 1999). The basal and induced expression levels in each condition were measured and compared between isogenes. In all conditions, *ALD2* exhibited lower expression levels compared with *ALD3*, suggesting a potentially larger role for Ald3p in yeast adaptation to osmo-induced stress. In addition, more recent evidence suggests that Ald2p and Ald3p may play a role in beta-alanine synthesis and in the cellular biosynthesis of coenzyme A (White *et al*. 2003).

However, in conditions that stimulated glycerol and acetic acid production in *S. cerevisiae* though LiCl stress, *GPD1*, *ALD2* and *ALD3* were increased in expression at the mRNA and protein levels, whereas *ALD6* was down-regulated (Bro *et al*. 2003). During fermentation of sake, another high sugar matrix, *ALD2* and *ALD3* were the only *ALD* isogenes determined to be up-regulated in an *S. cerevisiae* sake yeast strain, correlating with an increase in acetate production (Akamatsu *et al*. 2000). Contrary to these findings,

*ALD2*, *ALD3*, *ALD4* and *ALD6* were all up-regulated in response to sugar-induced osmotic stress 2 hours following exposure to the high osmolarity conditions (Erasmus *et al*. 2003; Erasmus and van Vuuren 2009). The transcription of the *ALD* isogenes, along with 585 other genes in an industrial strain of *S. cerevisiae*, were affected more than two-fold in chaptalized Riesling grape juice containing 40% (w/ v) sugars, including glycolytic and pentose phosphate genes. However, only the initial response of yeast to the osmo-induced sugar stress was monitored and it is not known whether the initial expression was transient or sustained throughout the length of the fermentation, which typically lasts for an additional 400-500 hours (Kontkanen *et al*. 2004; Pigeau and Inglis 2005).

Furthermore, yeast grown in the 40% (w/ v) sugar conditions expectantly produced higher levels of acetic acid (4.5-fold increase) compared to yeast fermenting at the lower sugar concentration containing 22% (w/ v) sugar (Erasmus *et al*. 2004). Of the isogenes that were up-regulated, *ALD6* was expressed at the highest level in both strains examined, followed by *ALD4* (Erasmus *et al*. 2009), which is a result consistent with the findings of Remize *et al*. (2000). If transcript levels do correlate with enzyme activity levels, these results suggest Ald6p to have a major role in acetic acid production during high sugar ferments, although it uses $NADP^+$ and not $NAD^+$ as a coenzyme in acetic acid formation (Wang *et al*. 1998). As a concluding remark, Erasmus and van Vuuren (2009) linked the high levels of acetic acid generated under osmotic stress to NADPH production, possibly as a way to compensate for the down-regulation of NADPH generated through the pentose phosphate pathway (PPP) (Bro *et al*. 2003; Erasmus and van Vuuren 2009). Erasmus *et al*. (2003) showed the transcription of several genes encoding enzymes in the oxidative and non-oxidative parts of the PPP was affected when *S. cerevisiae* was hyperosmotically

stressed, which altered metabolic flux through the pathway. Under these conditions, a potential shortage in NADPH could result, establishing the need to regenerate it through acetic acid biosynthesis via an $NADP^+$-dependent Aldp isoform such as Ald6p (Erasmus and van Vuuren 2009).

In contrast to these results, *ALD3* was the only *ALD* isogene increased in expression during fermentation in Icewine juice over that found throughout table wine production, which corresponded to an increase in acetaldehyde and acetic acid production (Pigeau and Inglis 2005; 2007). The results indicated *ALD3* displayed a 6.2-fold up-regulation on day 4 of fermentation compared to the table wine juice, which could account for the elevated level of acetic acid found in Icewine. *ALD3* was also found to be the only *ALD* further up-regulated by acetaldehyde stress during fermentation (Pigeau *et al*. 2007), although the enzyme activity levels have not yet been measured.

The findings of Erasmus *et al*. (2003; 2004) and Erasmus and van Vuuren (2009), question the linkage of acetic acid production under hyperosmotic stress to glycerol production and NADH requirements. Thus, important answers concerning the involvement of each *ALD* isogene in acetic acid formation and cofactor balance remain unclear, and additional research needs to be conducted to determine the metabolic role of acetic acid in the yeast hyperosmotic stress response and to define the contribution of each Aldp isoform to elevated acetic acid and intracellular redox balance during high sugar fermentations. A fundamental topic that has not been addressed during high sugar fermentations pertains to understanding the altered redox state of the cells during fermentation and specifically questions the ratio of $NAD^+$/NADH versus $NADP^+$/NADPH in wine yeast before and after exposure to hyperosmotic stress. Thus, it will be important in future research to assess the

redox balance of the coenzyme systems in cells under high versus low osmotic stress and to determine their roles as metabolic triggers for acetic acid production.

## 1.2. Formation of other metabolites and the relationship to acetic acid and wine quality

### 1.2.1. Formation of acetaldehyde

Acetaldehyde is an early metabolic by-product of fermentation produced from pyruvate, the end product of glycolysis in *S. cerevisiae* (Romano *et al.* 2004). Organoleptically, acetaldehyde is one of the most important sensory carbonyl compounds formed during fermentation and has an important impact on wine quality. At low levels, the compound contributes pleasant fruity aromas to wine, whereas at high levels it elicits an aroma reminiscent of bruised apples (Liu and Pilone 2000). Once formed, acetaldehyde can be secreted from the cell and remain in wine or be used intracellularly as a precursor for the formation of other metabolites such as ethanol and acetic acid (Fig 1.2 and 1.3). Functionally, acetaldehyde serves as the electron acceptor used for NADH re-oxidation during fermentative growth and is reduced to ethanol by alcohol dehydrogenase (Voet and Voet 2004), while acetic acid can form from the oxidation of acetaldehyde by aldehyde dehydrogenase, with the concomitant reduction of $NAD(P)^+$ to NAD(P)H.

### 1.2.2. Formation of acetylCoA

Via the pyruvate dehydrogenase (PDH) bypass, acetylCoA can form during fermentation from acetic acid (reviewed in Pronk *et al*. 1996). In this pathway, pyruvate is decarboxylated by pyvuvate decarboxylase (Pdcp) to acetaldehyde, which is then oxidized to acetate via aldehyde dehydrogenase (Aldp). In the final reaction, acetylCoA synthetase (Acsp) catalyzes the formation of acetylCoA from acetate and Coenzyme A (CoA). CoA

can also be regenerated from the activity of acetylCoA hydrolyase (Achp), which catalyzes the hydrolysis of acetylCoA (Lee *et al*. 1996). Through this reaction sequence, the availability of acetylCoA increases in the cytosol where it can be used in anabolic reactions including lipid, sterol and amino acid biosynthesis (reviewed in Pronk *et al*. 1996), as well as ester synthesis (Verstrepen *et al*. 2004). For ester biosynthesis to take place, the carboxylic acid moiety needs to be activated with CoA prior to reaction, and energy is required from the thioester linkage of acetylCoA (Verstrepen *et al*. 2004).

In *S. cerevisiae*, two genes (*ACS1* and *ACS2*) have been identified for encoding for proteins responsible for catalyzing the formation of acetylCoA from acetate via the PDH bypass and are reported to differ with respect to their cellular localization, substrate specificity and kinetic properties (Satyanarayana and Klein 1974). Of the enzymes, Acs1p is the mitochondrial isoform required for respiratory growth on non-fermentable carbon sources and is glucose repressed (Kratzer and Schüller 1995; Van den Berg *et al*. 1996), while Acs2p is the cytosolic isoform required for growth on glucose under fermentation conditions and is constituently expressed (Van den Berg and Steensma 1995).

Akamatsu *et al*. (2000) determined that genes encoding for acetylCoA synthetases (*ACS1/2*) and acetylCoA hydrolyase (*ACH1*) were expressed by an *S. cerevisiae* sake yeast strain fermenting sake mash, along with *ALD2/3* encoding for cytosolic aldehyde dehydrogenases. The transcription of these genes was limited to the early stage of normal sake mash and was induced by high osmolarity under fermentative conditions in the presence of high glucose, which corresponded to an increase in acetate production. Akamatsu *et al*. (2000) also reported that overexpression of *ACS2* resulted in low acetate

production during small-scale sake fermentations, while overexpression of *ACS1* did not significantly change acetate productivity.

The work of Akamatsu *et al*. (2000) suggests a possible connection between aldehyde dehydrogenase and acetylCoA synthetase activity on acetic acid production by yeast during fermentation. This connection was further investigated under Icewine fermentation conditions to determine whether the expression of genes involved in acetic acid synthesis and degradation may contribute to the overall levels produced by wine yeast as they adapt to hyperosmotic stress. Martin (2008) showed through microarray and Northern Blot analysis of acetylCoA synthetases that both *ACS* isoforms were strongly down-regulated in Icewine juice fermenting yeast cells in comparison to yeast fermenting table wine juice. Since *ACS1* is glucose repressed and present during respiratory growth, it unlikely contributes to acetylCoA formation during fermentation (Pigeau and Inglis 2007). In contrast, the expression level of *ACS2* greatly influences acetylCoA biosynthesis and acetic acid degradation. Low expression of *ACS2* reduces the need for acetate as a substrate for acetylCoA synthetase, thereby reducing the formation of acetylCoA from acetate. Thus, it is possible that the high levels of acetic acid formed during Icewine fermentation could be the consequence of a decrease in acetylCoA formation due to low *ACS2* expression (Martin 2008).

Furthermore, since acetylCoA is a substrate for alcohol acetyltransferases, acetylCoA levels formed during Icewine fermentation may affect the amount of ethyl acetate produced in Icewine or other high sugar fermentations (Fig. 1.3). Lower acetylCoA levels would reduce the amount of substrate available to acetyltransferases for catalysis, thereby reducing the amount of ethyl acetate formed during fermentation. Heit (2011) and

Heit and Inglis (2012) determined no positive correlation between ethyl acetate production and increased osmotic stress to exist during Icewine fermentation as higher levels of ethyl acetate were produced by wine yeast fermenting table wine juice compared to Icewine juice. Down-regulation of *ACS* genes not only agree with the lower ethyl acetate levels formed during Icewine fermentation, but also with the down-regulation of fatty acid synthesis genes and reduced yeast cell growth in this matrix (Martin 2008).

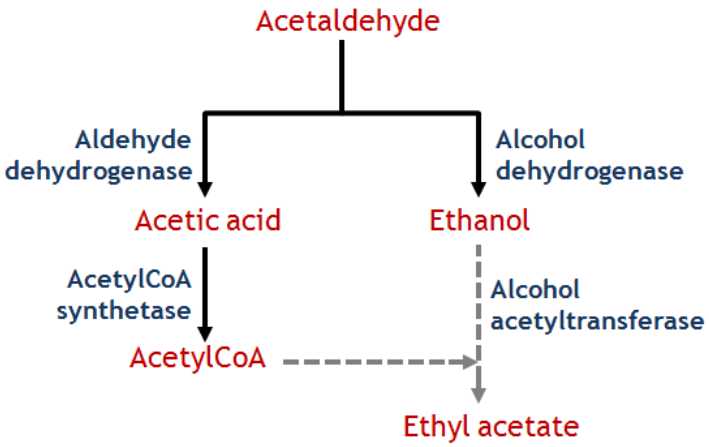


**Figure 1.3: Relationship of metabolites formed by *S. cerevisiae* during fermentation.**

### 1.2.3. Formation of ethyl acetate

Volatile esters represent the largest and most important group of flavour compounds formed during alcoholic fermentation (Cordente *et al.* 2006). Of these diverse compounds in wine, ethyl esters and acetate esters are found in the highest concentrations (Sumby *et al*. 2010). With respect to structure, ethyl esters contain an alcohol moiety (ethanol) and an acid group, specifically a medium-chain fatty acid, while acetate esters are comprised of an acid moiety (acetate) and an alcohol group, specifically ethanol or another complex alcohol derived from amino acid metabolism (Saerens *et al*. 2008). Although produced in trace amounts, esters greatly influence the organoleptic properties

of wine, affecting both composition and quality. Volatile esters are responsible for the fruity and candy-like characteristics of wine, and include notable compounds such as ethyl acetate (nail polish, solvent-like aroma), phenyl ethyl acetate (flowery, rose aroma) and isoamyl acetate (banana aroma), all of which are acetate esters, and ethyl caprylate (sour apple aroma), a (C6) short chain fatty acid ethyl ester (Dufour *et al*. 2002; Lambrechts and Pretorius 2000).

Plata *et al*. (2003) indicates acetate esters to be formed biochemically through an enzyme-catalyzed condensation reaction between an activated acylCoA component and a higher alcohol, and chemically through an esterification reaction between a carboxylic acid and an alcohol. However, the reaction rate of its chemical synthesis has been suggested to be too slow to account for the ester concentrations measured in alcoholic beverages (Mason and Dufour 2000), thereby attributing the majority of these compounds formed to the biochemical activity of the yeast cells. During fermentation, the enzymatic synthesis of esters is known to result primarily from alcohol acyltransferases, although esterases may also contribute, albeit to a much lesser extent (Lilly *et al*. 2000; Mason and Dufour 2000; Verstrepen *et al*. 2003).

Ester formation is primarily influenced by two factors: the concentration of the co-substrates and the activity level(s) of the ester synthetase(s) involved in catalysis. For ethyl acetate specifically, its formation is determined by the availability of acetylCoA and ethanol in the fermenting medium (Plata *et al*. 2003; Mason and Dufour 2000), and the activity levels of alcohol acyltransfereases (Verstrepen *et al*. 2003). At low levels, less acetylCoA and/ or ethanol is available to bind to the catalytic site of an alcohol acyltransferase, thereby limiting the amount of product that can be formed. Yeast growth

and cell requirements for lipid and sterol biosynthesis also influence acetylCoA levels, and therefore substrate availability and overall ester formation. Once fermentation commences, ester synthesis is initially slow due to the intracellular demand for acetylCoA to support yeast growth and metabolism (Thurston *et al*. 1992). As a consequence, little acetylCoA is diverted away from lipid and sterol biosynthesis and towards other metabolic processes, such as ester synthesis, at this time, resulting in low ethyl acetate levels. However, when lipid and sterol biosynthesis decreases, the large increase in cellular acetylCoA levels and acyltransferase activities leads to an increase in ester biosynthesis in yeast.

Alcohol acetyltransferases are the most well-known enzymes involved in ester synthesis and function in catalyzing the transfer of CoA-bound acetyls to an alcohol molecule (Nordstrom 1962; 1963; 1964; Malcorps and Dufour 1992; Yoshimoto *et al*. 1998). To date, three alcohol acetyltransferases capable of catalyzing this reaction have been identified in yeast and include Atf1p (encoded by *ATF1*), its closely related homologue Lg-Atf1p (encoded by Lg-*ATF1*) and Atf2p (encoded by *ATF2*) (Yoshioka and Hashimoto 1984; Yoshimoto *et al*. 1998; 1999). Atf1p and Atf2p have been reported to be present in *S. cerevisiae* and the lager yeast *S. pastorianus*, while Lg-Atf1p is found only in *S. pastorianus* (Malcorps and Dufour 1992; Saerens *et al*. 2006). Of these enzymes, Atf1p has been researched in the greatest detail and has been shown to be majorly involved in ethyl acetate and isoamyl acetate production (Lilly *et al.* 2000).

Verstrepen *et al.* (2003) investigated and compared the roles of the known *S. cerevisiae* alcohol acetyltransferases in volatile ester production by deleting or overexpressing *ATF1*, Lg-*ATF1* and *ATF2* in a laboratory strain and a commercial brewing strain. The resulting expression levels of *ATF1* and *ATF2* were determined to affect the

formation of both ethyl acetate and isoamyl acetate during fermentation. Overexpression of *ATF1* resulted in a 30-fold increase in ethyl acetate production and a 180-fold increase in isoamyl acetate production compared to wild-type cells. For most other esters analyzed, *ATF1* deletion resulted in a 60 to 90% reduction compared to wild-type levels. On the other hand, overexpression and deletion of *ATF2* produced more modest increases and decreases in ester concentration, respectively, whereas the contribution of Lg-*ATF1* was determined to be very limited, indicating the respective gene products to have only minor roles in ester formation compared to that of Atf1p.

Although the physiological roles of esters in yeast metabolism have yet to be completely elucidated, current literature suggests a variety of functions for this family of compounds. Verstrepen *et al*. (2003) indicates ester synthesis may be used as a mechanism to recycle free CoA under conditions in which normal regeneration of acetylCoA is prevented, while Bardi *et al*. (1998) suggests its formation to be related to an intracellular necessity for CoA from acylCoAs. Ester formation may also be used as a detoxification strategy against high levels of medium-chain fatty acids, acetic acid and ethanol (Bardi *et al*. 1998), all of which can negatively affect the metabolic activity and longevity of the fermenting yeast cells (Casal *et al*. 1996).

Despite the important roles esters may play in yeast, the formation of ethyl acetate during alcoholic fermentation can have a negative impact on wine composition and overall wine quality when produced in sufficient concentrations or above the sensory detection threshold (Heit and Inglis 2013). Along with other minor volatile acids, ethyl acetate and its precursor, acetic acid, make up volatile acidity. In Canada, Vintners Quality Alliance (VQA) regulates VA levels in all wine styles and defines the permissible concentration to

be 2.1 g $l^{-1}$ in Icewine and 1.3 g $l^{-1}$ acetic acid in table wine (VQA 2013). Although these maximal levels are rarely surpassed following chemical analyses, these compounds do contribute to wine aroma when their concentrations are present above the respective sensory threshold levels. Nurgel *et al.* (2004) reports the levels of acetic acid and ethyl acetate in Canadian Icewine to range from 0.49 to 2.29 g $l^{-1}$ and 0.086 to 0.369 g $l^{-1}$, respectively. Although produced in higher concentration than ethyl acetate, the level of acetic acid in Icewine is lower than its sensory threshold, which was determined to be 3.185 g $l^{-1}$ (Cliff and Pickering 2006). In contrast, the threshold level of ethyl acetate (0.198 g $l^{-1}$) falls within the range produced in Canadian Icewines currently on the market, enabling its perception in Icewine to be easier than acetic acid.

Since the concentration of ethyl acetate formed during Icewine fermentation is close to its sensory threshold level, minor concentration changes can majorly impact the sensory profile of a wine, potentially implicating its overall quality. Since a wine must also undergo sensory analysis prior to receiving the VQA designation, ethyl acetate formation is a ubiquitous concern within the wine industry for producers requiring their wines sufficiently meet the quality standards stipulated by VQA. As a consequence of these concerns, it is important that the production of ethyl acetate be controlled during fermentation in order to mitigate its negative effect on wine composition and quality due to its association with spoilage. Such control will require a better understanding of its biochemical formation during high and low sugar fermentations, focusing on both the availability of substrates and the activity levels of enzymes directly and indirectly involved in ethyl acetate synthesis in fermenting wine yeast cells.

### 1.3. Introduction to wine yeast: *Saccharomyces cerevisiae* and *Saccharomyces bayanus*

Although the development of certain management strategies for controlling VA production will rely on understanding the mechanisms for both acetic acid and ethyl acetate formation during fermentation, an alternative method for controlling high VA levels has been evaluated in the interim. Recent studies have focused on assessing the different acetic acid and ethyl acetate production capacities of specific wine yeast strains (Heit 2011; Heit and Inglis 2012; 2013; Yang 2010), and comparing their abilities to affect the chemical composition and aroma profile of the resulting wine (Eglinton *et al*. 2000; Antonelli *et al*. 1999). Of these yeasts, the majority of commercial strains belong to *Saccharomyces cerevisiae* and are widely used in the fermentation industry for wine, beer and sake production. Despite *S. cerevisiae* being primarily responsible for alcoholic fermentation (Pretorius 2000), other species of the genus *Saccharomyces* have been isolated from wine (Naumov *et al*. 2000; Masneuf-Pomarede *et al*. 2010; Gonzalez *et al*. 2006) and beer fermentations (Nguyen and Gaillardin 2005), as well as cider production (Naumov *et al*. 2001), which has generated substantial interest amongst producers for their potential use in commercial fermentations.

Unlike natural *Saccharomyces* strains, industrial strains have been domesticated through human activity, resulting in the development of an array of individual strains that have been selected for phenotypically desired traits (Borneman *et al*. 2011). Such characteristics include their fermentation properties, physiological adaptation to different environments and stress conditions, and ability to efficiently ferment glucose into ethanol and carbon dioxide without adversely affecting sensory quality through the production of unwanted flavour compounds (Pretorius 2000). As expected from these diverse

characteristics, genetic differences between species and strains of *Saccharomyces*, both industrial and natural, inevitably result in altered metabolism and stress responses to perturbed environmental conditions, including high osmotic pressure, hypoxia, high concentrations of sugar and ethanol and low nitrogen levels (Marks *et al*. 2008). Due to such trait variation among strains, yeasts produce phenotypically distinct outcomes from each other as they behave differently during the fermentation course, varying not only in their fermentation performances, but also in their production of certain metabolic by-products and overall contribution to wine flavour and aroma.

Of the non-*Saccharomyces cerevisiae* yeast strains, *S. bayanus* is a species involved in beer fermentation that has recently gained interest for use in sweet wine production due to its cryotolerance property and ability to produce flavour and aroma compounds distinct from industrial strains of *S. cerevisiae*. Previous studies have determined differences exist in the chemical composition of wines fermented by either *S. bayanus* or *S. cerevisiae* strains (Castellari *et al*. 1992; 1994; Kishimoto 1994; Massoutier *et al*. 1998; Antonelli *et al*. 1999), where wines made with *S. bayanus* generally contained higher concentrations of glycerol and succinic acid, and lower levels of acetic acid and ethanol. Malic acid levels in wines fermented by cryotolerant versus non-cryotolerant strains of *S. cerevisiae*, *S. uvarum* and *S. bayanus* were also observed to differ as the cryotolerant strains were found to degrade rather than synthesize this compound, resulting in lower levels in the final wine (Castellari *et al*. 1992). As a consequence of such traits, the fermentative capabilities of cryotolerant strains, and more specifically of *S. bayanus*, can result in wines with not only a distinct chemical composition, but also more unique organoleptic properties than those produced from ordinary non-cryotolerant and *S. cerevisiae* strains (Castellari *et al*. 1992).

To assess the suitability of two selected *S. bayanus* strains (AWRI 1176 and AWRI 1375) for winemaking, Eglinton *et al*. (2000) investigated their chemical and sensory impact on wine. Detailed chemical analysis of wine composition combined with sensory descriptive analysis elucidated differences between the *S. cerevisiae* (AWRI 838) and two *S. bayanus* isolates investigated following fermentation in Chardonnay table wine juice. When compared to *S. cerevisiae*, wine fermented by *S. bayanus* contained higher levels of glycerol, succinic acid and acetaldehyde, and lower levels of malic acid, acetic acid, ethanol and ethyl acetate. The work presented from this study also determined the aroma profiles of the resulting *S. bayanus* wines to be distinctly different from those fermented by *S. cerevisiae*. *S. bayanus* strains were associated with aroma attributes such as 'cooked orange peel', 'yeasty', 'honey', 'nutty' and 'aldehyde', whereas the *S. cerevisiae* isolate was associated with 'estery', 'pineapple', 'peach' and 'citrus' aromas.

Furthermore, Anotonelli *et al*. (1999) investigated the abilities of different yeast strains to form volatile compounds during the fermentation of Trebbiano table wine must. In total, nine strains of *S. cerevisiae* and four strains of *S. bayanus* were evaluated in the study and generated results similar to that of Eglinton *et al*. (2000) as the strains were significantly different in their production of certain compounds. The results of the chemical analyses indicated strains of *S. bayanus* produced higher levels of malic acid, glycerol and volatile compounds, mainly in the form of phenylethanol and ethyl lactate, compared to *S. cerevisiae*, which formed higher levels of acetic acid and $SO_2$, and lower levels of succinic acid. In addition, all *S. bayanus* strains produced low quantities of acetic acid while some *S. cerevisiae* strains reached the highest quantities. Due to the low acetic acid levels formed, along with other undesirable compounds such as sulfur anhydride, *S. bayanus* was

considered to be of applicative interest to the wine industry. Eglinton *et al*. (2000) acknowledges the importance of strain differences in winemaking, indicating that the different chemical composition and sensory profile of *S. bayanus*-fermented wine could be used to produce wines distinct from those of *S. cerevisiae*.

Since acetic acid and ethyl acetate are two concerning compounds in Icewine, the ability of *S. bayanus* to form low levels of acetic acid, the precursor to ethyl acetate, would be of benefit to the wine industry as it may provide a way to control or reduce their levels in wine. Heit (2011) and Heit and Inglis (2013) assessed the ability of a natural isolate of *S. bayanus* to ferment Icewine as compared to the commercial yeast *S. cerevisiae* K1-V1116, and evaluated differences in acetic acid and ethyl acetate production between the strains. Although the yeasts differed in the amount of sugar consumed during the fermentation course, *S. bayanus* produced significantly less acetic acid per gram of sugar metabolized than K1-V1116, with no significant difference in glycerol production (Heit and Inglis 2013). This finding is consistent with past studies demonstrating that acetic acid production is strain dependent (Patel and Shibamoto 2002; Torrens *et al*. 2008; Erasmus *et al*. 2004). Furthermore, *S. bayanus* demonstrated trends consistent with lower ethyl acetate production compared to *S. cerevisiae*. Although *S. bayanus* exhibited fermentation difficulties in the high sugar condition, as demonstrated by its slower sugar consumption and fermentation time, and lower cell concentration, its ability to generate low levels of acetic acid and ethyl acetate during the fermentation course and in the final wines shows potential for its use in less osmotically stressful environments such as that resulting from the concentrated sugars in semi-dried grapes used to produce appassimento-style wine.

## 1.4. Literature Cited


Albertyn, J., S. Hohmann, J.M. Thevelein and B.A. Prior. 1994. *GPD1*, which encodes glycerol-3-phosphate dehydrogenase is essential for growth in *Saccharomyces cerevisiae* and its expression is regulated by the high-osmolarity glycerol response pathway. Mole Cell Biol. 14:4135-4144.

Akamatsu, S., K. Kamiya, N. Yamashita, T. Motoyoshi, N. Goto-Yamamoto, T. Ishikawa, N. Okazaki and A. Nishimura. 2000. Effect of aldehyde dehydrogenase and acetyl-CoA synthetases on acetate formation in sake mash. J Biosci Bioeng. 90:555-560.

Akhtar, N., A. Blomberg and L. Alder. 1997. Osmoregulation and protein expression in a *pbs2J1* mutant of *Saccharomyces cerevisiae* during adaptation to hypersaline stress. FEBS Lett. 403:173-180.

Ansell, R., K. Granath, J.M. Thevelein and L. Adler. 1997. The two isozymes for yeast $NAD^+$-dependent glycerol-3-phosphate dehydrogenase encoded by *GPD1* and *GPD2* have distinct roles in osmoadaptation and redox regulation. EMBO J. 16:2333-2340.

Antonelli, A., L. Castellari, C. Zambonelli and A. Carnacini. 1999. Yeast influence on volatile composition of wine. J Agric Food Chem. 47:1139-1144.

Bardi, L., C. Crivelli and M. Marzona. 1998. Esterase activity and release of ethyl esters of medium chain fatty acids by *Saccharomyces cerevisiae* during anaerobic growth. J Microbial. 44:1171-1176.

Billi, D. and M. Potts. 2002. Life and death of dried prokaryotes. Res Microbiol. 153:7-12.

Blomberg, A. 2000. Metabolic surprises in *Saccharomyces cerevisiae* during adaptation to saline conditions: questions, some answers, and a model. FEMS Microbiol Lett. 182:1-8.

Blomberg, A. and L. Alder. 1992. Physiology of osmotolerance in fungi. Adv Microb Physiol. 33:145-212.

Blomberg, A. and L. Alder. 1989. Roles of glycerol and glycerol-3-phosphate dehydrogenase ($NAD^+$) in acquired osmotolerance of *Saccharomyces cerevisiae*. J Bacteriol. 171:1087-1092.

Boisnard, S., G. Ruprich-Robert, M. Florent, B. Da Silva, F. Chapeland-Leclerc and N. Papon. 2008. Insight into the role of HOG pathway components Ssk2p, Pbs2p, and Hog1p in the opportunistic yeast *Candida lusitaniae*. Eukaryotic Cell. 7:2179-2183.

Borneman, A., B.A. Desany, D. Riches, J.P. Affourtit, A.H. Forgan, I.S. Pretorius, M. Egholm and P.J. Chambers. 2011. Whole genome comparison reveals novel genetic

elements that characterize the genome of industrial strains of *Saccharomyces cerevisiae*. Plos Genetics. 7:1-10.

Brewster, J.L., T. de Valoir, N.D. Dwyer, E. Winter and M.C. Gustin. 1993. An osmosensing signal transduction pathway in yeast. Science. 259:1760-1763.

Bro, C., B. Regenberg, G. Lagniel, J. Labarre, M. Montero-Lomeli and J. Nielsen. 2003. Transcriptional, proteonomic, and metabolic responses to lithium in galactose-grown yeast cells. J Biol Chem. 278:31141-32149.

Casal, M., H. Cardosa and C. Leão. 1996. Mechanisms regulating the transport of acetic acid in *Saccharomyces cerevisiae*. Microbiol. 142:1385-1390.

Castellari, L., G. Pacchioli, C. Zambonelli, V. Tini and L. Grazia. 1992. Isolation and initial characterization of cryotolerant *Saccharomyces* strains. Ital J Food Sci. 4:179-186.

Castellari, L., M. Ferruzzi, A. Magrini, P. Giudici, P. Passarelli and C. Zambonelli. 1994. Unbalanced wine fermentation by cryotolerant vs. non-cryotolerant *Saccharomyces* strains. Vitis 33:49-52.

Cheetham, J., D.A. Smith, A. Silva Dantas, K.S. Doris, M.J. Patterson, C.R. Bruce and J. Quinn. 2007. A single MAPKKK regulates the Hog1 MAPK pathway in the pathogenic fungus *Candida albicans*. Mol Biol Cell. 18:4603-4614.

Chen, R.E. and J. Thorner. 2007. Function and regulation in MAPK signaling pathways: Lessons learned from the yeast *Saccharomyces cerevisiae*. Biochim Biophys Acta. 1773:1311-1340.

Cliff, M.A. and G.J. Pickering. 2006. Determination of odor detection thresholds for acetic acid and ethyl acetate in ice wine. Aust J Wine Res. 17:45-52

Cordente, A., J.H. Sweigers, F.G. Hergardt and I.S. Pretorius. 2006. Modulating aroma compounds during wine fermentation by manipulating carnitine acetyltransferases in *Saccharomyces cerevisiae*. FEMS Microbial Lett. 267:159-166.

Cuevas, B.D., A.N. Abell and G.L. Johnson. 2007. Role of mitogen-activated protein kinase kinase kinases in signal integration. Oncogene. 26:3159-3171.

Dufour, J.P., K.J. Verstrepen and G. Derdelinckx. Brewing yeasts. 2002. In *Yeasts in food*, T. Boekhour, V. Robert (eds). Behr's Verlag: Hamburg; 347-388.

Eglinton, J.M., A.J. Heinrich, A.P. Pollmitz, P. Langridge, P.A. Henschke and M. De Barros Lopes. 2002. Decreasing acetic acid accumulation by a glycerol overproducing

strain of *Saccharomyces cerevisiae* by deleting the *ALD6* aldehyde dehydrogenase gene. Yeast. 19:295-301.

Eglinton, J.M., S.J. McWilliams, M.W. Fogarty, I.L. Francis, M.J. Kwiatkowski, P.B. Høj and P.A. Henschke. 2000. The effect of *Saccharomyces bayanus*-mediated fermentation on the chemical composition and aroma profile of Chardonnay wine. Aust J Wine Res. 6:190-196.

Erasmus, D.J., G.K. van der Merwe and H.J. van Vuuren. 2003. Genome-wide expression analyses: metabolic adaptation of *Saccharomyces cerevisiae* to high sugar stress. FEMS. 34:375-399.

Erasmus, D.J. and H.J.J. van Vuuren. 2009. Genetic basis for osmosensitivity and genetic instability of the wine yeast *Saccharomyces cerevisiae* V1N7. Am J Enol Vitic. 60:145-154.

Erasmus, D.J., M. Cliff and H.J.J. van Vuuren. 2004. Impact of yeast strain on the production of acetic acid, glycerol, and the sensory attributes of Icewine. Am J Enol Vitic. 55:371-378.

Eriksson, P., L. Andre, R. Ansell, A. Blomberg and L. Adler. 1995. Cloning and characterization of *GPD2*, a second gene encoding sn-glycerol 3-phosphate dehydrogenase ($NAD^+$) in *Saccharomyces cerevisiae*, and its comparison with *GPD1*. Mol Microbiol. 17:95-107.

Ferrigno, P., F. Posas, D. Koepp, H. Saito and P.A. Silver. 1998. Regulated nucleo/ cytoplasmic exchange of HOG1 MAPK requires the importin b homologs NMD5 and XPO1. EMBO J. 17:5606-5614.

Furukawa, K. and S. Hohmann. 2013. Synthetic biology: lessons from engineering yeast MAPK signalling pathways. Mol Microbiol. 88:5-19.

Gonzalez S., E. Barrio, J. Gafner and A. Querol. 2006. Natural hybrids from *Saccharomyces cerevisiae*, *Saccharomyces bayanus* and *Saccharomyces kudriavzevii* in wine fermentations. FEMS Yeast Res. 6:1221-1234.

Heit, C. and D. Inglis. 2013. Acetic acid and ethyl acetate production during high brix fermentations: effect of yeast strain. Am J Enol Vitic. 64:4.

Heit, C. and D. Inglis. 2012. An investigation of the relationship between ethyl acetate production and osmotic stress in *Saccharomyces cerevisiae* K1-V1116 during high brix fermentations. Am J Enol Vitic. 63:4.

Heit, C. 2011. Effect of yeast strain and sugar concentration on ethyl acetate production in Icewine juice. BSc Hons Thesis. Brock University, ON.

Hirayama, T., T. Maeda, H. Saito and K. Shinozaki. 1995. Cloning and characterization of seven cDNAs for hyperosmolarity-responsive (*HOR*) genes of *Saccharomyces cerevisiae.* Mol Gen Genet. 249:127-138.

Hohmann, S. 2002. Osmotic stress signaling and osmoadaptation in yeasts. Microbiol Mol Biol Rev. 66:300-371.

Hohmann, S. 2009. Control of high osmolarity signaling in the yeast *Saccharomyces cerevisiae*. FEBS Lett. 583:4025-4029.

Jain, V.K., B. Divol, B.A. Prior and F.F. Bauer. 2012. Effect of alternative $NAD^+$-regenerating pathways on the formation and primary and secondary aroma compounds in *Saccharomyces cerevisiae* glycerol-defective mutant. Appl Microbiol Biotechnol. 93:131-141.

Jansen, G., F. Buhring, C.P. Hollenberg and M. Ramezani Rad. 2001. Mutations in the SAM domain of STE50 differentially influence the MAP kinase-mediated pathways for mating, filamentous growth and osmotolerance in *Saccharomyces cerevisiae.* Mol Genet Genom. 265: 102-117.

Kishimoto, M. 1994. Fermentation characteristics of hybrids between the cryophilic wine yeast *Saccharomyces bayanus* and the mesophilic wine yeast *Saccharomyces cerevisiae*. J Ferment Bioeng. 77:432-435.

Kontkanen, D., D. Inglis, G. Pickering and A. Reynolds. 2004. Effect of yeast inoculation rate, acclimatization, and nutrient addition on Icewine fermentation. Am J Enol Vitic. 55:363-370.

Kratzer, S. and H. J. Schüller. 1995. Carbon source-dependent regulation of the acetyl coenzyme A synthetases-encoding gene *ACS1* from *Saccharomyces cerevisiae*. Gene. 161:75-79.

Kukec, A., M. Berovic, M. Wondra, S. Celan and T. Kosmerl. 2003. Influence of temperature shock on the glycerol production in cv. Sauvignon blanc fermentation. Vitis. 42:205-206.

Lambrechts, M.G. and I.S. Pretorius. 2000. Yeast and its importance to wine aroma: a review. S Aft J Enol Vitic. 21:97-129.

Larsson, C., I.L. Påhlman, R. Ansell, M. Rigoulet, L. Adler and L. Gustafsson. 1998. The importance of the glycerol-3-phosphate shuttle during aerobic growth of *S. cerevisiae*. Yeast. 14:347-357.

Lee, F., L. Lin and J.A. Smith. 1996. Acetyl-CoA hydrolase involved in acetate utilization in *Saccharomyces cerevisiae*. Biochim Biophys Acta. 1297:99-104.

Lilly, M., M.G. Lambrechts and I.S. Pretorius. 2000. Effect of increased acetyltransferase activity on flavour profiles of wine and distillates. Appl Environ. Microbiol. 66:744-753.

Liu, S.Q. and G.J. Pilone. 2000. An overview of formation and roles of acetaldehyde in winemaking with emphasis on microbiological implications. Int J Food Sci Technol. 35:49-61.

Logothetis, S., G. Walker and E.T. Nerantzis. 2007. Effect of salt hyperosmotic stress on yeast cell viability. Proc Natl Sci. 113:171-184.

Maeda, T., M. Takekawa and H. Saito. 1995. Activation of yeast PBS2 MAPKK by MAPKKKs or by binding of an SH3-containing osmosensor. Science. 269:554-558.

Maeda, T., S.M. Wurgler-Murphy and H. Saito. 1994. A two-component system that regulates osmosensing MAP kinase cascade in yeast. Nature. 369:242-245.

Malcorps, P. and J.P. Dufour. 1992. Short-chain and medium chain aliphatic ester synthesis in *Saccharomyces cerevisiae*. Eur J Biochem. 210:1015-1022.

Marks, V.D., S.J. Ho Suiz, D. Erasmus, G.K. van der Merwe, J. Brumm, W.W. Wasserman, J. Bryan and H.J.J. van Vuuren. 2008. Dynamics of the yeast transcriptome during wine fermentation reveals a novel fermentation stress response. FEMS Yeast Res. 8:35-52.

Martin, D.D., R.A. Ciulla and M.F. Roberts. 1999. Osmoadaptation in archaea. Appl Environ Microbial. 65:1815-1825.

Martin, S.J. 2008. The osmoadaptive response of the wine yeast *S. cerevisiae* K1-V1116 during Icewine fermentation. PhD Thesis. Brock University, ON.

Masneuf-Pomarede, I., M. Bely, P. Marullo, A. Lonvaud-Funel and D. Dubourdieu. 2010. Reassessment of phenotypic traits for *Saccharomyces bayanus* var. *uvarum* wine yeast strains. Int J Food Microbiol. 139:79-86.

Mason, A.B. and J.P. Dufour. 2000. Alcohol acetyltransferases and the significance of ester synthesis in yeast. Yeast. 16:1287-1298.

Massoutier, C., H. Alexandre, M. Feuillat and C. Charpentier. 1998. Isolation and characterization of cryotolerant *Saccharomyces* strains. Vitis. 37:55-59.

Mettetal, J.T., D. Muzzey, C. Gómez-Uribe and A. van Oudenaardem. 2008. The frequency dependence of osmo-adaptation in *Saccharomyces cerevisiae*. Science. 319:482-484.

Miermont, A., J. Uhlendorf, M. McClean and P. Hersen. 2011. The dynamical systems properties of the HOG signaling cascade. J Signal Transduct. 2011:1-12.

Mollapour, M. and P.W. Piper. 2006. Hog1p mitogen-activated protein kinase determines acetic acid resistance in *Saccharomyces cerevisiae*. FEMS Yeast Res. 6:1274-1280.

Nadal, E., P.M. Alepuz and F. Posas. 2002. Dealing with osmostress through MAP kinase activation. Euro Mol Biol Org. 3:735-740.

Naumov, G., I. Masneuf, E.S. Naumova, M. Aigle and D. Dubourdieu. 2000. Association of *Saccharomyces bayanus* var. *uvarum* with some French wines: genetic analysis of yeast populations. Res Microbiol. 151: 683-691.

Naumov, G.I., H.V. Nguyen, E.S. Naumova, A. Michel, M. Aigle and C. Gaillardin. 2001. Genetic identification of *Saccharomyces bayanus* var. *uvarum*, a cider-fermenting yeast. Int J Food Microbiol. 65:163-171.

Nguyen, H.V. and C. Gaillardin. 2005. Evolutionary relationships between the former species *Saccharomyces uvarum* and the hybrids *Saccharomyces bayanus* and *Saccharomyces pastorianus*; reinstatement of *Saccharomyces uvarum* (Beijerinck) as a distinct species. FEMS Yeast Res. 5:471-483.

Navarro-Avino, J.P., R. Prasad, V.J. Miralles, R.M. Benito and R. Serreno. 1999. A proposal of nomenclature of aldehyde dehydrogenases in *Saccharomyces cerevisiae* and characterization of the stress-inducible *ALD2* and *ALD3* genes. Yeast. 15:829-842.

Neviogt, E. and U. Stahl. 1997. Osmoregulation and glycerol metabolism in the yeast *Saccharomyces cerevisiae*. FEMS Microbiol Rev. 213:231-271.

Norbeck, J. and A. Blomberg. 2000. The level of cAMP-dependent protein kinase A activity strongly affects osmotolerance and osmo-instigated gene expression in *S. cerevisiae*. Yeast. 16:121-137.

Norbeck, J., A. Påhlman, N. Akhtar, A. Blomberg and L. Adler. 1996. Purification and characterization of two isoenzymes of DL-glycerol-3-phosphatase from *Saccharomyces cerevisiae.* J Biol Chem. 271:13875-13881.

Nordström, K. 1964. Formation of esters from alcohols by brewer's yeast. J Inst Brew. 70:328-336.

Nordström, K. 1962. Formation of ethyl acetate in fermentation with brewer's yeast III: participation of coenzyme A. J Inst Brew. 68:398-407.

Nordström, K. 1963. Formation of ethyl acetate in fermentation with brewer's yeast IV: metabolism of acetyl coenzyme A. J Inst Brew. 69:142-153.

Nurgel, C., G.J. Pickering and D.L. Inglis. 2004. Sensory and chemical characteristics of Canadian ice wines. J Sci Food Agric. 84:1675-1684.

O'Rourke, S.M. and I. Herskowitz. 2004. Unique and redundant roles for HOG MAPK pathway components as revealed by whole-genome expression analysis. Mol Biol Cell. 15:532-542.

O'Rourke, S.M., I. Herskowitz and E.K. O'Shea. 2002. Yeast go the whole HOG for the hyperosmotic stress response. Trends Genet. 18:405-412.

Ostrander, D.B. and J.A. Gorman. 1999. The extracellular domain of the *Saccharomyces cerevisiae* Sln1p membrane osmolarity sensor is necessary for kinase activity. J Bacteriol. 181:2527-2534.

Påhlman, A.K., K. Granath, R. Ansell, S. Hohmann and L. Alder. 2001. The yeast glycerol 3-phosphatases Gpp1p and Gpp2p are required for glycerol biosynthesis and differentially involved in the cellular responses to osmotic, anaerobic, and oxidative stress. Biol Chem. 276:3555-3563.

Parmar, J.H., S. Bhartiya and K.V. Venkatesh. 2011. Characterization of the adaptive response and growth upon hyperosmotic shock in *Saccharomyces cerevisiae*. Mole BioSyst. 7:1138-1148.

Patel, S. and S. Shibamoto. 2002. Effect of different strains of *Saccharomyces cerevisiae* on production of volatiles in Napa Gamay wine and Petit sirah wine. J Agric Food Chem. 50:5649-5653.

Petelenz-Kurdzuel, E., E. Eriksson, M. Smedh, C. Beck, S. Hohmann and M. Gokso. 2011. Quantification of cell volume changes upon hyperosmotic stress in *Saccharomyces cerevisiae.* Integr Biol. 3:1120-1126.

Pigeau, G.M. and D.L. Inglis. 2007. Response of wine yeast (*Saccharomyces cerevisiae)* aldehyde dehydrogenase to acetaldehyde stress during Icewine fermentation. J Appl Microbiol. 103:1576-1586.

Pigeau, G.M. and D.L. Inglis. 2005. Upregulation of *ALD3* and *GPD1* in *Saccharomyces cerevisiae* during Icewine fermentation. J Appl Microbiol. 99:112-125.

Pigeau, G.M., E. Bozza, K. Kaiser and D.L. Inglis. 2007. Concentration effect of Riesling Icewine juice on yeast performance and wine acidity. J Appl Microbiol. 103:1961-1698.

Plata, C., C. Millán, J.C. Mauricio and J.M. Ortega. 2003. Formation of ethyl acetate and isoamyl acetate by various species of wine yeasts. Food Microbiol. 20:217-224.

Posas, F. and H. Saito. 1998. Activation of the yeast SSK2 MAP kinase kinase kinase by the SSK1 two-component response regulator. EBMO. 17:1385-1394.

Posas, F. and H. Saito. 1997. Osmotic activation of the HOG MAPK pathway via Ste11p MAPKKK: scaffold role of Pbs2p MAPKK. Science. 276:1702-1705.

Posa, F., S.M. Wurgler-Murphy, T. Maeda, E.A. Witten, T.C. Thai and H. Saito. 1996. Yeast HOG1 MAP kinase cascade is regulated by a multistep phophorelay mechanism in the SLNI-YPDI-SSK1 "two-component" osmosensor. Cell. 86:865-875.

Pretorius, I.S. 2000. Tailoring wine yeast for the new millennium: novel approaches to the ancient art of winemaking. Yeast. 16:675-729.

Pronk, J.T., H.Y. Steensma and J.P. van Dijken. 1996. Pyruvate metabolism in *Saccharomyces cerevisiae*. Yeast. 12:1607-1633.

Raitt, D.C., F. Posas and H. Saito. 2000. Yeast Cdc42 GTPase and Ste20 PAK-like kinase regulate Shol-dependent activation of the Hogl MAPK pathway. EMBO J. 19:4623-4631.

Reiser, V., S.M. Salah and G. Ammerer. 2000. Polarized localization of yeast Pbs2 depends on osmostress, the membrane protein Sho1 and Cdc42. Nat Cell Biol. 2:620-627.

Rep, M., J. Albertyn, J.M. Thevelein, B.A. Prior and S. Hohmann. 1999. Different signalling pathways contribute to the control of *GPD1* expression by osmotic stress in *Saccharomyces cerevisiae.* Microbiol. 145:715-727.

Rep, M., M. Krantz, J.M. Thevelein and S. Hohmann. (2000). The transcriptional response of *Saccharomyces cerevisiae* to osmotic shock. J Biol Chem. 275: 8290-8300.

Remize, F., E. Andrieu and S. Dequin. 2000. Engineering of the pyruvate dehydrogenase bypass in *Saccharomyces cerevisiae*: role of the cytosolic $Mg^{2+}$ and mitochondrial $K^{+}$ acetaldehyde dehydrogenases Ald6p and Ald4p in acetate formation during alcoholic fermentation. Appl and Environ Microbiol. 66:3151-3159.

Remize, F., J.L. Roustan, J.M. Sablayrolles, P. Barre, and S. Dequin. 1999. Glycerol overproduction by engineered *Saccharomyces cerevisiae* wine yeast strains leads to substantial changes in by-product formation and to a stimulation of fermentation rate in stationary phase. Appl Environ Microbiol. 65:143-149.

Romano, P., G. Suzzi, L. Turbani and M. Polsinelli. 1994. Acetaldehyde production in *Saccharomyces cerevisiae* wine yeasts. FEMS Microbiol Lett. 118:213-218.

Saint-Prix. F., L. Bönquist and S. Dequin. 2004. Functional analysis of the *ALD* gene family of *Saccharomyces cerevisiae* during anaerobic growth on glucose: the $NADP^+$-dependent Ald6p and Ald5p isoforms play a major role in acetate formation. Microbiol. 150:2209-2220.

Saito, H. and K. Tatebayashi. 2004. Regulation of the osmoregulatory HOG MAPK cascade in yeast. J Biochem. 136: 267-272.

Saerens, S.M.G., P.J. Verbelen, N. Vanbeneden, J.M. Thevelein and F.R. Delvaux. 2008. Monitoring the influence of high-gravity brewing and fermentation temperature on flavour formation by analysis of gene expression levels in brewing yeast. Appl Microbiol Biotechnol. 80:1039-1051.

Saerens, S.M.G., K.J. Verstrepen, S.D.M. Van Laere, A.R.D. Voet, P. Van Dijck, F.R. Delvaux and J.M. Thevelein. 2006. The *Saccharomyces cerevisiae EHT1* and *EEB1* genes encode novel enzymes with medium-chain fatty acid ethyl ester synthesis and hydrolysis capacity. Biol Chem. 281:4446-4456.

Satyanarayana, T., A.D. Mandel and H.P. Klein. 1974. Evidence for two immunologically distinct acetyl-coenzyme A synthetases in yeast. Biochem Biophys Acta. 341:396-401.

Schoodermark-Stolk, S.A., M. Tabernero, J. Chapman, E.G. Ter Schure, C.T. Verrips, A.J. Verkleij and J. Boonstra. 2005. Bat2p is essential in *Saccharomyces cerevisiae* for fusel alcohol production on the non-fermentable carbon source ethanol. FEMS Yeast Res. 5:757-766.

Sumby, K.M., P.R. Grbin and V. Jiranek. 2010. Microbial modulation of aromatic esters in wine: current knowledge and future prospects. Food Chem. 121:1-16.

Tamas, M.J., M. Rep, J.M. Thevelein and S. Hohmann. 2000. Stimulation of the yeast high osmolarity glycerol (HOG) pathway: evidence for a signal generated by a change in turgor rather than by water stress. FEBS Lett. 472:159-165.

Tamás, M.J. and S. Hohmann. 2003. The osmotic stress response of *Saccharomyces cerevisiae*. Yeast stress response. Springer-Verlag, Berlin. 199.

Thorne, T.W., H. Ho, M. Huvet, K. Haynes and M.P.H. Stumpf. 2011. Prediction of putative protein interactions through evolutionary analysis of osmotic stress response in the model yeast *Saccharomyces cerevisiae*. Fungal Genet Biol. 48:504-511.

Thursten, P.A., D.E. Quain and R.S. Tubb. 1992. Lipid metabolism and the regulation of volatile ester synthesis in *Saccharomyces cerevisiae*. J Inst Brew. 88:90-94.

Torrens, J., P. Urpi, M. Riu-Aumatell, S. Vichi, E. Lopez-Tamanes and S. Buxaderas. 2008. Different commercial yeast strains affecting volatile and sensory profile of cava base wine. Int J Food Microbiol. 124:48-57.

Van den Berg, M.A. and H.Y. Steensma. 1995. *ACS2*, a *Saccharomyces cerevisiae* gene encoding acetyl-coenzyme A synthetase, essential for growth on glucose. Eur J Biochem. 231:704-713.

Van den Berg, M.A., P. de Jong-Gubbels, C.J. Kortland, J.P. van Dijken, J.T. Pronk and H.Y. Steensma. 1996. The two acetyl-coenzyme A synthetases of *Saccharomyces cerevisiae* differ with respect to kinetic properties and transcriptional regulation. Biol Chem. 271:28953-28959.

van Dijken, J. and W. Sheffers. 1986. Redox balances in the metabolism of sugars by yeasts. FEMS Microbiol Rev. 32:199-224.

Varela, J.C.S. and W. H. Mager. 1996. Response of *Saccharomyces cerevisiae* to changes in external osmolarity. Microbiol. 142:721-731.

Verduyn, C., E. Postma, A. Scheffers and J.P. van Dijken. 1990. Physiology of *Saccharomyces cerevisiae* in anaerobic glucose-limited chemostat culture. J Gen Microbiol. 136:395-403.

Verstrepen, K.J., G. Derdelinckx, J.P. Dufour, J. Winderickx, J.M. Thevelein, J. Pretorius and F.R. Delvaux. 2003. Adding fruitiness to beer. J Biosci Bioeng. 96:110-118.

Verstrepen, K.J., S.D.M. Van Laere, B.M.P. Vanderhaegen, G. Derdelinckx, J.P. Dufour, I.S. Pretorius, J. Winderickx, J.M. Thevelein and F.R. Delvaux. 2003. Expression levels of the yeast alcohol acetyltransferase genes *ATF1*, *Lg-ATF1*, and *ATF2* control of the formation of a broad range of volatile esters. Appl and Environ Microbiol. 69:5228-5237.

Verstrepen, K.J., S.D.M. Van Laere, J. Vercammen, G. Derdelinckx, J.P. Dufour, I.S. Pretorius, J. Winderickx, J.M. Thevelein and F.R. Delvaux. 2004. The *Saccharomyces cerevisiae* alcohol acetyltransferase Atf1p is localized in lipid particles. Yeast. 21:367-377.

Voet and Voet. 2004. Biochemistry. John Wiley & Sons, New York. 1392.

VQA Ontario. 2013. Wine standards. Retrieved from: http://www.vqaontario.com/Regulations/Standards

Wang, X.P., C.J. Mann, Y.L. Bai, L. Ni and H. Weiner. 1998. Molecular cloning, characterization, and potential rules of cytosolic and mitochondrial aldehyde dehydrogenases in ethanol metabolism in *Saccharomyces cerevisiae*. J Bacteriol. 180:822-830.

White, W.H., P.L. Skatrud, Z. Xue and J.H. Toyn. 2003. Specialization of function among aldehyde dehydrogenases: the *ALD2* and *ALD3* genes are required for beta-alanine biosynthesis in *Saccharomyces cerevisiae*. Genetics. 163:69-77.

Yang, F. 2011. Study of new yeast strains as novel starter cultures for Riesling Icewine production. MSc Thesis. Brock University, ON.

Yoshimoto, H., D. Fujiwara, T. Momma, K. Tanaka, H. Sone, N. Nagasawa and T. Tamai. 1999. Isolation and characterization of the *ATF2* gene alcohol acetyltransferase II in the bottom fermenting yeast *Saccharomyces pastorianus*. Yeast. 15:409-417.

Yoshimoto, H., T. Momma, D. Fujiwara, H. Sone, Y. Kaneko and T. Tamai. 1998. Characterization of the *AFT1* and *Lg-ATF1* genes encoding alcohol acetyltransferases in the bottom fermenting yeast *Saccharomyces pastorianus*. J. Ferment Bioeng. 86:15-20.

Yoshioka, K. and N. Hashimoto. 1984. Acetyl-CoA of brewer's yeast and formation of acetate esters. Agric Biol Chem. 48:207-209.

# Chapter 2

## 2. Acetic Acid and Ethyl Acetate Formation during Fermentation in Appassimento-Type Must: Effect of Yeast Strain and Sugar Concentration

**Heit, C.[1,2] and D.L. Inglis[1,2,3]**

1 Cool Climate Oenology and Viticulture Institute, Brock University, St. Catharines, ON, Canada
2 Centre for Biotechnology, Brock University, St. Catharines, ON, Canada
3 Department of Biological Sciences, Brock University, St. Catharines, ON, Canada

Formatted for the Journal of Applied Microbiology

### 2.1. Abstract

**Aims:** To study the metabolomics and fermentation performances of *Saccharomyces cerevisiae* and *Saccharomyces bayanus* strains under high sugar stress during the vinification of partially dried grapes. The production of glycerol, acetaldehyde, ethanol, acetic acid and ethyl acetate were followed to relate metabolites in wine involved in the yeast's osmotic stress response to acetic acid and ethyl acetate production during high sugar fermentations. Kinetic and metabolic differences between the wine yeast strains were also compared to evaluate their abilities to form acetic acid and ethyl acetate, and to ferment must produced using an appassimento-type process.

**Methods and Results:** Appassimento-type must (27°Brix; 244 ± 19 g $l^{-1}$ sugar) and table wine must (18°Brix; 179 ± 5 g $l^{-1}$ sugar) were fermented in triplicate using the commercial wine yeast *S. cerevisiae* strain EC-1118 and a natural strain of *S. bayanus*. Acetic acid production increased 41.2% in the 27°Brix condition in comparison to the 18°Brix condition fermented by EC-1118, accompanied by an 80.6% decrease in ethyl acetate production over that determined in table wine. Acetic acid production by *S. bayanus* in the 27°Brix must was lower than that observed in the 18°Brix condition, although starting levels were higher as a result of the drying process. Ethyl acetate production was also lower in the concentrated grape must, resulting in a 96.4% decrease over that found in the reference condition. The fermentation performances and kinetic behavior of the wine yeasts were similar in the high and low sugar conditions. Between strains, sugar utilization and ethanol production were comparable as no significant differences were determined, although differences in viable cell concentrations existed.

**Conclusions:** This study investigated the different acetic acid and ethyl acetate production capacities of two wine yeasts fermenting under high and low sugar conditions. Higher acetic acid and lower ethyl acetate levels were formed by EC-1118 in appassimento-style wine compared to table wine, while lower levels of both metabolites were formed by *S.*

*bayanus* fermenting under high sugar stress. Of the two strains studied, *S. bayanus* produced less acetic acid and ethyl acetate compared to EC-1118 fermenting the high and low sugar musts, which is consistent with our previous studies. In light of the differences in metabolite formation between yeasts, both strains displayed appreciable capabilities to overcome osmotic stress and to yield ethanol after fermenting the concentrated grape must.

**Significance and Impact:** The results provided insights on the abilities of two wine yeasts to ferment high sugar must produced using an appassimento-type process, and strain differences in the production of metabolites involved in the stress response leading to acetic acid and ethyl acetate formation. Taken together, this work assisted in our understanding of the stress response of wine yeasts to solutes concentrated in grape juices and of possible factors contributing to the formation of yeast metabolites, namely acetic acid and ethyl acetate, under these conditions. This investigation is of applicative interest for the wine industry that uses high sugar musts.

**Keywords:** *Saccharomyces cerevisiae*, *Saccharomyces bayanus*, appassimento process, hyperosmotic stress, glycerol, acetaldehyde, ethanol, acetic acid, ethyl acetate, aldehyde dehydrogenase, redox balance.

## 2.2. Introduction

Ontario's wine appellations include the Niagara Peninsula and the adjacent regions of Lake Erie Northshore, now including Pelee Island, and Prince Edward County (VQA 2013A). Of these appellations, the Niagara Peninsula is the largest and most diverse Viticultural Area in Canada, and is denoted as a cool-climate region as it is situated at approximately N43°latitude, with relatively high changes in day-night temperature and considerable sunshine during the growing season, lasting from April through to October (VQA 2013A). On average, the number of growing degree days within the region is reported to be 1413, while the number of frost-free days is 198 (VQA 2013A). Due to its climatic characteristics, Niagara supports the quality production of selected wine grape varieties including *Vitis vinifera* varietals such as Pinot noir, Cabernet franc, Sauvignon blanc and Riesling (VQA 2013A), although its cool and relatively humid climate and short

growing season impact both grape composition and wine quality (Jackson and Lombard 1993).

Meso-climate site characteristics, including temperature, relative humidity and rain, combined with good canopy management and crop control, are critical in capturing sufficient heat to fully ripen fruit, thereby allowing it to reach maturity (Jones and Hellman 2002). Aside from basic climatic constraints in Niagara, annual weather variability within the region and extreme climatic events, including early freezes, mid-winter thaws and spring frosts, pose additional challenges for the Ontario wine industry as these factors also influence grape and wine quality (Hakimi Rezaei and Reynolds 2010; Shaw 2005). Climatic variation can further result in insufficient heat units to fully ripen some varieties, and fall weather may include excessive rain, potentially precluding the fruit from reaching its full flavour potential through ripening on-vine (Jackson and Lombard 1993; Winkler 1954). However, ripening the fruit off-vine postharvest using an appassimento-type process represents a new and exciting innovation for the Ontario wine industry to overcome this climatic barrier and to produce high quality wines. This process involves drying grapes already picked from the vine, which increases the sugar content due to water loss, resulting in berry dry weight reductions of 10 to 40%, and induces changes both within and on the grape surface that alter flavour (Rizzini *et al*. 2009).

Traditionally, the "passito" method has been employed in Mediterranean civilizations with hot climates using grapes that have either been dried naturally through withering or dehydrated using a particular drying process (Barbanti *et al*. 2008). Under dehydration conditions, postharvest water stress and subsequent over-ripening can be achieved in berries by placing them in shady, dry or ventilated areas or in closed

environments where the temperature, relative humidity and airflow are artificially controlled (Bellincontro *et al*. 2004). Controlled environmental conditions have been shown to be important for obtaining high-quality dehydrated berries as they permit more uniform dehydration and postponed water stress compared to traditional, uncontrolled conditions (Chkaibain *et al*. 2007). In addition to sugar concentration, research conducted for wine production has also shown organic acid, phenolic and aroma compounds to be produced or concentrated, suggesting positive postharvest flavour development can occur as a consequence of the drying process (Bellincontro *et al*. 2004; Constantini *et al*. 2006; Moreno *et al*. 2008). Ratios of tartaric/ malic acid have been shown to increase due to a loss off malic acid from increased respiration (Rizzini *et al*. 2009), along with phenolics, including stilbenes (trans-resveratrol, trans-piceid) and catechins (Mencarelli *et al*. 2010), acetaldehyde and ethyl acetate (Constanti *et al*. 2006).

However, fermenting must from dried grapes presents many challenges for wine yeast (López de Lerma and Peinado 2011). The high solute concentrations expose yeast to extreme conditions of hyperosmotic stress, leading to altered metabolism, growth, and fermentation difficulties (Pigeau and Inglis 2005; 2007; Heit 2011). Under these conditions, target alcohol levels may not be attained and metabolic by-products of stress responses such as glycerol and acetic acid may impact wine composition (Heit and Inglis 2013). Both glycerol and acetic acid have been implicated in allowing yeast to maintain cytosolic osmotic and redox balance, respectively, under high osmolarity (Pigeau and Inglis 2005; Erasmus *et al.* 2004). The further metabolism of acetic acid to acetylCoA by an acetylCoA synthetase (Mason and Dufour 2000) facilitates the biosynthesis of ethyl acetate, a volatile compound that can further impact the chemical composition and overall

quality of the resulting wine (Heit and Inglis 2013). When present in sufficient concentrations, ethyl acetate and acetic acid affect the organoleptic properties of wine and may cause the volatile acid levels to exceed legal limits. Alcohol acetyltransferases are the most well-known enzymes involved in ester synthesis and catalyze the condensation of acetylCoA and ethanol (Nordstrom 1962; 1963).

The mechanisms (both transcriptional and non-transcriptional) involved in yeast osmoregulation and osmoadaptation have been extensively studied in laboratory strains of *S. cerevisiae* in response to salt-induced osmotic stress (Hohmann *et al*. 2002), and to a lesser extent in wine *S. cerevisiae* in response to sugar-induced osmotic stress during fermentation (Pigeau and Inglis 2005; Erasmus *et al*. 2003). However, aerobically grown *S. cerevisiae* have been shown to synthesize glycerol under salt stress accompanied by acetic acid production (Blomberg and Alder 1989), which is consistent for *S. cerevisiae* exposed to sugar stress during wine fermentation, with a linear correlation between glycerol and acetic acid production (Pigeau and Inglis 2007). Glycerol is the main osmolyte in *S. cerevisiae* and is synthesized under osmotic stress (Blomberg and Alder 1989; Brewster *et al*. 1993; Nevoigt and Stahl 1997; Blomberg 2000). The rate-limiting step in its biosynthesis is the expression of glycerol-3-phosphate dehydrogenase (encoded by *GPD1* and *GPD2*), which catalyzes the reduction of dihydroxyacetone phosphate (DHAP) to glyceraldehyde-3-phosphate, with the oxidation of NADH (Remize *et al*. 2001). In a subsequent reaction, glycerol-3-phosphate is dephosphorylated by glycerol-3-phosphatases (encoded by *GPP1* and *GPP2*) to form glycerol (Påhlman *et al.* 2001).

Since yeast lack a transhydrogenase to convert reducing equivalents between coenzyme systems ($NAD^+$/ NADH, $NADP^+$/ NADPH) (Bruinenberg *et al*. 1983), they rely

on metabolite formation to maintain the intracellular redox balance, specifically through redox reactions that can reduce the excess $NAD^+$ produced during glycerol synthesis. Acetic acid biosynthesis has been suggested as a mechanism that yeast can use to balance $NAD^+$ produced in response to osmotic stress by regenerating NADH (Blomberg and Alder 1989). The NADH consumed during DHAP reduction could be provided by the $NAD^+$-dependent oxidation of acetaldehyde to acetic acid by a cytosolic aldehyde dehydrogenase (Aldp), resulting in the reduction of $NAD^+$ to NADH (Pigeau and Inglis 2007). In *S. cerevisiae*, there are five Aldp isoforms that are capable of catalyzing this reaction, two of which are cytosolic and $NAD^+$-dependent (encoded by *ALD2* and *ALD3*) (Navarro-Avino *et al*. 1999) and one of which is cytosolic and $NADP^+$-dependent (encoded by *ALD*6) (Meaden *et al*. 1997). To date it remains unclear which cofactor system and Aldp isoform is responsible for acetic acid production during high sugar fermentations and the linkage to hyperosmotic stress and NADH requirements (Pigeau and Inglis 2005; 2007; Erasmus *et al*. 2003; 2004).

Since acetic acid is a precursor to ethyl acetate, understanding the factors contributing to their biosynthesis is important for ultimately determining what controls acetic acid and ethyl acetate formation by wine yeast fermenting under high sugar stress. With respect to substrate availability for the Aldp isozymes, acetaldehyde levels have been shown to quickly increase during Icewine fermentation over that found in table wine juice (Pigeau and Inglis 2005; Heit 2011; Heit and Inglis 2012; 2013), which was followed by a decrease in acetaldehyde and a large increase in acetic acid (Pigeau and Inglis 2005; Heit 2011; Heit and Inglis 2012; 2103). Of the *ALD* isogenes, Pigeau and Inglis (2005; 2007) reported only *ALD3* to be differentially up-regulated in response to osmotic stress during

Icewine fermentation, which corresponded to a large-fold increase in acetic acid. They concluded that Ald3p contributes, in part, to the elevated acetic acid found in Icewines. In contrast, Erasmus *et al*. (2003) found *ALD2*, *ALD3*, *ALD4* and *ALD6* to all be up-regulated under high osmolarity 2 hours after exposure to 40% (w/v) sugar, also corresponding to an increase in acetic acid produced days later during the fermentation. However, $NADP^+$-dependent Ald6p was recently reported to be responsible for the majority of acetic acid generated in a laboratory *S. cerevisiae* strain grown under aerobic conditions exposed to 40% (w/v) glucose, linking acetic acid generation under osmotic stress to NADPH production, possibly as a way to compensate for the down-regulation of NADPH generated through the pentose phosphate pathway (Bro *et al*. 2003; Erasmus and van Vuuren 2009).

Elevated acetic acid in Icewine also appears due to lack of conversion to acetylCoA from the down-regulation in gene expression of acetylCoA sythetases encoded by *ACS2* and *ACS1* (Martin and Inglis 2006; Martin 2008). Under these conditions, low expression of *ACS2* in osmotically stressed cells may also reduce the formation of acetylCoA from acetate, thereby reducing the amount of substrate available to acetyltransferases for ethyl acetate formation. The down-regulation of *ACS* genes corresponded to a down-regulation of fatty acid synthesis genes and reduced growth in the Icewine condition (Martin 2008) as acetylCoA is required for lipid, sterol and amino acid biosynthesis (Pronk *et al*. 1996). This result was further substantiated by the lower ethyl acetate levels measured in Icewine compared to table wine, whereby acetylCoA is required for the esterification to ethanol by alcohol acetyltransferase (Heit 2011; Heit and Inglis 2012). Lower ethyl acetate levels in Icewine could also be due to the reduced acetyltransferase activity, although this variable has not been measured.

In Ontario and elsewhere, the high sugar musts associated with Icewine and appassimento-type wine production pose challenges in the management of volatile acidity (VA) (Heit and Inglis 2013). With the maximum allowable limit of VA at 2.1 g $l^{-1}$ and 1.3 g $l^{-1}$ acetic acid in Icewine and table wine (VQA 2013B), respectively, it is important to understand the fermenting yeast's adapted response during high sugar fermentation to determine how and why acetic acid is produced and the controlling factors of ethyl acetate formation due to their impact on wine quality. In addition, investigating the use of wine yeast strains as control agents for acetic acid and ethyl acetate production during high sugar ferments will be important for developing a strategy for managing VA levels during fermentation.

To address VA concerns in high sugar wines, this research sought to achieve three objectives: (1) to use appassimeto-type must and table wine must to evaluate differences in the produced yeast metabolites involved in the stress response leading to acetic acid and ethyl acetate formation; (2) to evaluate differences in metabolites produced between two wine yeast strains, commercial *S. cerevisiae* EC-1118 and a natural isolate of *S. bayanus*, in appassimento-type must containing high starting concentrations of acetaldehyde and acetic acid; (3) and to assess the ability of *S. bayanus* to ferment wine using the appassimento process. To achieve these objectives, we followed the time course of glycerol, acetaldehyde, ethanol, acetic acid and ethyl acetate produced in wines during the fermentation of appassimento-type must and compared these profiles with that found in yeast fermenting table wine must. Along with the metabolomics, the overall production of each metabolite was also compared between strains fermenting under high and low sugar stress to ascertain differences in the concentrations generated during fermentation.

## 2.3. Materials and Methods

**2.3.1. Yeast strains.** Two yeast strains were used in this study for wine fermentations: the commercial yeast *S. cerevisiae* strain EC-1118 was supplied by Lallemand Inc. (Montreal, QC, Canada) and the natural yeast strain *S. bayanus* was isolated from Brock University from the bloom of Riesling Icewine grapes (St. Catharines, ON, Canada).

**2.3.2. Grape musts.** To investigate the impact of hyperosmotic stress on wine yeast, appassimento-type must was produced from *V. vinifera* L.cv. Cabernet franc grapes harvested at Cherry Avenue Research Station (Vineland, ON, Canada) and dried using a modern tobacco kiln at Reif Estate Winery (Niagara-on-the-Lake, ON, Canada). Two fermentation conditions were investigated using the control and dried grapes: table wine must at 18°Brix (179 ± 5 g $l^{-1}$) and appassimento-type must at 27°Brix (244 ± 19 g $l^{-1}$).

**2.3.3. Grape harvesting and withering.** Grape clusters from the Cherry Avenue vineyard were harvested in the 2011 season at a soluble solids content of 18°Brix. Five-hundred and seventeen kilograms were handpicked, with any diseased fruit culled after inspection, and placed in plastic, perforated drying containers in a single layer. After picking, the grapes were divided into two lots. One lot (207 kg) was taken to the Cool Climate Oenology and Viticulture Institute (CCOVI) to be processed and used for wine production (Teaching Winery, Brock University). Upon arrival at CCOVI, the grapes were stored at room temperature overnight to allow them to warm, and were processed the following day. The remaining lot (310 kg) was placed inside a tobacco kiln with control of temperature and relative humidity (RH). The starting temperature and RH of the kiln were recorded as 20.9°C and 64.8%, respectively, as determined by a data logger, and appeared to fluctuate throughout the drying period, averaging values of 32.1°C and 26.6%, respectively. Grapes

were sampled every day during the drying period. At each sampling time, 15 clusters were selected at random from trays arranged in the tobacco kiln. On receipt of the samples, 7 berries per cluster were randomly selected, removed from the rachis and weighed for berry weight determination. The extra berries were manually crushed inside the bag and filtered using a metal strainer. The grape juice obtained was immediately subjected to chemical analysis of soluble solids, titratable acidity and pH. The remaining juice samples for analysis of glucose, fructose, glycerol, acetaldehyde, ethanol, acetic acid and ethyl acetate were centrifuged at 10 000 rpm for 5 min at 4°C (Sorvall RC5C Plus, rotor model SLA-1500; Newtown, CT, USA) to remove microorganisms and grape particulate matter. The supernatant was recovered and a 5 $ml^{-1}$ sample was removed and centrifuged at 12 000 rpm for 4 min at room temperature using a microcentrifuge (Sorvall MC12). Samples were decanted and supernatants were stored at -30°C until analyzed. After 114 hours of drying (over 5 days) the grapes reached 27°Brix and were ready for vinification and removed from the kiln for processing.

**2.3.4. Chemical analyses of initial juices.** Soluble solids of the starting unfermented juices were determined using an ABBE bench top refractometer (Model 10450, American Optical). Reducing sugar content was determined using the commercial enzyme assay kit for glucose and fructose (K-FRUGL) according to the manufacturer's instructions (Megazyme International Ireland, Ltd.; Bray Co., Wicklow, IRE). Juice acidity was determined by measuring pH using a Corning pH meter (model 455) first calibrated to pH 4.0, pH 7.0 and pH 10.0, and titratable acidity by titration with 0.1 N NaOH to an endpoint of pH 8.2 (Zoecklein *et al*. 1996). Ammonia and amino nitrogen levels were assayed by

the enzymatic method (K-AMIAR and K-PANOPA, Megazyme).Yeast assimilable nitrogen content (YANC) was the sum of the two concentrations.

**2.3.5. Must fermentation and sampling:** A total of four fermentation treatments were studied in this experiment, with each performed in triplicate. These included: wine produced from fruit harvested at approximately 18°Brix and inoculated with EC-1118 (1) and *S. bayanus* (2); and fruit harvested at approximately 18°Brix and kiln-dried to approximately 27°Brix and inoculated with EC-1118 (3) and *S. bayanus* (4). Before processing, control and semi-dried grapes were divided randomly and equally into three replicates based on weight (25 kg grapes/ replicate), and each replicate was processed separately through the crusher/destemmer. Musts were aliquoted into plastic pails (30 l), blanketed with carbon dioxide, sealed with a plastic lid and stored at 22°C to increase the temperature prior to yeast inoculation. To the starting musts, 0.75 g $l^{-1}$ of DAP was added prior to inoculation, and on day 3 of fermentation 0.25 g $l^{-1}$ was added, totalling 1 g $l^{-1}$.

**2.3.6. Yeast inoculation procedure for fermentations.** Five grams of active freeze dried wine yeast (*S. cerevisiae* EC-1118) were rehydrated in 50 ml of sterile, 40°C water (RiOs-16; Millipore, Etobicoke, ON, Canada) for 15 minutes, gently swirling every 5 minutes to encourage aeration. Thirty microlitres of the EC-1118 starter culture and frozen (-80°C) working cell bank of *S. bayanus* were subsequently plated on YPD media (1% yeast extract, 2% peptone, 2% dextrose, 2% agar) and incubated in a growth chamber at 30°C before use in the fermentations. Yeast starter cultures were prepared using a step-wise acclimatization method outlined by Kontkanen *et al*. (2004). For the appassimento fermentations, juice required for the starter cultures was clarified prior to use via racking and centrifugation at 10 000 rpm for 5 min at 4°C (Sorvall RC5C Plus, rotor model SLA-

1500). To prepare the growth media to build up the starter cultures, Cabernet franc table wine juice was first diluted from 18°Brix to 10°Brix with sterile, distilled water (RiOs-16, Millipore) and 2 g $l^{-1}$ of diammonium phosphate (DAP) was added to 450 ml of the dilute juice. Using a sterile wire loop, a loop-full of each yeast strain was inoculated from the YPD plate into the respective growth medium. These cultures were grown aerobically at 25°C with shaking at 130 rpm in a temperature controlled orbital shaker (Weiss Gallenkamp) until the total cell concentration reached 2 x $10^8$ cells $ml^{-1}$, as determined using a haemocytometer counting chamber, light microscope (40x magnification) and methylene blue indicator. The three starter cultures of each strain were combined in a 2 l Erlenmeyer flask, gently swirled to homogenize the sample, and aliquoted into new, sterile flasks. To acclimatize the yeasts to the two growth mediums, an equal volume of 18°Brix juice was added to each culture. The starter cultures were incubated at 25°C in a water bath for 1 h, swirling gently every 30 min. For the controls, a 900 ml starter culture was used to inoculate 18.75 l of each replicate to achieve a total cell concentration of 4.78 x $10^6$ cells $ml^{-1}$ and inoculum rate of 0.35 g $l^{-1}$, in a final volume of approximately 19.65 l. To acclimatize the remaining cultures to the high Brix juice, an equal volume of appassimento juice was added to each starter culture. The cultures were held at 20°C for 2 h, swirling gently every 30 min. A 800 ml starter culture was then used to inoculate 11 l of appassimento must to achieve a total cell concentration of 4.8 x $10^6$ cells $ml^{-1}$ and an inoculum rate of 0.35 g $l^{-1}$ in a final volume of 11.80 l. After inoculation, the culture and skins were mixed back into the juice using a punch-down tool to initiate fermentation.

**2.3.7. Experimental winemaking and fermentation monitoring.** Fermentations were carried out in a temperature controlled room at 22°C and were monitored by sugar

consumption. The fermentations continued to dryness (less than 3 g $l^{-1}$ reducing sugar, as determined by the FOSS WineScan™; Hillerød, Denmark) or until the yeast stopped consuming sugar, as determined by no further change in sugar concentration for three days. When all fermentations were complete, individual replicates from each treatment were pressed using a pneumatic bladder press that applied a constant pressure up to 1 bar for 2 minutes, allowing consistent pressing. Wines had 50 ppm $SO_2$ added before being settled at room temperature, racked, and cold stored at -2°C. Sampling of the fermentations occurred daily after mixing to ensure homogeneity, which was performed by moving the punch-down disc up and down. During the fermentation course, replicates received two sets of plunges per day. Beginning the morning after yeast inoculation, replicates received 20 plunges per set, and as the fermentation progressed, plunging replicates were reduced and did not exceed 4 per set by the end of fermentation. The punch-down tool was washed with water and sprayed with 70% ethanol and wiped down before and after mixing to prevent contamination. After mixing, a 60 ml sample from each replicate was removed and immediately assessed for soluble solids, temperature, and yeast cell concentration. Soluble solids were measured using a degree Brix hydrometer, temperature was determined using a thermometer labeled in degree Celsius, and viable cell concentrations were monitored by CFU counts on YPD agar after appropriate dilutions. The remaining samples were centrifuged at 10 000 rpm for 5 min at 4°C (Sorvall RC5C Plus, rotor model SLA-1500) to remove fermenting yeast cells and grape particulate matter. Samples (5 ml) for metabolite analysis were removed from the supernatant and centrifuged again at 12 000 rpm for 4 min at room temperature using a microcentrifuge (Sorvall MC12), and subsequently stored in sterile Eppendorf tubes at -30°C until analyzed. Enzymatic UV test

kits for determination of glucose, fructose, glycerol, acetaldehyde, ethanol and acetic acid by an enzymatic reaction and spectrophotometric quantification were supplied by Megazyme (K-FRUGL, K-GCROL, K-ACHD, K-ETOH, K-ACET). Ethyl acetate was evaluated by gas chromatography against an ethyl acetate standard curve using a Hewlett-Packard 6890 series gas chromatograph (Agilent Technologies Inc.; Palo Alto, CA, USA). The GC was equipped with a flame ionization detector (FID), split/split-less injector, and Chemstation software. Separations were carried out with a DB®-WAX (30 m, 0.25 mm, 0.25 µm) GC column (122-7032 model; Agilent) with helium as the carrier gas at a flow rate of 1.5 ml $min^{-1}$. Samples were not diluted and contained 5% 4-methyl-2-pentanol as the internal standard. All juice and wine measurements were tested in duplicate. In all treatments, yeast strains were evaluated for their generation of each metabolite, which was determined by subtracting the metabolite concentration measured on day 0 of fermentation (the day of inoculation) from the level determined on the final day of fermentation. The resulting value was used to calculate the normalized production of each metabolite, which was determined by dividing the amount of metabolite produced by the grams of sugar consumed by the respective yeast strain during the fermentation course. The final concentration of each metabolite was also determined by measuring the amount present in the resulting wines after pressing.

**2.3.8. Statistical analysis.** Differences between variables were determined by XLSTAT statistical software package released by Addinsoft (Version 7.1; New York, NY). Statistical methods used were analysis of variance (ANOVA) with mean separation by Fisher's Least Significant Difference (LSD) test ($p < 0.05$).

## 2.4. Results

**2.4.1. Initial appassimento-type must.** The chemical compositions of Cabernet franc musts, 18˚Brix and 27˚Brix, are given in Table 2.1. As a consequence of the drying process, the non-sterile appassimento-type juice had higher starting concentrations of glycerol, acetaldehyde and acetic acid compared to the table wine must, and a lower ethanol concentration, while the ethyl acetate content was not detectable in both. In addition to concentrating grape sugars, thereby increasing the glucose and fructose content in the berries, the concentration of titratable acids was also higher in the 27°Brix musts, as was the pH. By comparison, the total assimilable nitrogen (N) content to support yeast growth was low, hence the necessity to supplement the musts with DAP. As an entirety, the high concentration of fermentable sugars, high titratable acidity and low pH in the starting must created a stressful environment for yeast growth and fermentation as demonstrated by their slower sugar utilization and prolonged fermentation times.

**Table 2.1:** Chemical composition of Cabernet franc musts prior to fermentation (mean ± SD).

| | 18°Brix | 27°Brix |
|---|---|---|
| Soluble solids (°Brix) | 18.4 ± 0.1 | 27.2 ± 0.1 |
| Glucose + fructose (g $l^{-1}$) | 179 ± 5 | 244 ± 19 |
| Titratable acidity (g $l^{-1}$) | 6.69 ± 0.22 | 7.18 ± 0.20 |
| pH | 3.25 ± 0.02 | 3.54 ± 0.02 |
| ◆Free amino acid nitrogen (mg N $l^{-1}$) | 26 ± 2 | 46 ± 1 |
| Ammonia nitrogen (mg N $l^{-1}$) | 5 ± 4 | 6 ± 1 |
| Glycerol (g $l^{-1}$) | 0.21 ± 0.03 | 0.25 ± 0.02 |
| Acetaldehyde (mg $l^{-1}$) | 4.8 ± 1.0 | 11.7 ± 0.0 |
| Ethanol (% v/v) | 0.2 ± 0.0 | 0.1 ± 0.0 |
| Acetic acid (g $l^{-1}$) | 0.01 ± 0.00 | 0.05 ± 0.00 |
| Ethyl acetate (mg $l^{-1}$) | *ND | *ND |

◆This measurement does not include proline.

*ND= Not detected.

**2.4.2. Fermentation kinetics.** Yeast fermenting the table wine must and appassimento-type must began to consume sugar almost immediately following inoculation, with consumption differences existing between the strains in each fermentation condition (Fig. 2.1A). In the high sugar ferments (27°Brix), all of the available fermentable sugars were consumed by EC-1118 after 291.5 hours (12 days), while only 1± 0 g $l^{-1}$ remained in the wines fermented by *S. bayanus* after 339.5 hours (14 days) (Fig. 2.1A and 2.1B). These results differ from the low sugar ferments (18°Brix), where the yeast exhibited a more rapid fermentation rate. Under these conditions, the fermentation lengths were shorter, lasting only 162 hours (7 days), and both EC-1118 and *S. bayanus* were able to consume all of the available fermentable sugars in this time (Fig. 2.1A and 2.1B). Although the strains took the same amount of time to complete fermentation, *S. bayanus* fermented the low sugar must more rapidly than EC-1118, consuming more grams of reducing sugar per liter of solution at any sampling hour (Fig. 2.1A). A similar result was observed in the high sugar condition, but the robustness of the *S. bayanus* strain appeared to diminish around 120 hours, allowing EC-1118 to complete the fermentation first.

As sugar concentration decreased during the fermentations, ethanol production increased (Fig. 2.2A). Of the two sugar conditions, higher levels of ethanol were produced in the 27°Brix ferments compared to the 18°Brix ferments as the starting musts had higher initial sugar concentrations and were fermented to dryness. Although the ethanol levels between sugar conditions differed significantly, there were no statistically significant differences between strains within each condition. For the amount of sugar consumed by EC-1118 and *S. bayanus* during fermentation, similar amounts of ethanol were produced in the two sugar conditions (Fig. 2.3). As expected, yeast strains fermenting appassimento-

type must took longer to complete the fermentation as this condition contained approximately 100 g $l^{-1}$ more reducing sugar compared to the table wine condition. Unexpectedly, however, yeast strains grew to higher peak cell concentrations in the 27°Brix condition compared to the 18°Brix condition, although the higher cell density was not enough to shorten the overall fermentation time (Fig. 2.4). Residual nitrogenous compounds were measured in all four treatments and found to be 19 ± 2 mg N $l^{-1}$ and 26 ± 7 mg N $l^{-1}$ in the table wines fermented by EC-1118 and *S. bayanus*, respectively, and 26 ± 1 mg N $l^{-1}$ and 45 ± 2 mg N $l^{-1}$ in the appassimento-style wines fermented by EC-1118 and *S. bayanus*, respectively (Appendix I, Table 1).

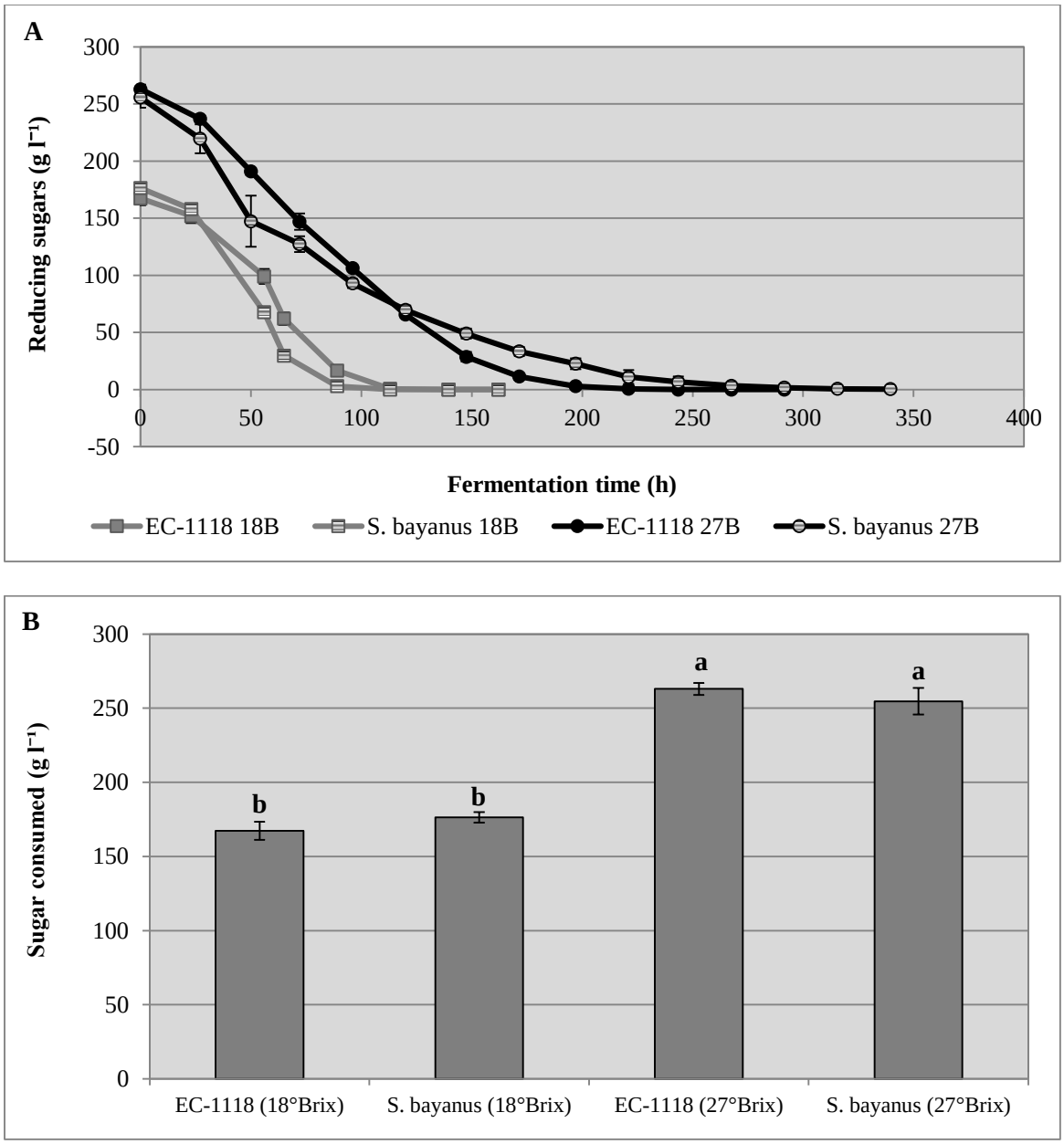


**Figure 2.1: Sugar consumption during fermentation of table wine must and appassimento-type must.** Sugar consumption was followed throughout the course of the fermentations (A), and the total sugar consumed was compared between yeast strains in high versus low sugar environments (B). Fermentations were performed in triplicate and samples from each treatment were analyzed in duplicate, for an n = 6 for each measurement. The mean values (± SD) of the triplicate fermentations are shown; where the error bars are not visible, they are within the symbol. Treatments were compared to each other and analyzed statistically using analysis of variance (ANOVA) with mean separation by Fisher's Least Significant Difference (LSD) test ($p < 0.05$). In descending order, lowercase letters indicate a unique group based on statistical difference using Fisher's $LSD_{0.05}$.

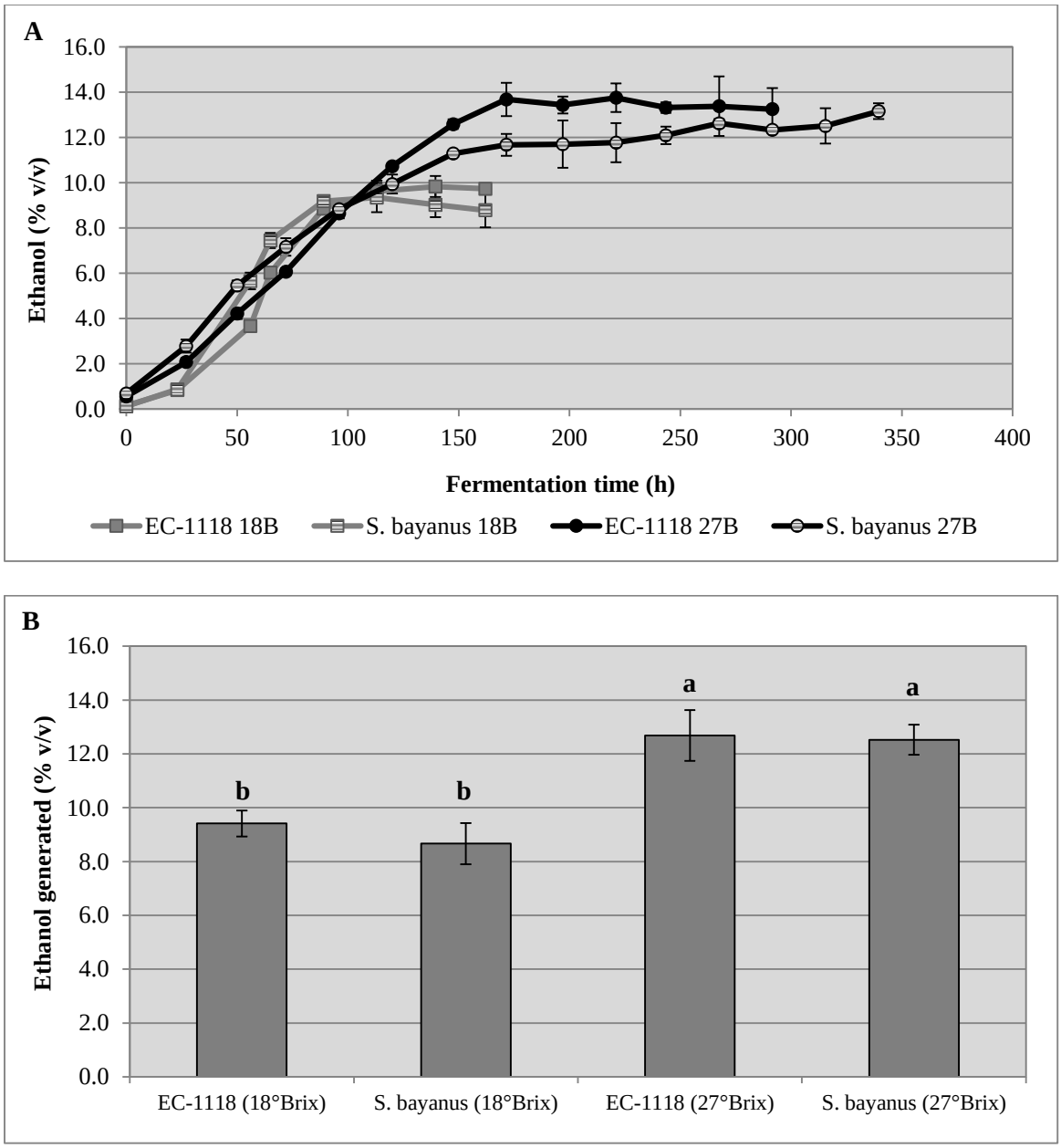


**Figure 2.2: Ethanol production during fermentation of table wine must and appassimento-type must.** Ethanol was measured throughout the course of the fermentations (A) and the total ethanol production was compared between yeast strains in high versus low sugar environments (B). Metabolite production was determined by substracting the concentration measured on day 0 of fermentation (inoculation day) from the level determined on the final day of fermentation. Fermentations were performed in triplicate and samples from each treatment were analyzed in duplicate, for an n = 6 for each measurement. The mean values (± SD) of the triplicate fermentations are shown; where the error bars are not visible, they are within the symbol. Treatments were compared to each other and analyzed statistically using analysis of variance (ANOVA) with mean separation by Fisher's Least Significant Difference (LSD) test ($p < 0.05$). In descending order, lowercase letters indicate a unique group based on statistical difference using Fisher's $LSD_{0.05}$.

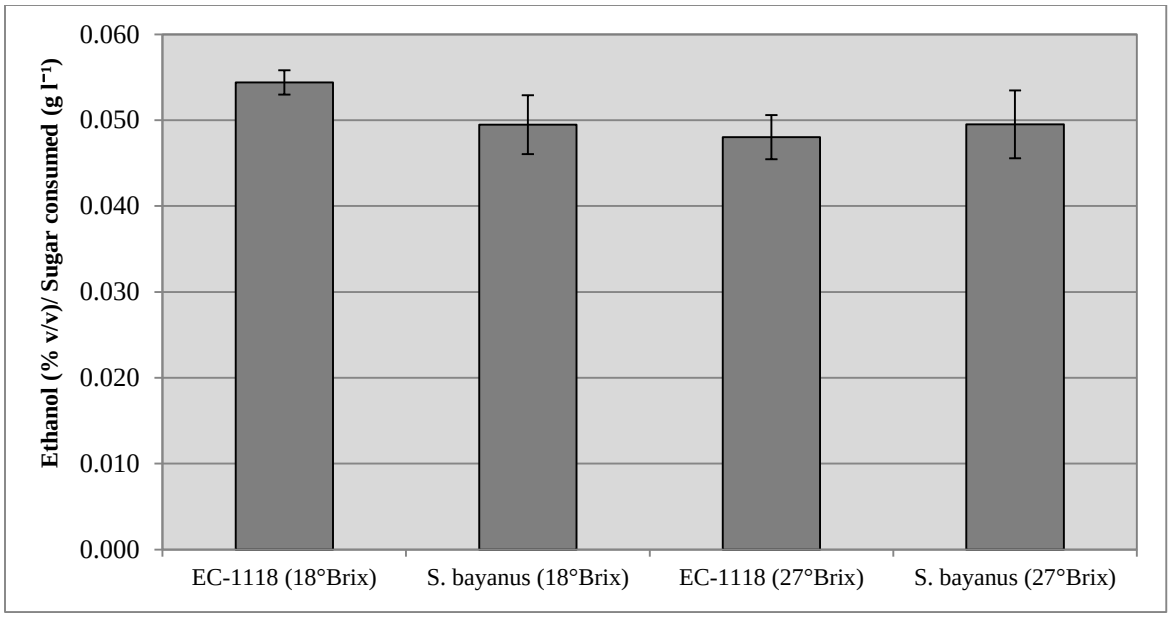


**Figure 2.3: Ethanol produced/ sugar consumed during fermentation of table wine must and appassimento-type must.** Total ethanol production was normalized to the amount of sugar consumed during the course of the fermentations, and compared between yeast strains. Fermentations were performed in triplicate and samples from each treatment were analyzed in duplicate (n = 6). Ethanol values represent the average ± standard deviation of the mean from duplicate fermentations. The statistical method used was analysis of variance (ANOVA).

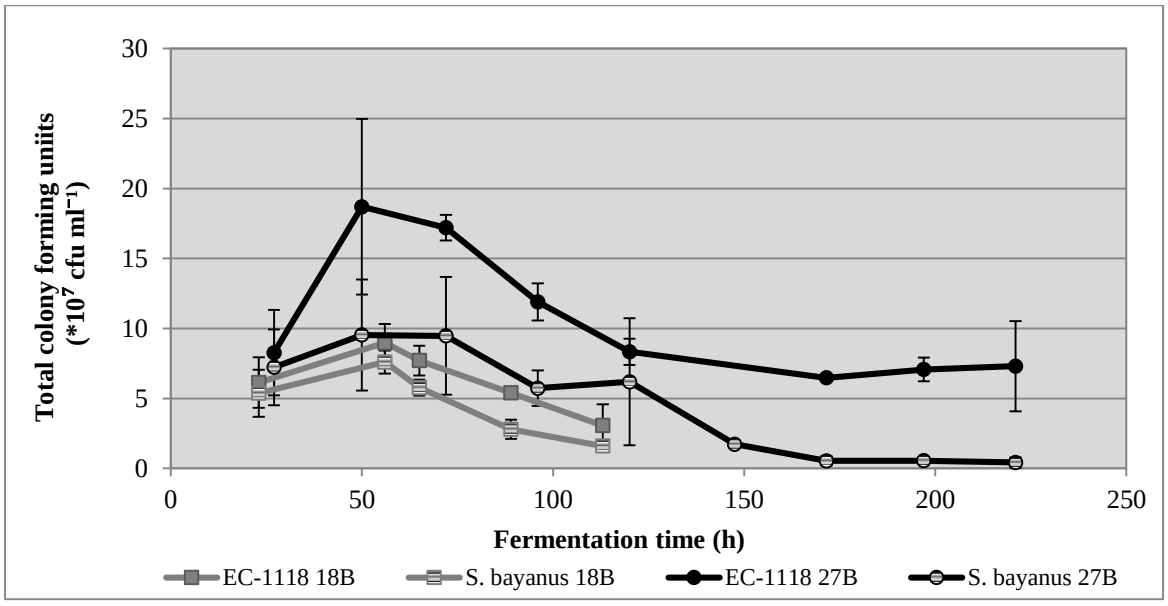


**Figure 2.4: Total colony forming units during fermentation.** Total colony forming units were measured throughout the course of the fermentations. Fermentations were performed in triplicate and samples were tested in singlet (n = 3). The mean values (± SD) of the triplicate fermentations are shown; where the error bars are not visible, they are within the symbol.

### 2.4.3. Acetic acid production

Acetic acid production differed between strains in the two fermentation conditions. In both the 18°Brix and 27°Brix musts, acetic acid was produced in significantly higher concentrations during the fermentation by EC-1118 compared to *S. bayanus*. In the 18°Brix ferments, acetic acid concentrations increased during the first 23-56 hours of fermentation, after which levels proceeded to decrease once the peak concentration was reached (Fig. 2.5A). As sugar consumption continued, acetic acid levels fluctuated slightly and gradually increased towards the end of fermentation from the minimum concentration that was achieved. In the 27°Brix ferments, starting levels of acetic acid at time zero were 5.7 times higher than those observed in the low sugar treatments. During fermentation, acetic acid levels decreased from the high starting concentrations after which levels increased and remained relatively constant as sugar consumption continued.

With respect to yeast strain, fermentations by *S. bayanus* in the 18°Brix and 27°Brix musts displayed the lowest acetic acid production during the process and in the final wine, followed by EC-1118 in the low and high sugar conditions, respectively (Fig. 2.5B). As yeast fermenting the two sugar conditions consumed different amounts of sugar, and yeast metabolites are by-products of sugar consumption, the acetic acid produced was normalized to the grams of sugar consumed and compared between strains in each condition. Similar to the unnormalized data, *S. bayanus* produced significantly lower levels of acetic acid in both the 18°Brix and 27°Brix conditions compared to EC-1118 fermenting under the same sugar conditions (Fig. 2.6).

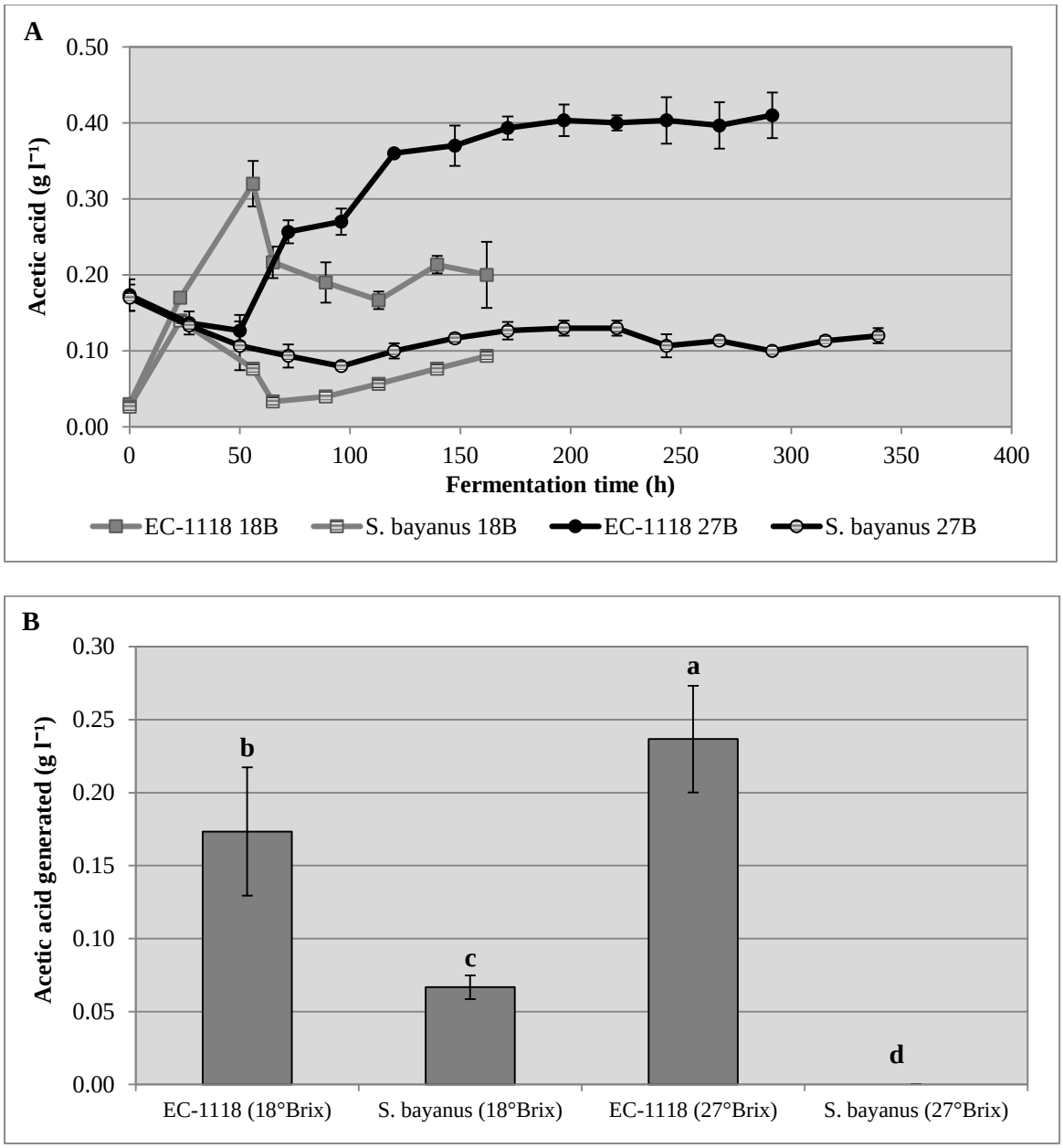


**Figure 2.5: Acetic acid production during fermentation of table wine must and appassimento-type must.** Acetic acid was measured throughout the course of the fermentations (A), and the total acetic acid production was compared between yeast strains in high versus low sugar environments (B). Metabolite production was determined by substracting the concentration measured on day 0 of fermentation (inoculation day) from the level determined on the final day of fermentation. Fermentations were performed in triplicate and samples from each treatment were analyzed in duplicate, for an n = 6 for each measurement. The mean values (± SD) of the triplicate fermentations are shown; where the error bars are not visible, they are within the symbol. Treatments were compared to each other and analyzed statistically using analysis of variance (ANOVA) with mean separation by Fisher's Least Significant Difference (LSD) test ($p < 0.05$). In descending order, lowercase letters indicate a unique group based on statistical difference using Fisher's $LSD_{0.05}$.

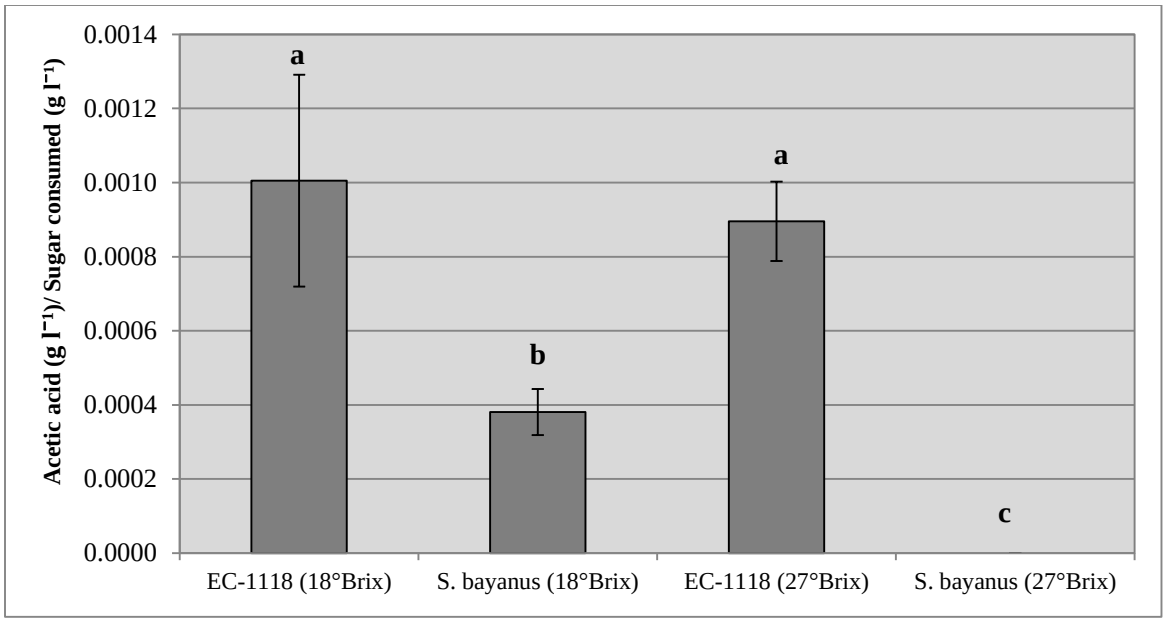


**Figure 2.6: Acetic acid produced/ sugar consumed during fermentation of table wine must and appassimento-type must.** Total acetic acid production was normalized to the amount of sugar consumed during the course of the fermentations, and compared between yeast strains. Fermentations were performed in triplicate and samples from each treatment were analyzed in duplicate, for an n = 6 for each measurement. The mean values (± SD) of the triplicate fermentations are shown. Treatments were compared to each other and analyzed statistically using analysis of variance (ANOVA) with mean separation by Fisher's Least Significant Difference (LSD) test ($p < 0.05$). In descending order, lowercase letters indicate a unique group based on statistical difference using Fisher's $LSD_{0.05}$.

.

### 2.4.4. Ethyl acetate production

Ethyl acetate production differed between strains in the two fermentation conditions. As a general trend in most treatments, ethyl acetate production increased to a peak concentration after which levels subsequently decreased as sugar consumption continued (Fig. 2.7A). However, in the 27°Brix must fermented by *S. bayanus*, ethyl acetate accumulation continued to increase slowly throughout the fermentation course, reaching its peak concentration by only the final day of fermentation. Higher peak ethyl acetate levels were obtained in the low sugar musts fermented by *S. bayanus* and EC-1118. In the 18°Brix condition specifically, peak ethyl acetate production was 9.0-times higher in the fermentation by *S. bayanus* and 3.7-times higher in the fermentation by EC-1118 compared to the same strains fermenting in the 27°Brix condition.

With respect to yeast strain, fermentation by *S. bayanus* in the 27°Brix must displayed the lowest ethyl acetate production during the fermentation course and in the final wine, followed by EC-1118 in the 27°Brix must, and *S. bayanus* and EC-1118, respectively, in the 18°Brix must (Fig. 2.7B). Since ethyl acetate is a by-product of sugar consumption, the ethyl acetate produced was normalized to the grams of sugar consumed and compared between yeast strains in each fermentation condition. Similar to the unnormalized data, *S. bayanus* tended to produce lower levels of ethyl acetate in both the 18°Brix must and 27°Brix must compared to EC-1118 fermenting under the same sugar conditions (Fig. 2.8).

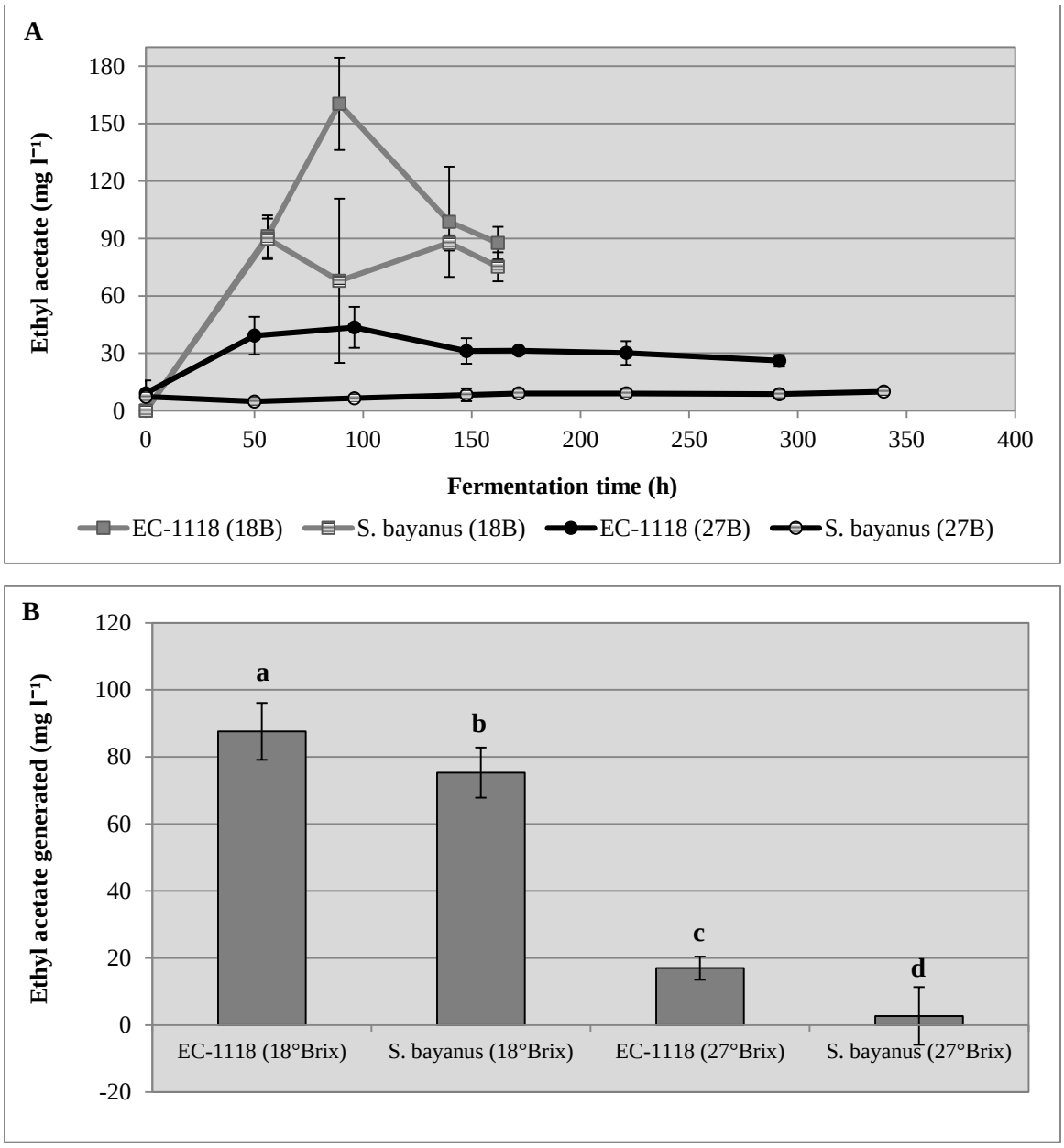


**Figure 2.7: Ethyl acetate production during fermentation of table wine must and appassimento-type must.** Ethyl acetate was measured throughout the course of the fermentations (A), and the total ethyl acetate production was compared between yeast strains in high versus low sugar environments (B). Metabolite production was determined by substracting the concentration measured on day 0 of fermentation (inoculation day) from the level determined on the final day of fermentation. Fermentations were performed in triplicate and samples from each treatment were analyzed in duplicate, for an n= 6 for each measurement. The mean values (± SD) of the triplicate fermentations are shown; where the error bars are not visible, they are within the symbol. Treatments were compared to each other and analyzed statistically using analysis of variance (ANOVA) with mean separation by Fisher's Least Significant Difference (LSD) test ($p < 0.05$). In descending order, lowercase letters indicate a unique group based on statistical difference using Fisher's $LSD_{0.05}$.

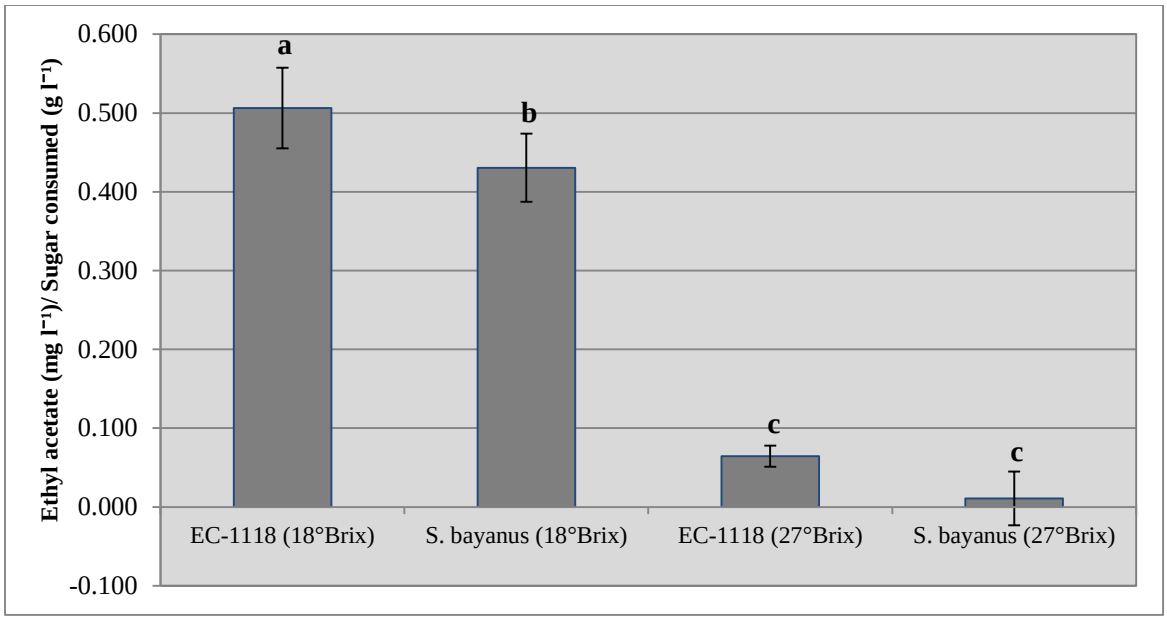


**Figure 2.8: Ethyl acetate produced/ sugar consumed during fermentation of table wine must and appassimento-type must.** Total ethyl acetate production was normalized to the amount of sugar consumed during the course of the fermentations, and compared between yeast strains. Fermentations were performed in triplicate and samples from each treatment were analyzed in duplicate, for an n= 6 for each measurement. The mean values (± SD) of the triplicate fermentations are shown. Treatments were compared to each other and analyzed statistically using analysis of variance (ANOVA) with mean separation by Fisher's Least Significant Difference (LSD) test ($p < 0.05$). In descending order, lowercase letters indicate a unique group based on statistical difference using Fisher's $LSD_{0.05}$.

### 2.4.5. Metabolomics analysis towards understanding acetic acid and ethyl acetate formation

#### 2.4.5.1. *S. cerevisiae* EC-1118 fermenting under high and low sugar stress

Ethyl acetate production was compared amongst yeast strains in high versus low sugar environments to determine its relationship to the stress response of wine yeast to high sugar conditions (Fig. 2.7B). Lower levels of ethyl acetate were produced by both yeast strains fermenting the 27˚Brix must compared to the 18˚Brix must.

The kinetics of metabolite formation during fermentation in the high and low sugar conditions were compared within yeast strains strains to understand the factors contributing to acetic acid and ethyl acetate production (Fig 2.9). In brief, 27˚Brix must fermented by EC-1118 formed higher levels of glycerol, acetaldehyde, ethanol and acetic acid during the fermentation course, and lower levels of ethyl acetate compared to EC-1118 fermenting the 18˚Brix must (Fig. 2.9). In both conditions, an initial increase in glycerol concentration was followed by a plateau, resulting in final levels 1.6-times higher in the 27˚Brix condition ($12.14 \pm 0.34$ g $l^{-1}$) compared to the 18˚Brix condition ($7.79 \pm 0.22$ g $l^{-1}$).

As glycerol continued to form, acetaldehyde was also produced as one of the early metabolic by-products of fermentation. Acetaldehyde production occurred between 0 and 89 hours of fermentation in the low sugar must, and between 0 to 50 hours in the high sugar must. Peak acetaldehyde levels were determined to be the highest in the 27˚Brix condition, measuring $90.6 \pm 5.1$ mg $l^{-1}$. Concentrations in both sugar conditions eventually decreased and then plateaued, resulting in levels 1.7-times higher in the appassimento-style wine ($81.9 \pm 8.9$ mg $l^{-1}$) compared to the table wine ($48.8 \pm 4.0$ mg $l^{-1}$).

At the same time as acetaldehyde levels were decreasing, an increase in ethanol, acetic acid, and ethyl acetate occurred in both fermentations. Ethanol was produced more rapidly in the table wine must condition in comparison to the appassimento-type must condition, although a higher production level was measured in the latter (Fig. 2.2B). As yeast fermenting the two sugar conditions consumed different amounts of sugar and yeast metabolites are by-products of sugar consumption, ethanol production was normalized to the grams of sugar consumed. For the amount of sugar consumed by EC-1118 in each fermentation condition, ethanol production was not significantly different (Fig 2.3).

As ethanol continued to increase, acetic acid was simultaneously produced. In the 18˚Brix must, acetic acid reached its peak concentration within 56 hours of fermentation ($0.32 \pm 0.03$ g $l^{-1}$), after which levels decreased and fluctuated between concentrations of $0.19 \pm 0.03$ g $l^{-1}$ and $0.21 \pm 0.01$ g $l^{-1}$ as sugar consumption continued. In contrast, in the 27˚Brix must, acetic acid levels initially decreased in the first 56 hours of fermentation, after which an increase was observed up until the final day of fermentation when a peak concentration of $0.41 \pm 0.03$ g $l^{-1}$ was determined in the wine. By the end of fermentation, acetic acid production was 2.1-times higher in the 27˚Brix condition ($0.41 \pm 0.03$ g $l^{-1}$) compared to the 18˚Brix condition ($0.20 \pm 0.04$ g $l^{-1}$).

Ethyl acetate production was also found to differ between the two sugar conditions. In contrast to ethanol and acetic acid production, ethyl acetate formed to a much lower level during fermentation in the 27˚Brix must versus the 18˚Brix must, although production trends were similar. Ethyl acetate production was 5.2-times lower in the 27˚Brix condition in comparison to the 18˚Brix condition, resulting in $26 \pm 3$ mg $l^{-1}$ and $88 \pm 9$ mg $l^{-1}$, respectively, on the final day of fermentation.

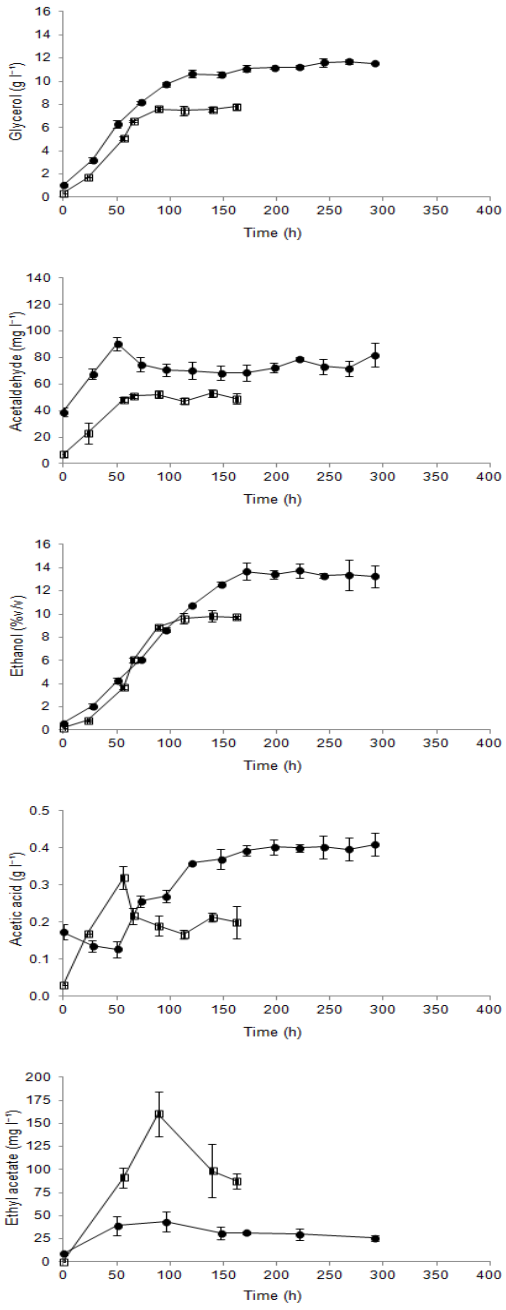


**Figure 2.9: Metabolite production during fermentation by *S. cerevisiae* EC-1118.** Fermentations of appassimento-type must (●) and table wine must (□) were monitored for (a) glycerol, (b) acetaldehyde, (c) ethanol, (d) acetic acid and (e) ethyl acetate formation during fermentation, and compared between sugar conditions. Metabolite production was determined by substracting the concentration measured on day 0 of fermentation (inoculation day) from the level determined on the final day of fermentation. Fermentations were performed in triplicate and samples from each treatment were analyzed in duplicate, for an n = 6 for each measurement. The mean values (± SD) of the triplicate fermentations are shown; where the error bars are not visible, they are within the symbol.

### 2.4.5.2. *S. bayanus* fermenting under high and low sugar stress

Appassimento-type must fermented by *S. bayanus* formed higher levels of glycerol and ethanol during the course of the fermentation, and lower levels of acetaldehyde, acetic acid and ethyl acetate (Fig. 2.10) in comparison to table wine. In both fermentation conditions, an initial increase in glycerol was followed by a plateau, resulting in levels 1.6-times higher in the 27˚Brix condition (14.53 ± 0.16 g $l^{-1}$) compared to the 18˚Brix condition (9.33 ± 0.43 g $l^{-1}$) on the final day of fermentation.

As glycerol continued to form, acetaldehyde was also produced as one of the early metabolic by-products of fermentation. Acetaldehyde production occurred between 0 and 65 hours of fermentation in the low sugar must, and between 0 to 89 hours in the high sugar must. Peak levels were the highest in the 27˚Brix ferment, measuring 101.9 ± 1.0 mg $l^{-1}$. Acetaldehyde levels in both sugar conditions eventually decreased and then plateaued, resulting in levels 1.3-times higher in the appassimento-style wine (58.9 ± 3.7 mg $l^{-1}$) compared to the table wine (46.9 ± 0.9 mg $l^{-1}$).

At the same time as acetaldehyde levels were decreasing, an increase in ethanol and ethyl acetate production occurred in both fermentations. Ethanol was produced more rapidly in the 18˚Brix condition in comparison to the 27˚Brix condition, although a higher production level was measured in the latter (Fig. 2.2B). As yeast fermenting the two sugar conditions consumed different amounts of sugar and yeast metabolites are by-products of sugar consumption, ethanol production was normalized to the grams of sugar consumed. For the amount of sugar consumed by *S. bayanus* in each fermentation condition, ethanol production was not significantly different (Fig 2.3).

As ethanol concentration continued to increase, acetic acid was simultaneously produced. Acetic acid levels decreased from the high starting concentration measured at time zero in the 27˚Brix condition and then plateaued, while concentrations were observed to increase at the beginning of fermentation in the 18˚Brix must. In this condition, acetic acid reached its peak concentration within 23 hours of fermentation ($0.14 \pm 0.00$ g $l^{-1}$) after which levels decreased and then fluctuated between concentrations of $0.03 \pm 0.01$ g $l^{-1}$ and $0.09 \pm 0.01$ g $l^{-1}$ as sugar consumption continued. However, acetic acid levels were determined to be 1.3-times higher in the 27˚Brix must condition ($0.12 \pm 0.01$ g $l^{-1}$) compared to the 18˚Brix must ($0.09 \pm 0.01$ g $l^{-1}$) by the end of fermentation.

Ethyl acetate production was also found to differ between the two sugar conditions. Similar to the result determined for acetic acid production, ethyl acetate formed to a much lower level during fermentation in 27˚Brix must versus 18˚Brix must. Ethyl acetate production was 27.6-times lower in the 27˚Brix condition in comparison to the 18˚Brix condition, resulting in $10 \pm 1$ mg $l^{-1}$ and $75 \pm 3$ mg $l^{-1}$, respectively, measured on the final day of fermentation.

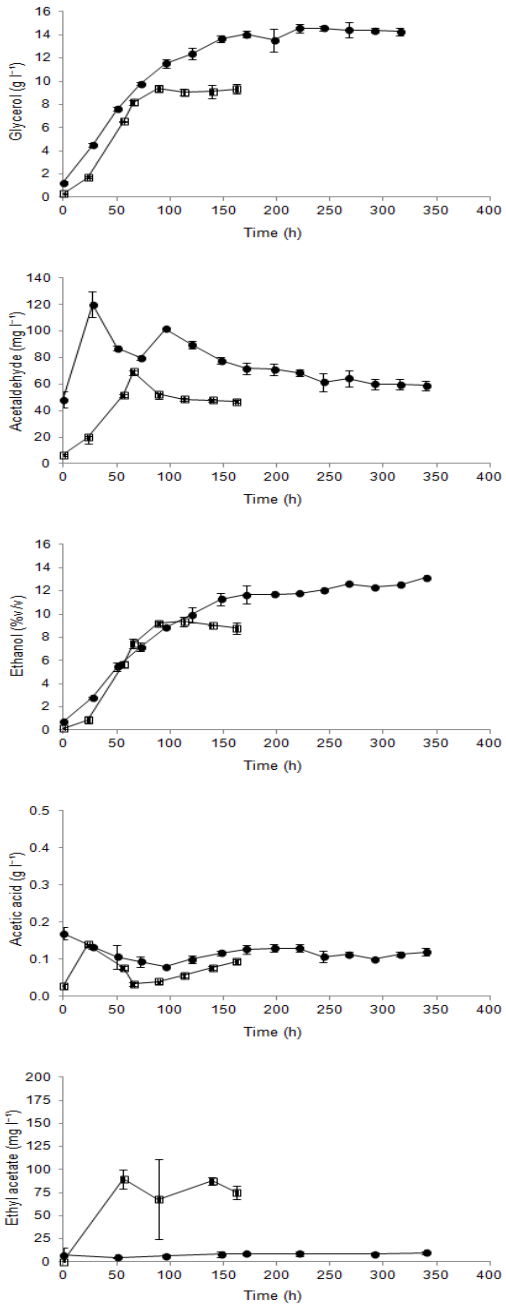


**Figure 2.10: Metabolite production during fermentation by *S. bayanus*.** Fermentations of appassimento-type must (●) and table wine must (□) were monitored for (a) glycerol, (b) acetaldehyde, (c) ethanol, (d) acetic acid and (e) ethyl acetate formation during fermentation, and compared between sugar conditions. Metabolite production was determined by substracting the concentration measured on day 0 of fermentation (inoculation day) from the level determined on the final day of fermentation. Fermentations were performed in triplicate and samples from each treatment were analyzed in duplicate, for an n = 6 for each measurement. The mean values (± SD) of the triplicate fermentations are shown; where the error bars are not visible, they are within the symbol.

## 2.5. Discussion

### 2.5.1. Understanding acetic acid and ethyl acetate formation during fermentation

In enzyme-catalyzed reactions, the amount of product can be controlled by substrate availability, the enzyme activity or a combination of both. Increased substrate availability or enzyme activity will increase the amount of product formed in the 27°Brix condition, while limited substrate availability or decreased enzyme activity will reduce the amount of product. In order to understand the factors controlling acetic acid and ethyl acetate formation during fermentation in high sugar grape must, such as that produced using an appassimento-type process, factors contributing to the production of these metabolites were measured and will be discussed.

### 2.5.2. Acetic acid production during fermentation

Higher levels of acetic acid were produced in the appassimento-style wine fermented by EC-1118 in comparison to the table wine. During the fermentation by *S. bayanus,* acetic acid levels also reached higher concentrations in the 27˚Brix condition compared to that in the 18˚Brix condition. However, lower levels of acetic acid were produced by the final day of the 27°Brix fermentation due to the high starting concentration measured at time zero in this condition and the low levels that formed as the fermentation progressed. The reason for elevated acetic acid production by wine yeast under hyperosmotic stress is still unresolved, but may be due to a combination of metabolic and transcriptional regulation, leading to a build-up of acetic acid due to a lack of further conversion to acetylCoA (Pigeau and Inglis 2005; 2007; Martin 2008).

From Figure 2.11, acetaldehyde can be reduced to ethanol by alcohol dehydrogenase or oxidized to acetic acid by aldehyde dehydrogenase. During fermentation

by EC-1118 in the high sugar must, elevated acetic acid may have resulted from (1) the higher substrate availability of acetaldehyde and/ or oxidized nicotinamide coenzymes ($NAD^+$, $NADP^+$), (2) the up-regulation of *ALD* genes encoding for aldehyde dehydrogenases, leading to increased enzyme activity of Aldp, or (3) the down-regulation of *ACS* genes encoding for acetylCoA synthetases, leading to decreased activity of Acsp.

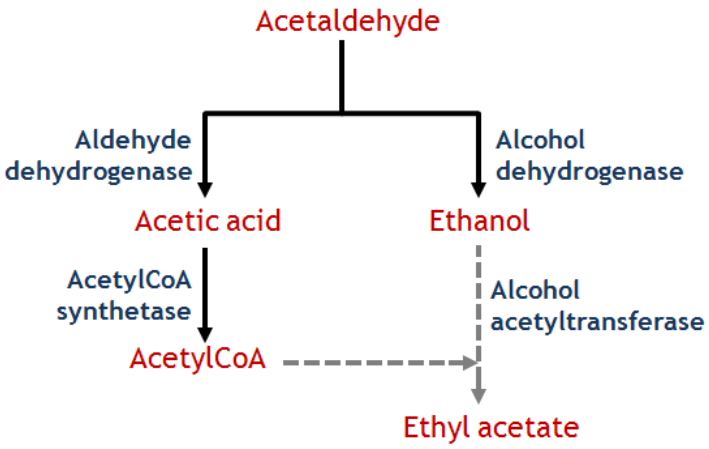


**Figure 2.11: Relationship of metabolites formed by *S. cerevisiae* during fermentation.**

Several studies investigating hyperosmotic stress in wine yeast have determined increased substrate availability for the aldehyde dehydrogenases during Icewine fermentation as acetaldehyde levels rapidly increased to a greater extent in Icewine juice compared to table wine juice (Pigeau and Inglis 2005; 2007; Martin 2008; Heit 2011; Heit and Inglis 2012). Increased acetaldehyde production preceeded *ALD3* expression, encoding a cytosolic $NAD^+$-dependent Aldp isoform. Pigeau and Inglis (2005; 2007) reported *ALD3* was the only *ALD* to be differentially up-regulated in Icewine over that found in table wine, which corresponded to a large fold increase in acetic acid production, and stimulated by acetaldehyde stress (Pigeau and Inglis 2007).

Furthermore, Martin (2008) determined two acetylCoA synthestaes, encoded by *ACS1* and *ACS2*, to be strongly down-regulated during fermentation in Icewine juice over that found in table wine juice, resulting in a 19-fold and 11-fold reduction in *ACS1* and *ACS2* expression, respectively. In addition, two-fold lower levels of ethyl acetate were determined in Icewine (60 mg $l^{-1}$) compared to that found in table wine (120 mg $l^{-1}$) (Heit 2011; Heit and Inglis 2012; 2013), whereby acetylCoA is required for esterification to ethanol by alcohol acetyltransferases in yeast-catalyzed ethyl acetate production (Fig. 2.11). Thus, lower ethyl acetate formation in appassimento-style wine by *S. cerevisiae* may be due to lower acetylCoA levels resulting from lower Acsp activity, which would reduce the amount of substrate available to alcohol acetyltransferases for catalysis.

In agreement with these findings, *S. cerevisiae* EC-1118 showed a 41.2% increase in acetic acid concentration in appassimento-style wine compared to table wine (Appendix 1, Table 1). Taken together, the increased expression of *ALD3* in conjunction with the down-regulation of *ACS* genes, as observed in the Icewine fermentation studies, may contribute to the elevated levels of acetic acid in appassimento-style wine. The increased gene expression of *ALD3* should increase the activity level of the corresponding enzyme, leading to increased conversion of acetaldehyde to acetic acid with the concomitant reduction of $NAD^+$ to NADH. On the other hand, the decreased gene expression of *ACS2* would reduce the activity level of Acs2p, resulting in a decrease in the transformation of acetic acid to acetylCoA and the accumulation of acetic acid.

### 2.5.3. Ethyl acetate production during fermentation

Lower levels of ethyl acetate were produced in appassimento-style wine in comparison to table wine. From Figure 2.11, ethyl acetate can be formed from the esterification of acetylCoA with ethanol by alcohol acetyltransferases. During the high sugar fermentations, lower levels of ethyl acetate may have formed as a consequence of (1) the decreased expression of *ACS* genes encoding for acetylCoA synthetases, leading to decreased enzyme activity of Acsp, (2) the lower substrate availability of acetylCoA and/ or ethanol in fermenting yeast cells, or (3) the decreased expression of *ATF* genes encoding for alcohol acetyltranferases, leading to decreased Atfp activity.

Martin (2008) showed a decrease in the expression levels of *ACS1* and *ACS2* during fermentation in Icewine juice. Under Icewine fermentation conditions, low *ACS2* expression in osmotically stressed cells may reduce the concentration of acetylCoA available to alcohol acetyltransferases for ethyl acetate formation as a result of its lack of conversion from acetate. When considering substrate availability further, ethanol production was significantly higher in strains fermenting under high sugar stress versus low sugar stress as the apasssimento-type must contained higher initial sugar concentrations as a result of the kiln-drying process and the yeasts fermented these wines to dryness. The higher ethanol levels in the resulting appassimento-style wines would, if anything, provide higher substrate availability for ethyl acetate formation, but lower ethyl acetate levels were determined. However, the ethanol obtained in the 27˚Brix ferments would unlikely be a limiting substrate contributing to low ethyl acetate formation in the appassimento-style wines because its concentration was so high. Likely, the limiting substrate was acetylCoA, although levels were not measured to verify this.

### 2.5.4. Strain differences in acetic acid and ethyl acetate production

Significantly lower levels of acetic acid and ethyl acetate were produced in appassimento-style wine fermented by *S. bayanus*. In comparison to *S. cerevisiae* EC-1118, *S. bayanus* displayed lower acetic acid and ethyl acetate production as a function of time (Appendix 1, Figure 8) and in the final wine (Appendix 1, Table 1). *S. bayanus* also displayed lower ratios of acetic acid and ethyl acetate production to sugar consumed, indicating that each metabolite was produced at different concentrations across the two strains when the same amount of sugar was consumed (Appendix 1, Table 3). Differences in acetic acid and ethyl acetate production between wine yeasts may be due to (1) substrate availability or (2) enzyme activity.

During alcoholic fermentation, acetic acid can form from the oxidation of acetaldehyde by aldehyde dehydrogenase, along with the concomitant reduction of $NAD(P)^+$ to NAD(P)H (Fig. 2.11). With respect to substrate availability for aldehyde dehydrogenase, yeast strains differed in the concentrations of acetaldehyde produced in the appassimento-style wines, with *S. bayanus* producing significantly lower levels in comparison to EC-1118. Thus, it is possible that the lower acetaldehyde levels produced by *S. bayanus* contributed to lower acetic acid formation during fermentation. At lower concentrations, less acetaldehyde would be available as a substrate for aldehyde dehydrogenase reducing the level of acetic acid formed. Yeast-catalyzed acetic acid biosynthesis is also influenced by $NAD(P)^+$ availability and aldehyde dehydrogenase activity, both of which at low levels would also reduce acetic acid formation. However, these variables were not measured to define their contributions to higher acetic acid formation by *S. cerevisiae* and lower acetic acid formation by *S. bayanus*.

As alcoholic fermentation progresses, acetylCoA can form from acetic acid via the pyruvate dehydrogenase bypass in a reaction catalyzed by acetylCoA synthetase (Fig. 2.11). In a subsequent reaction, acetylCoA can esterify with ethanol to form ethyl acetate in a reaction catalyzed by alcohol acetyltransferase. With respect to substrate availability, *S. bayanus* and *S. cerevisiae* strains differed in the concentrations of acetic acid produced. Of the two strains, *S. bayanus* displayed lower acetic acid production during the fermentation course and in the final wine compared to EC-1118. Although significant differences in acetic acid production existed between strains, no significant differences in ethanol concentration were determined. In addition, the ethanol obtained in the 27˚Brix ferments would unlikely be a limiting substrate contributing to lower ethyl acetate formation by *S. bayanus* because its concentration was high in all treatments. Likely, the limiting substrate was acetylCoA, but differences in its availability between strains were not measured to verify this. Although it is possible that the lower acetic acid produced by *S. bayanus* contributed to lower ethyl acetate formation, the activity levels of acetylCoA synthetases and alcohol acetyltransferases were also not measured, and therefore their contributions are unclear.

Furthermore, it is possible that *S. cerevisiae* and *S. bayanus* strans differed in their biosynthetic requirements for acetic acid and in its conversion to other metabolites. Viable cell concentrations differed between strains fermenting under increased osmotic stress as the EC-1118 ferment reached a higher peak cell concentration compared to that obtained in the *S. bayanus* ferment (Fig. 2.4). As a result of differences in viable cell density, yeast strains may have differed in their metabolic needs for various biosynthetic reactions, such as those involved in lipid and ergosterol synthesis, which require the input of acetylCoA,

as well as ester synthesis. A higher demand for acetylCoA to support yeast cell growth would increase acetic acid degradation, while also decreasing its availability for ethyl acetate formation. One of the aforementioned limitations of this study was that yeast strains were not evaluated for their metabolic production of acetylCoA. As a result, the kinetics of this metabolite could not be compared between wine yeasts to determine its contribution to acetic acid and ethyl acetate formation during fermentation in high sugar grape must.

Moreover, it is also possible that *S. cerevisiae* and *S. bayanus* strains differed in their hyperosmotic stress response to the high sugar environment. During fermentation in appassimento-type must, *S. bayanus* produced a higher concentration of glycerol in comparision to EC-1118, indicating that this strain may require more glycerol to act as a compatible solute for adaptation to the high osmotic stress, or that they have decreased ability to retain glycerol as an osmolyte in the cytoplasm upon hyperosmotic shock, hence the higher levels measured in the final wine (Erasmus *et al*. 2004).

However, the higher concentration of glycerol produced by *S. bayanus* did not result in a higher level of acetic acid when compared to the level produced by EC-11118. Under high osmolarity, higher acetic acid production would be expected as it has been implicated in NADH regeneration in response to glycerol overproduction by yeast fermenting under increased osmotic stress, possibly to compensate for the high levels of $NAD^+$ produced. The results obtained herein demonstrate that yeast strains fermenting under the same condition of osmotic pressure may respond differently to the stress, producing different concentrations of glycerol and acetic acid for cytosolic osmotic and redox balance, respectively. However, the higher glycerol and lower acetic acid levels produced by *S. bayanus* in comparison to EC-1118 in the 27°Brix ferments also suggest

that *S. bayanus* cells may not depend on acetic acid biosynthesis for NADH regeneration under high osmolarity, but instead rely on a different mechanism for maintaining redox balance within the $NAD^+$:NADH coenzyme system during adaptation to high sugar stress.

### 2.5.5. Application of *S. bayanus* to appassimento-style winemaking

Wine yeasts can produce acetic acid as a by-product of the hyperosmotic stress response resulting from high sugar concentrations in grape must. In the presence of ethanol, acetic acid can lead to the formation of ethyl acetate, another volatile compound that can further impact wine quality, often causing volatile acid levels to exceed legal limits (Erasmus *et al.* 2004). Prior to this study, strain differences in fermentation performance and metabolite formation between *S. cerevisiae* and *S. bayanus* strains had only been evaluated in Icewine (Heit 2011; Heit and Inglis 2013). These Icewine studies illustrated the effect of wine yeast on the production of high volatile acidity during Icewine fermentation and emphasized the importance of the choice of yeast strain. Although *S. bayanus* produced significantly less acetic acid per gram of sugar metabolized compared to *S. cerevisiae* K1-V1116 fermenting Icewine juice and demonstrated trends consistent with lower ethyl acetate production, it exhibited fermentation difficulties during Icewine fermentation (Heit 2011; Heit and Inglis 2013). The increased osmotic stress placed on *S. bayanus* negatively impacted cell growth and sugar consumption, as reflected in the longer lag phase at the start of fermentation, the lower cell population, the prolonged fermentation time, and the lower ethanol production, thereby making it a poorer fermenter in Icewine juice in comparison to *S. cerevisiae.*

In contrast to the Icewine studies, the results reported in this appassimento study demonstrated *S. cerevisiae* EC-1118 and *S. bayanus* to be similar in their kinetic behaviour

during fermentation. Between strains, sugar consumption and ethanol production levels were comparable, and fermentation lengths only differed by approximately two days, with *S. bayanus* lagging behind. However, *S. bayanus* produced significantly lower levels of acetic acid and ethyl acetate compared to *S. cerevisiae* fermenting appassimento-type must. Thus, the strong fermentation capability of *S. bayanus*, in combination with its low VA generation in response to increased osmotic stress, make it a suitable yeast strain for the production of appassimento-style wine and a possible candidate for commercialization, at least over the sugar concentration range tested in the 27°Brix condition. Future studies should target the optimal sugar concentration range over which *S. bayanus* is able to complete the fermentation and/ or to reach the desired ethanol level for the wine style.

## 2.6. Conclusions

This study investigated the different acetic acid and ethyl acetate production capacities of two wine yeasts fermenting under high and low sugar conditions. *S. cerevisiae* EC-1118 formed higher levels of acetic acid and lower levels of ethyl acetate in appassimento-style wine compared to table wine, while *S. bayanus* formed lower levels of both metabolites under increased sugar stress. Between strains, *S. bayanus* produced less acetic acid and ethyl acetate compared to EC-1118 in both fermentation conditions. In light of strain differences in metabolite formation, wine yeasts displayed appreciable capability to overcome osmotic stress and to yield ethanol fermenting the concentrated grape must. Between strains, sugar utilization and ethanol production levels were comparable as no significant differences were determined, although differences in viable cell concentration existed.

## 2.7. Literature Cited


Barbanti, D., B. Mora, R. Ferrarini, G.B. Torniella and M. Cipriani. 2008. Effect of various thermo-hygrometric conditions on the withering kinetics of grapes used from the production of "Amarone" and "Recioto" wines. J Food Eng. 85:350-358.

Bellincontro, A., D. De Santis, R. Botondi, I. Villa and F. Mencarelli. 2004. Different postharvest dehydration rates affect quality characteristics and volatile compounds of Malvasia, Trebbiano and Sangiovese grapes for wine production. J of the Sci Food Agr. 84:1791-1800.

Blomberg, A. and L. Alder. 1989. Roles of glycerol and glycerol-3-phosphate dehydrogenase ($NAD^+$) in acquired osmotolerance of *Saccharomyces cerevisiae*. J Bacteriol. 171:1087-1092.

Blomberg, A. 2000. Metabolic surprises in *Saccharomyces cerevisiae* during adaptation to saline conditions: questions, some answers, and a model. FEMS Microbiol Lett. 182:1-8.

Brewster, J.L., T. de Valoir, N.D. Dwyer, E. Winter and M.C. Gustin. 1993. An osmosensing signal transduction pathway in yeast. Science. 259:1760-1763.

Bro, C., B. Regenberg, G. Lagniel, J. Labarre, M. Montero-Lomeli and J. Nielsen. 2003. Transcriptional, proteonomic, and metabolic responses to lithium in galactose-grown yeast cells. J Biol Chem. 278:31141-32149.

Bruinenberg, P.M., J.P. van Dijken, and W.A. Scheffers. 1983. A theoretical analysis of NADPH production and consumption in yeasts. J. Gen Microbiol. 129:953-964.

Chkaiban, L., R. Botondi, A. Bellincontro, D. De Santis, P. Kefalas and F. Mencarelli. 2007. Influence of post-harvest water stress on lipoxygenase and alcohol dehydrogense activities, and on the composition of some volatile compounds in Gewürztraminer grapes dehydrated under controlled and uncontrolled thermohygrometric conditions. Aust J Grape Wine Res. 13:142-149.

Constantini, V., A. Bellicontro, D. De Santis, R. Botondi and F. Mencarelli. 2006. Metabolic changes of Malvasia grapes for wine production during postharvest drying. J Agric Food Chem. 54:3334-3340.

Erasmus, D.J., G.K. van der Merwe and H.J. van Vuuren. 2003. Genome-wide expression analyses: metabolic adaptation of *Saccharomyces cerevisiae* to high sugar stress. FEMS. 34:375-399.

Erasmus, D.J. and H.J.J. van Vuuren. 2009. Genetic basis for osmosensitivity and genetic instability of the wine yeast *Saccharomyces cerevisiae* V1N7. Am J Enol Vitic. 60:145-154.

Erasmus, D.J., M. Cliff and H.J.J. van Vuuren. 2004. Impact of yeast strain on the production of acetic acid, glycerol, and the sensory attributes of Icewine. Am J Enol Vitic. 55:371-378.

Hakimi Rezaei, J. and A.G. Reynolds. 2010. Characterization of Niagara peninsula Cabernet franc wines by sensory analysis. Am J Enol Vitic. 61:1-14.

Heit, C. and D. Inglis. 2013. Acetic acid and ethyl acetate production during high brix fermentations: effect of yeast strain. Am J Enol Vitic. 64:4.

Heit, C. and D. Inglis. 2012. An investigation of the relationship between ethyl acetate production and osmotics in *Saccharomyces cerevisiae* K1-V1116 during high brix fermentations. Am J Enol Vitic. 63:4.

Heit, C. 2011. Effect of yeast strain and sugar concentration on ethyl acetate production in Icewine juice. BSc Hons Thesis. Brock University, ON.

Hohmann, S. 2002. Osmotic stress signaling and osmoadaptation in yeasts. Microbiol Mol Biol Rev. 66:300-371.

Jackson, D.I. and P.B. Lombard. 1993. Environmental and management practices affecting grape composition and wine quality- a review. Am J Enol Vitic. 44:409-430.

Jones G.V. and E. Hellman. 2002. "Site assessment" in Oregon Viticulture. Edward Hellman, Editor, 5th Edition, OSU Press, 2002.

Kontkanen, D., D. Inglis, G. Pickering and A. Reynolds. 2004. Effect of yeast inoculation rate, acclimatization, and nutrient addition on Icewine fermentation. Am J Enol Vitic. 55:363-370.

López de Lerma, N. and R.A. Peinado. 2011. Use of two osmoethanol tolerant yeast strain to ferment from Tempranillo dried grapes: effect on wine composition. Int J Food Microbiol. 145:342-348.

Martin, S.J. and D. Inglis. 2006. Yeast osmoadaptive response during Icewine fermentation. Am J Enol Vitic. 57:527.

Martin, S.J. 2008. The osmoadaptive response of the wine yeast *S. cerevisiae* K1-V1116 during Icewine fermentation. PhD Thesis. Brock University, ON.

Meaden, P.G., F.M. Dickinson, A. Misfud, W. Tessier, J. Westwater, H. Bussey and M. Midgley. 1997. The *ALD6* gene of *Saccharomyces cerevisiae* encodes a cytosolic, $Mg^{2+}$-activated acetaldehyde dehydrogenase. Yeast. 13:1319-1327.

Mencarelli, F., A. Bellincontro, I. Nicoletti, M. Cirilli, R. Muleo and D. Corradini. 2010. Chemical and biochemical change of healthy phenolic fractions in winegrape by means of postharvest dehydration. J Agric Food Chem. 58:7557-7564.

Mollapour, M. and P.W. Piper. 2007. Hog1 mitogen-activated kinase phosphorylation targets the yeast Fps1 aquaglyceroporin for endocytosis, thereby rendering cells resistant to acetic acid. Mol Cell Biol. 27:6446-6456.

Moreno, J.J., F. Cerpa-Calderón, S.D. Cohen, Y. Fang, M. Qian and J.A. Kennedy. 2008. Effect of postharvest dehydration on the composition of Pinot noir grapes (*Vitis vinifera* L.) and wine. Food Chem. 1009:755-762.

Navarro-Avino, J.P., R. Prasad, V.J. Miralles, R.M. Benito and R. Serreno. 1999. A proposal of nomenclature of aldehyde dehydrogenases in *Saccharomyces cerevisiae* and characterization of the stress-inducible *ALD2* and *ALD3* genes. Yeast. 15:829-842.

Neviogt, E. and U. Stahl. 1997. Osmoregulation and glycerol metabolism in the yeast *Saccharomyces cerevisiae*. FEMS Microbiol Rev. 213:231-271.

Nordström, K. 1962. Formation of ethyl acetate in fermentation with brewer's yeast III: participation of coenzyme A. J Inst Brew. 68:398-407.

Nordström, K. 1963. Formation of ethyl acetate in fermentation with brewer's yeast IV: metabolism of acetyl coenzyme A. J Inst Brew. 69:142-153.

Påhlman, A.K., K. Granath, R. Ansell., S. Hohmann and L. Alder. 2001. The yeast glycerol 3-phosphatases Gpp1p and Gpp2p are required for glycerol biosynthesis and differentially involved in the cellular responses to osmotic, anaerobic, and oxidative stress. Biol Chem. 276:3555-3563.

Pigeau, G.M. and D.L. Inglis. 2007. Response of wine yeast (*Saccharomyces cerevisiae)* aldehyde dehydrogenase to acetaldehyde stress during Icewine fermentation. J Appl Microbiol. 103:1576-1586.

Pigeau, G.M. and D.L. Inglis. 2005. Upregulation of *ALD3* and *GPD1* in *Saccharomyces cerevisiae* during Icewine fermentation. J Appl Microbiol. 99:112-125.

Pigeau, G.M., E. Bozza, K. Kaiser and D.L. Inglis. 2007. Concentration effect of Riesling Icewine juice on yeast performance and wine acidity. J Appl Microbiol. 103:1961-1698.

Pronk, J.T., H.Y. Steensma and J.P. van Dijken. 1996. Pyruvate metabolism in *Saccharomyces cerevisiae*. Yeast. 12:1607-1633.

Rep, M., M. Krantz, J.M. Thevelein and S. Hohmann. (2000) The transcriptional response of *Saccharomyces cerevisiae* to osmotic shock. J Biol Chem. 275:8290-8300.

Remize, F., E. Andrieu and S. Dequin. 2000. Engineering of the pyruvate dehydrogenase bypass in *Saccharomyces cerevisiae*: role of the cytosolic $Mg^{2+}$ and mitochondrial $K^{+}$ acetaldehyde dehydrogenases Ald6p and Ald4p in acetate formation during alcoholic fermentation. Appl and Environ Microbiol. 66:3151-3159.

Remize, F., J.L. Roustan, J.M. Sablayrolles, P. Barre and S. Dequin. 1999. Glycerol overproduction by engineered *Saccharomyces cerevisiae* wine yeast strains leads to substantial changes in by-product formation and to a stimulation of fermentation rate in stationary phase. Appl Environ Microbiol. 65:143-149.

Remize, F., L. Barnavon and S. Dequin. 2001. Glycerol export and glycerol-3-phosphate dehydrogenase, but not glycerol phosphatase, are rate limiting for glycerol production in *Saccharomyces cerevisiae*. Metab Eng. 3:300-312.

Rizzini, F.M., C. Bonghia and P. Tonittib. 2009. Postharvest water loss induces marked changed in transcript profiling in skins of wine grape berries. Postharvest Biol Technol. 52:247-253.

Saint-Prix. F., L. Bönquist and S. Dequin. 2004. Functional analysis of the *ALD* gene family of *Saccharomyces cerevisiae* during anaerobic growth on glucose: the $NADP^{+}$-dependent Ald6p and Ald5p isoforms play a major role in acetate formation. Microbiol. 150:2209-2220.

Shaw, A. 2005. The Niagara peninsula viticultural area: a climatic analysis of Canada's largest wine region. J Wine Res. 16:85-103.

VQA Ontario. 2013A. The Niagara peninsula. Retrieved from: http://www.vqaontario.com/Appellations/NiagaraPeninsula

VQA Ontario. 2013B. Wine standards. Retrieved from: http://www.vqaontario.com/Regulations/Standards

Winkler, A.J. 1954. Effects of overcropping. Am J Enol Vitic. 5:4-12.

Zoecklein, B.W. 1994. Wine analysis and production. Chapman and Hall, New York.

# Chapter 3

## Evaluation of a UV Endpoint Enzymatic Method for Nicotinamide Coenzyme Determination in Wine Yeast Cell Lysate

**Heit, C.[1,2] and D.L. Inglis[1,2,3]**

1 Cool Climate Oenology and Viticulture Institute, Brock University, St. Catharines, ON, Canada
2 Centre for Biotechnology, Brock University, St. Catharines, ON, Canada
3 Department of Biological Sciences, Brock University, St. Catharines, ON, Canada

Formatted for the Journal of Applied Microbiology

### 3.1. Abstract

**Aims:** This study describes an evaluation of nicotinamide coenzyme determinations by the UV-endpoint method using a set of assay protocols outlined in Bergmeyer (1974) and the enzymes alcohol dehydrogenase (ADH, $NAD^+$ assay), glycerol-3-phosphate dehydrogenase (GPDH, NADH assay), glucose-6-phosphate dehydrogenase (G6P-DH, $NADP^+$ assay), and glutamate dehydrogenase (GlDH, NADPH assay). The biochemical interest of this determination lies in assessing the redox balance of the $NAD^+$/ NADH and $NADP^+$/ NADPH coenzyme systems to determine their respective roles as metabolic triggers for yeast-catalyzed acetic acid production.

**Methods:** The oxidized cofactors, $NAD^+$ and $NADP^+$, were quantified using pure ADH and G6P-DH, respectively. ADH catalyzed the reduction of $NAD^+$ to NADH and $H^+$ by the oxidation of ethanol to acetaldehyde, while G6P-DH catalyzed the oxidation of glucose-6-phosphate to gluconate-6-phosphate, with the concomitant reduction of $NADP^+$ to NADPH and $H^+$. The amount of NADH or NADPH formed was followed at 340 nm using a UV-Vis spectrophotometer, and directly proportional to the $NAD^+$ or $NADP^+$ concentration, respectively, present in the sample. The reduced cofactors, NADH and NADPH, were quantified using pure GPDH and GlDH, respectively. GPDH catalyzed the reduction of dihydroxyacetone phosophate to glycerol-3-phosphate, with the oxidation of NADH to $NAD^+$, while GlDH catalyzed the reductive amination of 2-oxoglutarate by ammonia to form glutamate, with the reduction of NADPH to $NADP^+$. The NADH or NADPH content was evaluated spectrophotometrically at 340 nm.

**Results and Comments:** During development of the assay here, we report that working assays for the measurement of $NAD^+$, NADH, $NADP^+$ and NADPH were established based on a set of protocols outlined in Bergmeyer (1974). The method was optimized to include a cell lysis buffer that was compatible with all assays, as well as filtration step to

deproteinize the lysate prior to coenzyme analyses. All assays underwent validation to ensure the established protocols were accurate and reproducible.

**Conclusions:** The adapted technique indicated high linearity, accuracy and precision of the analytical method but insufficient sensitivity for yeast extracts as the assays were unable to accurately quantify the low concentrations present in the cell lysate samples. Although the method was relatively simple, fast and inexpensive, further work is required to increase the sensitivity of the coenzyme detection and quantification in yeast extract.

**Keywords:** Nicotinamide coenzymes, enzyme assays, UV-Vis spectrophotometer, *Saccharomyces cerevisiae*, alcohol dehydrogenase, glycerol-3-phosphate dehydrogenase, glucose-6-phosphate dehydrogenase, glutamate dehydrogenase.

### 3.2. Introduction

β-Nicotinamide adenine dinucleotide ($NAD^+$) and β-Nicotinamide adenine dinucleotide phosphate ($NADP^+$) and their reduced forms (NADH and NADPH, respectively) are ubiquitous biomolecules found in eukaryotic and prokaryotic organisms (Xie 2008). In *Saccharomyces cerevisiae*, these coenzyme pairs play important roles as electron acceptors/ donors in over 300 biochemical reactions involving oxidation and reduction (Lui and Chen 2011; Forster *et al*. 2003), allowing them to have a critical effect on the metabolic status and redox state of the cell (Heux *et al.* 2006). Enzymes involved in these reactions are some of the most abundant and well-studied enzymes involved in energy metabolism, including glycolysis and the tricarboxylic acid cycle, and the pentose phosphate pathway (Kasimova *et al*. 2006). Due to the participation of coenzymes in these metabolic reaction networks, maintaining redox homeostasis is an important requirement for sustained metabolism and growth in all living cells (Vemuri *et al*. 2007).

Two pyridine nucleotide systems, NADH/ $NAD^+$ and NADPH/ $NADP^+$, determine the intracellular redox state, primarily through the NADH: $NAD^+$ ratio and to a lesser extent by the NADPH: $NADP^+$ ratio. Of the coenzymes, NADH is preferentially used as a reducing equivalent that is produced and consumed mainly in catabolic reactions, while

NADPH functions mainly as a reducing equivalent in anabolic processes (Bakker *et al*. 2001; van Dijken and Scheffers 1986). Since NADH is highly involved in the metabolic network, changes in the redox state of the NADH/ $NAD^+$ system results in extensive changes in yeast metabolism (Nielson 2003). Within the cell, carbon and nitrogen metabolism are responsible for the biosynthesis of building blocks and macromolecules, including proteins, lipids, DNA, RNA and carbohydrates (Nielson 2011). Therefore, changes within the redox state negatively impacting cellular metabolic processes can affect yeast cell function, growth and survival if balance is not restored.

To avoid nucleotide depletion and disruption of cellular redox balance, intracellular rates of formation and consumption of NADH/ $NAD^+$ and NADPH/ $NADP^+$ must be balanced (Nissen *et al*. 2001). Yeast redox metabolism is characterized by the absence of transhydrogenase activity (van Dijken and Scheffers 1986), making it necessary for the coenzyme systems to be separated within the yeast cell. As a consequence, maintenance of intracellular redox balance demands that reduced coenzymes be re-oxidized in the compartment where they are produced using distinct enzymatic mechanisms (Bakker *et al.* 2001) as opposed to transferring reducing equivalents between the coenzyme systems (van Dijken and Scheffers 1986).

During sugar metabolism in yeast under anaerobic conditions, NADH generated in glycolysis can be re-oxidized in the conversion of pyruvate to ethanol and carbon dioxide during alcoholic fermentation, thereby making the process redox-neutral (Kukec *et al*. 2003). However, when yeast cells are subjected to conditions of high osmolarity, redox balance within the NADH/ $NAD^+$ coenzyme system is offset as their stress response leads to the production of high levels of glycerol, the main osmolyte in *S. cerevisiae* (Blomberg

and Alder 1989; Brewster *et al*. 1993; Nevoigt and Stahl 1997; Blomberg 2000) while alcoholic fermentation still progresses. The rate-limiting step in its biosynthesis is the expression of glycerol-3-phosphate dehydrogenase (encoded by *GPD1* and *GPD2*), which catalyzes the reduction of dihydroxyacetone phosphate (DHAP) to glyceraldehyde-3-phosphate, with the oxidation of NADH to $NAD^+$ (Remize *et al*. 2001). In a subsequent reaction, glycerol-3-phosphate is dephosphorylated by glycerol-3-phosphatases (encoded by *GPP1* and *GPP2*) to form glycerol (Påhlman *et al.* 2001).

Under hyperosmotic stress, yeast rely on metabolite formation to maintain intracellular redox balance, specifically through redox reactions that can reduce the excess $NAD^+$ formed during glycerol biosynthesis. Acetic acid biosynthesis has been suggested as a mechanism that yeast can use to balance excess $NAD^+$ formed in response to hyperosmotic stress by regenerating NADH (Blomberg and Alder 1989). The NADH consumed during DHAP reduction could be provided by the $NAD^+$-dependent oxidation of acetaldehyde to acetic acid by a cytosolic aldehyde dehydrogenase (Aldp), resulting in the reduction of $NAD^+$ to NADH (Pigeau and Inglis 2007). But the main aldehyde dehydrogenase to produce acetic acid has been reported as an $NADP^+$-dependent form, challenging the role of acetic acid production for balance of the $NAD^+$/ NADH ratio (Remize *et al*. 1999; Englinton *et al.* 2002; Erasmus and van Vuuren 2009).

To date, it remains unclear which cofactor system and Aldp isoform is responsible for acetic acid production during high sugar fermentations. There are three cytosolic Aldp isoforms in *S. cerevisisae* that can catalyze this reaction, two of which are $NAD^+$-dependent (encoded by *ALD2* and *ALD3*) (Navarro-Avino *et al*. 1999) and one of which is $NADP^+$-dependent (encoded by *ALD6*) (Meaden *et al*. 1997). Previous research questions the

linkage of acetic acid production under hyperosmotic stress to glycerol production for maintaining intracellular redox balance (Erasmus *et al*. 2003; Erasmus and van Vuuren 2009), and thus additional studies need to be conducted to define the contribution of each isozyme to both elevated acetic acid and redox balance.

Current literature pertaining to elevated acetic acid during high sugar fermentations is confusing and controversial as different Aldp isoforms with distinct cofactor specificities have been suggested to be majorly responsible. Throughout Icewine fermentation, Pigeau and Inglis (2005) found only *ALD3* to be up-regulated in response to hyperosmotic shock, which corresponded to an increase in acetaldehyde and acetic acid production. *ALD3* displayed a 6.2-fold up-regulation on day 4 of fermentation over that found in the table wine juice, and was the only *ALD* further up-regulated by acetaldehyde stress during fermentation (Pigeau and Inglis 2007). Contrary to these findings, *ALD2*, *-3*, *-4* and *-6* were all up-regulated in response to sugar-induced osmotic stress after brief exposure to chaptalized grape juice (40% w/ v sugar) (Erasmus *et al*. 2003; Erasmus and van Vuuren 2009). *ALD6* was expressed at the highest level, followed by *ALD4* (Erasmus and van Vuuren 2009), which is consistent with the findings of Remize *et al*. (2000). If transcript levels do correlate with enzyme activity levels, Ald6p is suggested to have a major role in acetic acid production, possibly as a way to compensate for the down-regulation of NADPH generated through the pentose phosphate pathway (Bro *et al*. 2003; Erasmus and van Vuuren 2009). However, coenzyme levels have not yet been measured in fermenting yeast cells and will be fundamental in determining their impact on the metabolic regulation of acetic acid production.

An essential part of the research lies in understanding the altered redox state of the yeast cells during fermentation and elucidating their roles as metabolic triggers for acetic acid production. For these determinations to be made, the ratio of $NAD^+$/ NADH versus $NADP^+$/ NADPH in yeast before and after hyperosmotic stress under fermentative conditions needs to be measured, which will enable the redox status of both coenzyme systems to be assessed. The objective of this research was to develop a series of enzymatic assays for measuring $NAD^+$, $NADP^+$, NADH and NADPH content in yeast cytosolic extract using a UV-endpoint method based on a method outlined in Bergmeyer (1974), and to critically evaluate the use of these assays for application to Icewine and other wine styles involving high sugar juices.

### 3.3. Materials and Methods

**3.3.1. Yeast strain.** The commercial yeast *Saccharomyces cerevisiae* strain EC-1118 was used for the analysis of assay methods for quantifying $NAD^+$, NADH, $NADP^+$ and NADPH in cell extract and was acquired from Lallemand Inc. (Montreal, QB, Canada).

**3.3.2. Culture media.** For batch cultures, yeast cells were grown in a defined medium made up of minerals and vitamins according to Verduyn *et al*. (1992) and supplemented with glucose (20 g $l^{-1}$) (Agrimi *et al*. 2011). The mineral concentrations per liter included: $(NH_4)_2SO_4$, 5 g; $KH_2PO_4$, 3 g; EDTA, 15 mg; $MgSO_4 \cdot 7H_2O$, 0.5 g; $ZnSO_4 \cdot 7H_2O$, 4.5 mg; $CoCl_2 \cdot 6H_2O$, 0.3 mg; $MnCl_2 \cdot 4H_2O$, 1 mg; $H_3BO_3$, 1 mg; $CuSO_4 \cdot 5H_2O$, 0.3 mg; $CaCl_2 \cdot 2H_2O$, 4.5 mg; $FeSO_4 \cdot 7H_2O$, 3 mg; $NaMoO_4 \cdot 2H_2O$, 0.4 mg; and KI, 0.1 mg. The vitamin concentrations per liter included: biotin, 0.05 mg; nicotinic acid, 1 mg; calcium pantothenate, 1 mg; inositol, 25 mg; thiamine HCl, 1 mg; pyridoxine HCl, 1 mg; and para-amino benzoic acid, 0.2 mg. All individual stock solutions of the mineral components were

heat sterilized (120ºC) for 20 minutes and the vitamin mixture was filtered-sterilized through a 0.22 µm grade filter (Millipore) prior to storage at 4°C. To prepare a 1x working solution, appropriate volumes of the concentrated stock solutions were diluted with Milli-RiOs water (RiOs-16; Millipore, Etobicoke, ON, Canada). The final solution was adjusted to pH 5.0 with 1 N NaOH and filtered-sterilized through a 0.22 µm grade filter (Millipore) under a vacuum.

**3.3.3. Yeast inoculation procedure and growth conditions for batch cultures.** Five grams of active freeze dried yeast (*S. cerevisiae* EC-1118) were rehydrated in 50 ml of sterile, 40°C water (RiOs-16; Millipore) for 15 minutes, gently swirling every 5 minutes to encourage aeration. Thirty microliters of the EC-1118 starter culture were subsequently plated on YPD media (1% yeast extract, 2% peptone, 2% dextrose, 2% agar) and incubated in a growth chamber at 30°C before use (MIR-262; SANYO Electric Co., Ltd.). To prepare the pre-culture, a loop-full of the yeast from a freshly streaked plate was inoculated into 50 ml of defined medium contained in a 500 ml Erlenmeyer flask. The pre-culture was grown aerobically at 30°C with shaking at 160 rpm in a temperature-controlled orbital shaker (Weiss Gallenkamp) until an optical density at 600 nm ($OD_{600}$) of 0.4 to 0.7 was reached, as determined using a UV-Vis Spectrophotometer (Spectronic Genesys™ 2). One milliliter of the starter culture was then used to inoculate 100 ml batch cultures in 500 ml Erlenmeyer flasks to a starting $OD_{600}$ of ~0.002-0.010. Cultures were incubated at 30°C and 160 rpm until an $OD_{600}$ of 0.7 to 1.0 was reached to achieve approximately 1 g cell weight per 100 ml of culture.

**3.3.4. Determination of yeast wet weight.** Yeast wet weight was measured by the cell pellet weight after centrifugation of the cell culture. A pre-determined volume of yeast

culture was removed from each batch culture, combined, and added to pre-weighed centrifugation tubes. The cell suspensions were pelleted at 5000 rpm for 10 min at 4ºC using a Sorvall RC5C Plus ultra-centrifuge (rotor model SS-34; Newtown, CT, USA), after which the supernatants were decanted. The pellets were resuspended in sterile Milli-RiOs water (RiOs-16; Millipore) and pelleted as before. After centrifugation, the supernatant was decanted and the wet weight of the cells was determined by the difference in mass.

**3.3.5. Determination of yeast dry weight.** Yeast dry weight was determined using a filter retention assay. A pre-determined volume of yeast culture was removed from each batch culture, combined, and passed through a sterile, pre-weighed 0.22 µm grade filter (Millipore) under a vacuum. Filters were washed twice with Milli-RiOs water (RiOs-16; Millipore) and then dried at 60ºC for 2 days in an oven (MIR-212; SANYO Electric Co., Ltd.), after which time they were re-weighed. Dry weight was determined by the difference in mass.

**3.3.6. Preparation of yeast extracts for assays.** To obtain a cytosolic yeast extract, the following extraction protocol, modified from a procedure developed by Murdza-Inglis (1995) and Agrimi *et al*. (2011), was followed. Once an $OD_{600}$ of 0.7 to 1.0 was reached, yeast cells were harvested in the late exponential phase by centrifugation using a Sorvall RC5C Plus ultracentrifuge (rotor model SLA-3000). Yeast cells were pelleted at 5500 rpm for 10 min at 4 ºC, washed once with 2 ml sterile Milli-RiOs water (RiOs-16; Millipore), and were centrifuged as before. To prepare the whole cells for cell wall digestion, the pellet was resuspended in 2 ml/ g (wet weight) of Tris-dithiothreitol (DTT) buffer (100 mM Tris-$H_2SO_4$, pH 9.4; 10 mM DTT) and incubated for 20 minutes at 30 ºC in a temperature-controlled orbital shaker (Weiss Gallenkamp) with gentle shaking (90 rpm). The treated

cells were then collected by centrifugation at 3500 rpm for 5 min at 4ºC using an SS-34 rotor. The pellet was resuspended in 2 ml spheroplast buffer (1.2 M sorbitol; 20 mM potassium phosphate, pH 7.4) and the cells were centrifuged as before. After washing, spheroplasts were prepared using Zymolyase-100T (Cedarlane Labs Ltd., Burlington, ON, Canada), a cell-wall hydrolyzing enzyme. Cells were added to a mixture containing 1 mg of Zymolyase-100T/ g (wet weight) and 4 ml spheroplast buffer. The mixture was incubated for 45 minutes at 30 ºC in an orbital shaker (Weiss Gallenkamp) with gentle shaking (90 rpm). Spheroplast conversion was monitored by diluting 10 µl of the cell suspension in 990 µl of spheroplast buffer or Milli-RiOs water (RiOs-16; Millipore) and examining the cells using a light microscope (40x magnification) and haemocytometer counting chamber. Spheroplasts formation was considered complete when 80-90% of the cells suspended in water appeared ghost-like due to the loss of their cell walls and rapidly burst into cell debris in water. Spheroplasts are osmotically fragile and will lyse when transferred from a hypertonic to hypotonic medium. Following Zymolyase digestion, spheroplasts were collected by centrifugation at 3500 rpm for 5 min at 4 ºC (rotor model SS-34), washed twice in spheroplast buffer, and were pelleted as before. The spheroplasts were resuspended in 3.5 ml ice-cold cell breaking buffer (0.6 M mannitol; 20 mM HEPES-KOH, pH 7.4; 1 mM phenylmethylsulfonylfluoride [PMSF]; 0.1% w/v fatty acid free-Bovine Serum Albumin [BSA]) and were disrupted with 20 up-and-down strokes of the tight-fitting pestle of a pre-chilled Dounce homogenizer. Throughout this process, the Dounce homogenizer was kept on ice. The extent of cell lysis was determined by diluting 10 µl of the cell suspension in 990 µl spheroplast buffer and examining the cells using a light microscope (40x magnification) and haemocytometer counting chamber. After

homogenization, the lysate was transferred to pre-chilled microcentrifuge tubes and fractionated using differential centrifugation. The nuclear fraction was recovered at 3500 rpm for 5 min at 4ºC using an SS-34 rotor, and the mitochondrial fraction was recovered from the supernatant at 9000 rpm for 10 min at 4ºC. After centrifugation, the supernatant containing the cytosolic fraction was removed and kept on ice until analyzed for its nucleotide concentration.

**3.3.7. Inactivation of proteases in yeast cell extract using a protease inhibitor cocktail.** Prior to performing the enzymatic assays, cytosolic extract samples were inactivated using a protease inhibitor cocktail manufactured by Roche Applied Science (Complete Ultra Tablets, EDTA-free, glass vials, catalogue no. 05892953001). To prepare a 1x stock solution, 1 tablet was added directly to 50 ml of extraction medium, according to the manufacturer's instructions. All stock solutions were stirred on a stir plate until the tablets dissolved, and the solution was considered ready to use even if fine particles were visible in solution. The stock solutions were used for preparation of the calibration standards for $NAD^+$, NADH, $NADP^+$ and NADPH determination, as described in Section 3.3.9., and as the buffer for cell lysis.

**3.3.8. Deproteinization of yeast cell extract with spin filters.** Prior to enzymatic analysis, cytosolic extract samples were deproteinized using molecular weight cut-off (MWCO) spin filters manufactured by Pall Life Sciences (Microsep™ Centrifugal Device; catalogue no. OD010C46 (10 kDa) or Microsep™ Advance spin filter; catalogue no. OD010C33 (10 kDa) and OD030C3310 (30 kDa); Mississauga, ON, CAN). After cytosolic extraction, a measured volume of the sample was added to each centrifugation tube. Samples in the Microsep™ Advance tubes were centrifuged at 7920 rpm (as specified by the

manufacturer) at 4 ºC using the Sorvall RC5C Plus. All samples were centrifuged until the volume of filtrate did not change, indicating more sample was able to be filtered through. Prior to performing the assays, the volume of sample recovered was determined so that the nucleotide content could be normalized to this value.

**3.3.9. Overview: Determination of intracellular NAD(P)$^+$ and NAD(P)H concentrations.** Intracellular nucleotide concentrations were measured in standard and yeast cell extract samples using a UV-Vis spectrophotometer (Spectronic Genesys™ 2) and endpoint assay method outlined in Bergmeyer (1974). Reactions were prepared in semi-micro UV/ Vis cuvettes (1.5 ml, 10 mm optical path length, Fisher Scientific), and coenzymes were measured by monitoring changes in UV absorption of NADH and NADPH at 340 nm. Each standard curve was used to determine the respective coenzyme concentration in yeast cytosolic extract by comparing the absorbance of the extract sample with the standard solutions.

**3.3.9.1. Assay procedure for the determination of NAD$^+$.** The quantification of $NAD^+$ required a reaction catalyzed by alcohol dehydrogenase (ADH; EC1.1.1.1). In this reaction, ADH catalyzed the reduction of $NAD^+$ to NADH and $H^+$ by oxidation of ethanol to acetaldehyde (1). As a net result, the oxidation of ethanol generated an excess of NADH, allowing the reaction to be followed by measuring the increase in absorbance of the solution at 340 nm as the reaction reached equilibrium. The amount of NADH produced was proportional to the amount of $NAD^+$ in the cell lysate sample and was used as an indicator of the cellular $NAD^+$ concentration.

$$\text{(1) ethanol} + NAD^+ \overset{ADH}{\rightleftharpoons} \text{acetaldehyde} + NADH + H^+$$

The $NAD^+$ content was determined in a 2.02 ml reaction medium containing pyrophosphate buffer (pH 8.8) consisting of 50 mM tetrasodium pyrophosphate and 22 mM semicarbazide, and 1 ml of yeast cell extract or standard sample. To initiate the reaction, 10 µl of ethanol were added to the reaction cuvette, giving a final ethanol concentration of 85 mM, and an equal volume of water was added to the blank cuvette. The contents in each were thoroughly mixed via inversion and the reaction was left to incubate at room temperature. Prior to taking the first absorbance reading ($A_1$), the spectrophotometer was zeroed at 340 nm with the blank cuvette, and after 15 minutes the absorbance of the sample or standard was measured. Ten microliters of freshly prepared 1.2 mg/ ml ADH (409 U $mg^{-1}$, catalogue no.10127558001; Roche Applied Science, Laval, QB, Canada) were then added to the cuvette and the reaction was left to incubate for 6 minutes, after which time the $A_2$ reading was taken. The change in absorbance ($\Delta A$) due to the addition of ADH was determined, and the $NAD^+$ content was interpolated from the standard curve using the equation of the standard. Standard solutions for the determination of $NAD^+$ were prepared in water or cell breaking buffer from a 10 mM $NAD^+$ stock (β-Nicotinamide adenine dinucleotide hydrate, catalogue no. N7004, Sigma-Aldrich®) prepared in Milli- RiOs water (RiOs-16; Millipore) and included: 0 µM, 100 µM, 300 µM, 500 µM, 750 µM, 1000 µM and 1500 µM. Standards were tested in duplicate and the mean concentration (± SD) was plotted on the calibration curve. Yeast cell lysate samples were tested in singlet.

**3.3.9.2. Assay procedure for the determination of $NADP^+$.** The quantification of $NADP^+$ required a reaction catalyzed by glucose-6-phosphate dehydrogenase (G6P-DH; EC1.1.1.49). In this reaction, G6P-DH catalyzed the oxidation of glucose-6-phosphate to gluconate-6-phosphate, along with the concomitant reduction of $NADP^+$ to NADPH and

$H^+$ (2). The reaction was followed by measuring the increase in absorbance of the solution at 340 nm as NADPH formed and the reaction reached equilibrium. The NADPH formed was stoichiometric with the amount of $NADP^+$ in the cell lysate and was used as an indicator of the cellular $NADP^+$ content.

$$\text{(2) glucose-6-phosphate} + NADP^+ \overset{\text{G6P-DH}}{\rightleftharpoons} \text{gluconate-6-P} + NADPH + H^+$$

The $NADP^+$ was determined in a 2.07 ml reaction medium containing 5mM magnesium sulfate and 2 ml of yeast cell extract or standard sample. To initiate the reaction, 50 µl of glucose-6-phosphate were added to the reaction cuvette, giving a final glucose-6-phosphate concentration of 5 mM, and an equal volume of Milli-RiOs water (RiOs-16; Millipore) was added to the blank cuvette. The contents of the cuvette were thoroughly mixed via inversion and the reaction was left to incubate at room temperature. Prior to taking the first absorbance reading ($A_1$), the spectrophotometer was zeroed at 340 nm with the blank cuvette, and after 15 minutes the absorbance of the sample was measured. Ten microliters of freshly prepared 2 mg/ ml G6P-DH (463 U $mg^{-1}$, catalogue no.10127655001; Roche Applied Science) were then added to the cuvette and the reaction was left to incubate for 15 minutes, after which time the $A_2$ reading was taken. The change in absorbance ($\Delta A$) due to the addition of G6P-DH was determined, and the $NADP^+$ content was interpolated from the standard curve using the equation of the standard. Standard solutions for the determination of $NADP^+$ were prepared in water or cell breaking buffer from a 10 mM $NADP^+$ stock (β-Nicotinamide adenine dinucleotide phosphate hydrate, catalogue no. N5755, Sigma-Aldrich®) and included: 0 µM, 10, µM, 25 µM, 40 µM, 50 µM, and 75 µM. The pH of each standard and sample was adjusted to 7.2-7.4 if necessary with 1N NaOH.

Standards were tested in duplicate and the mean concentration (± SD) was plotted on the calibration curve. Yeast cell lysate samples were tested in singlet.

**3.3.9.3. Assay procedure for the determination of NADH and NADPH.** The quantification of NADH and NADPH required two enzymatic reactions; in the first reaction catalyzed by glycerol-3-phosphate dehydrogenase (GPDH; EC1.1.1.8), dihydroxyacetone phosophate (DHAP) was reduced to glycerol-3-phosphate by NADH (3). The oxidation of NADH in the previous reaction was followed by the determination of NADPH with glutamate dehydrogenase (GlDH; EC 1.4.1.3) (4). In this pathway, GlDH catalyzed the reductive amination of 2-oxoglutarate by ammonia to form glutamate in a reaction utilizing NADPH. Both reactions were followed by measuring the decrease in absorbance of the solution at 340 nm as NADH and NADPH were oxidized to $NAD^+$ and $NADP^+$ in the respective reactions.

$$\text{(3) DHAP + NADH + } H^+ \overset{\text{GPDH}}{\rightleftharpoons} \text{ glycerol-3-phosphate + } NAD^+$$

$$\text{(4) 2-oxoglutarate + } NH_4^+ \text{ + NADPH } \overset{\text{GlDH}}{\rightleftharpoons} \text{ glutamate + } H_2O \text{ + } NADP^+$$

The NADH and NADPH contents were determined in a reaction medium containing 0.5 mM dihydroxyacetone phosphate, 2.5 mM 2-oxoglutarate and 5 mM ammonium, all of which comprised the ‘substrate mixture’, and 2 ml of yeast cell extract or standard sample in a final volume of 2.01 ml for NADH determination and 2.02 ml for NADPH determination. To initiate the reaction, 50 µl of the substrate mixture were added to the reaction cuvette and an equal volume of water was added to the blank cuvette. The contents of the cuvette were thoroughly mixed via inversion and the reaction was left to incubate. Prior to taking the first absorbance reading ($A_1$), the spectrophotometer was zeroed at 340

nm with the blank cuvette, and after 5 minutes the absorbance of the sample was measured at room temperature. Five microliters of freshly prepared 1 mg/ ml GDH (255 U $mg^{-1}$, catalogue no.10127752001; Roche Applied Science) were then added and the reaction was left to incubate for 5 minutes following inversion, after which time the $A_2$ reading was taken. In the same cuvette, the reaction for NADPH was initiated by the addition of 5 µl of freshly prepared 2 mg/ ml GlDH (120 U $mg^{-1}$, catalogue no.10127558001; Roche Applied Science). The contents of the cuvette were mixed via inversion and the reaction was left to incubate for 5 minutes, after which time the $A_3$ reading was taken. The change in absorbance ($\Delta A$) due to the addition of GDH and GlDH was determined, and NADH and NADPH concentrations were interpolated from the respective standard curves using the equation of the standard. Standard solutions for the NADH determination were prepared in cell breaking buffer from a 5 mM NADH stock (β-Nicotinamide adenine dinucleotide reduced disodium salt hydrate, catalogue no. N8129, Sigma-Aldrich®) prepared in 0.01 M Tris-HCl (pH 8.5) and included: 0 µM, 10 µM, 25 µM, 50 µM, 75 µM and 100 µM. Standard solutions for NADPH determination were prepared cell breaking buffer from a 5 mM NADPH stock (β-Nicotinamide adenine dinucleotide 2'-phophate reduced tetrasodium salt hydrate, catalogue no. N1630, Sigma-Aldrich®) prepared in 0.01 M NaOH and included: 0 µM, 25 µM, 50 µM, 75 µM 100 µM and 150 µM. Standards were tested in duplicate and the mean concentration (± SD) was plotted on the calibration curve. Yeast cell lysate samples were tested in singlet.

**3.3.10. Enzymatic assay method for nucleotide determination in yeast cell extract.** The UV-endpoint method was evaluated based on a set of protocols outlined in Bergmeyer (1974). Before this method could be applied to yeast cell lysate, it had to first be considered

valid to ensure it was fit for the intended purpose. Method validation included specific laboratory investigations and procedures that demonstrated that this particular protocol used for the quantitative measurement of the desired analytes, $NAD^+$, NADH, $NADP^+$ and NADPH, in yeast cytosolic extract was reliable and reproducible. The fundamental parameters for validating this included: (1) linearity and range (calibration curve), (2) precision (repeatability), (3) sensitivity (lower limit of quantification), and (4) accuracy (recovery).

**3.3.10.1. Linearity, precision, sensitivity and accuracy provided by the method.** During the initial stage of the validation process, it was necessary to first construct calibration curves that defined the relationship between the known concentrations of each coenzyme and optical density at the desired wavelength. The initial calibration curves for $NAD^+$ and $NADP^+$ included standards from 0-1500 µM. A subsequent calibration curve using standards from 0-100 µM was established for each coenzyme to focus in on the lower concentration range expected in yeast extract. The linearity was evaluated by linear regression analysis. Regression analysis was calculated using the least square method (Microsoft Excel 2013), and was utilized to determine the linear correlation coefficient (R) and coefficient of determination ($R^2$) of standard curves for each standard. An R-value of $\geq$0.985 was used as criterion of linearity, while a high $R^2$-value of $\geq$0.980 was used as criterion for goodness of fit of the regression line. After conducting the preliminary calibration studies, the linear range of the assay was optimized such that the absorbance of each standard was directly proportional to the analyte concentration in the sample. The precision of the procedure was determined by analyzing duplicate samples of standard. The repeatability was expressed numerically as the coefficient of variation (CV) of the

duplicate measurements, which was defined as the: (standard deviation of the analyte assay values/ mean concentration of the analyte assay values) x 100. The precision was assessed for each concentration level and did not exceed more than 20% of the CV. Assay sensitivity was evaluated on the basis of the lower limit of quantification (LLOQ) using the concentration of the lowest detectable standard from the data set that was in the prescribed accuracy and precision of the assay. The accuracy of each assay method was based on the recovery of known standards in the assay based on standard addition. When preparing standard samples, known quantities of pure analyte were added to the sample matrix (cell breaking buffer) and the increase in measured concentration was determined. A comparison of the assayed coenzyme concentration versus the predicted amount provided the recovery of the method and an estimation of its accuracy, which was expressed as the: (average measured concentration of analyte/ predicted concentration of analyte) x 100. A percent recovery value found within ±10% of the standard concentration was considered acceptable.

## 3.4. Results

### 3.4.1. In-study validation of assays

#### 3.4.1.1. Evaluation of Bergmeyer (1974) assay using standards in water

The results demonstrated that the assay protocols described by Bergmeyer (1974) using $NAD^+$ or $NADP^+$ standards in water were precise, accurate and linear over the range of cofactor concentrations tested (Fig. 3.1A and 3.1B). The R-values were estimated to be 0.9999 and 0.9991 for $NAD^+$ and $NADP^+$, respectively, indicating a high degree of linearity, and the $R^2$-values were estimated to be 0.9999 for $NAD^+$ and 0.9984 for $NADP^+$, suggesting good fit of the data. For duplicate measurements at each concentration level, the calculated precision did not exceed more than 20% of the CV, and the acceptance criterion for recovery was met (±10%). These results demonstrated that the assay protocols described by Bergmeyer (1974) can be repeated within the lab with high precision, accuracy and linearity.

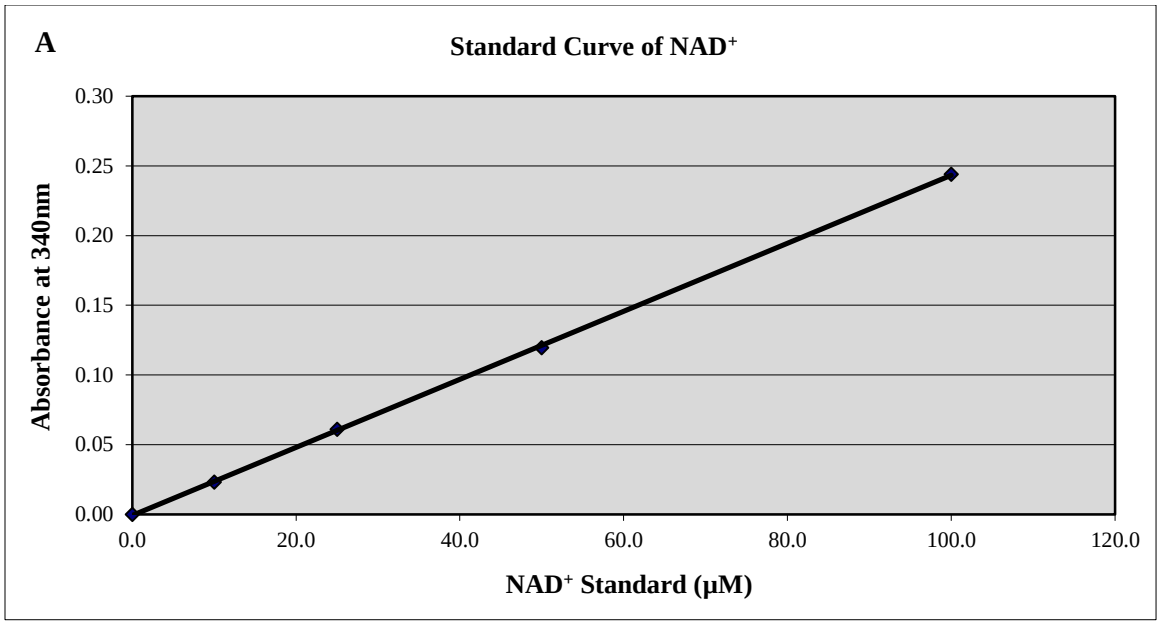


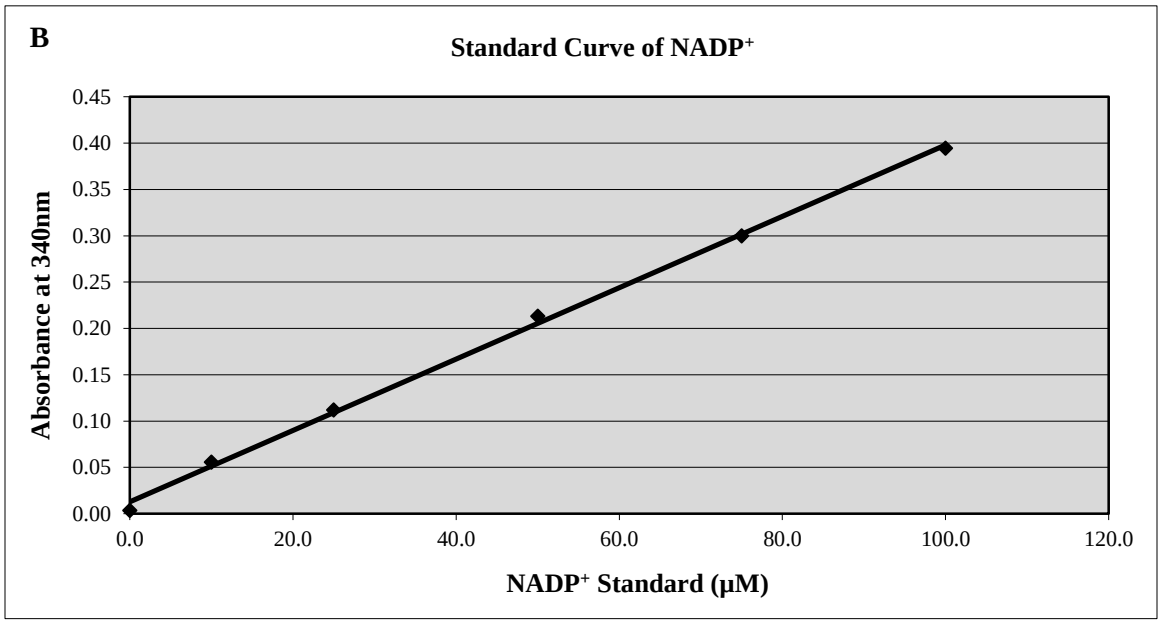


**Figure 3.1: Best-fit calibration curves of $NAD^+$ and $NADP^+$ with cofactor dissolved in water.** The Y axis represents the absorbance change at 340 nm during the reactions catalyzed by alcohol dehydrogenase in the $NAD^+$ assay (A) and glucose-6-phosphate dehydrogenase in the $NADP^+$ assay (B). Lines represent linear least squares fits to the data. The correlation coefficient (R) and coefficient of determination ($R^2$) were calculated using linear regression analysis. For (A), an R-value of 0.9999 and $R^2$-value of 0.9999 were determined; for (B) an R-value of 0.9991 and $R^2$-value of 0.9984 were determined. Standards were prepared in water and tested in duplicate (n = 2). The mean values (± SD) of the duplicate measurements are shown; where the error bars are not visible, they are within the symbol.

### 3.4.1.2. Recovery of $NADP^+$ standards made up in yeast extraction buffer

Standard recoveries from the curves in Figures 3.1 were tested using standards prepared in yeast extraction buffer. Two buffers used for cellular homogenization were assessed to determine the compatibility of each with the previously described enzymatic assay for $NADP^+$ (Section 3.3.9.2). The first buffer (Buffer 1) consisted of 0.6 M sorbitol, 10 mM Tris-HCl (pH 7.4), 1 mM EDTA, 1 mM PMSF and 0.2% (w/v) BSA, while the second (Buffer 2) contained 0.6 M mannitol, 20 mM HEPES-KOH (pH 7.4) and 0.1% (w/v) BSA. The various sample buffers spiked with 50 μM of $NADP^+$ standard stock (10 mM) were prepared (Table 3.1), and the recovery of each standard concentration was determined from the standard curve. For all samples derived from Buffer 1, less than 50% of the spiked concentration was recovered. When prepared in Buffer 2, a higher recovery of the standard concentration was measured (78.2%), and in the presence of PMSF, the standard recovery was determined to be 92%.

Table 3.1. Percent recoveries of buffer samples spiked with 50 μM of $NADP^+$ standard stock (n =1).

| **Sample** | **Recovery (%)** |
|---|---|
| Buffer 1 | 34.8 |
| Buffer 1<br>(without EDTA) | 45.7 |
| Buffer 1<br>(without EDTA and PMSF) | 32.1 |
| Buffer 1<br>(without EDTA and BSA) | 22.4 |
| Buffer 1<br>(substitution of sorbitol with mannitol) | 23.4 |
| Buffer 2 | 78.7 |
| Buffer 2<br>(with PMSF) | 92.0 |

### 3.4.1.3. $NAD^+$ assay in Buffer 2

Calibration samples prepared in Buffer 2, with the inclusion of 1 mM PMSF as a protease inhibitor, were used to construct standards curves of each cofactor. To verify whether $NAD^+$ can be quantified in cell breaking buffer by the UV-endpoint method, various amounts of standard $NAD^+$ were added to the reaction mixture in the presence of ADH used to catalyze the reaction, and absorbance changes were monitored by a UV-Vis spectrophotometer at 340 nm. Linear standard curves were obtained between final concentrations of 0 to 100 µM $NAD^+$ (Fig. 3.1A) and 100 to 750 µM $NAD^+$ (Appendix II, Fig. 2). The R-values were estimated to be 0.9999 for both the lower and upper linear regions of the calibration curve, indicating a high degree of linearity. The $R^2$-value of the lower region curve was estimated to be 0.9998, while that of the upper region was estimated to be 0.9999, both results suggesting each linear model to be a good fit of the data. For duplicate measurement at each concentration level, the calculated precision did not exceed more than 20% of the CV, and the acceptance criterion for recovery was met (±10%). These results demonstrated that $NAD^+$ can be precisely and accurately quantified within the established working range using the UV-endpoint method, and that the cell breaking buffer system is compatible with the assay. From the data set, the LLOQ was determined to be 10 µM, while the upper limit of quantification (ULOQ) was determined to be 750 µM. Similarly for the $NADP^+$, NADH and NADPH assays, the results demonstrated high precision, accuracy and linearity (Fig. 3.1B-D).

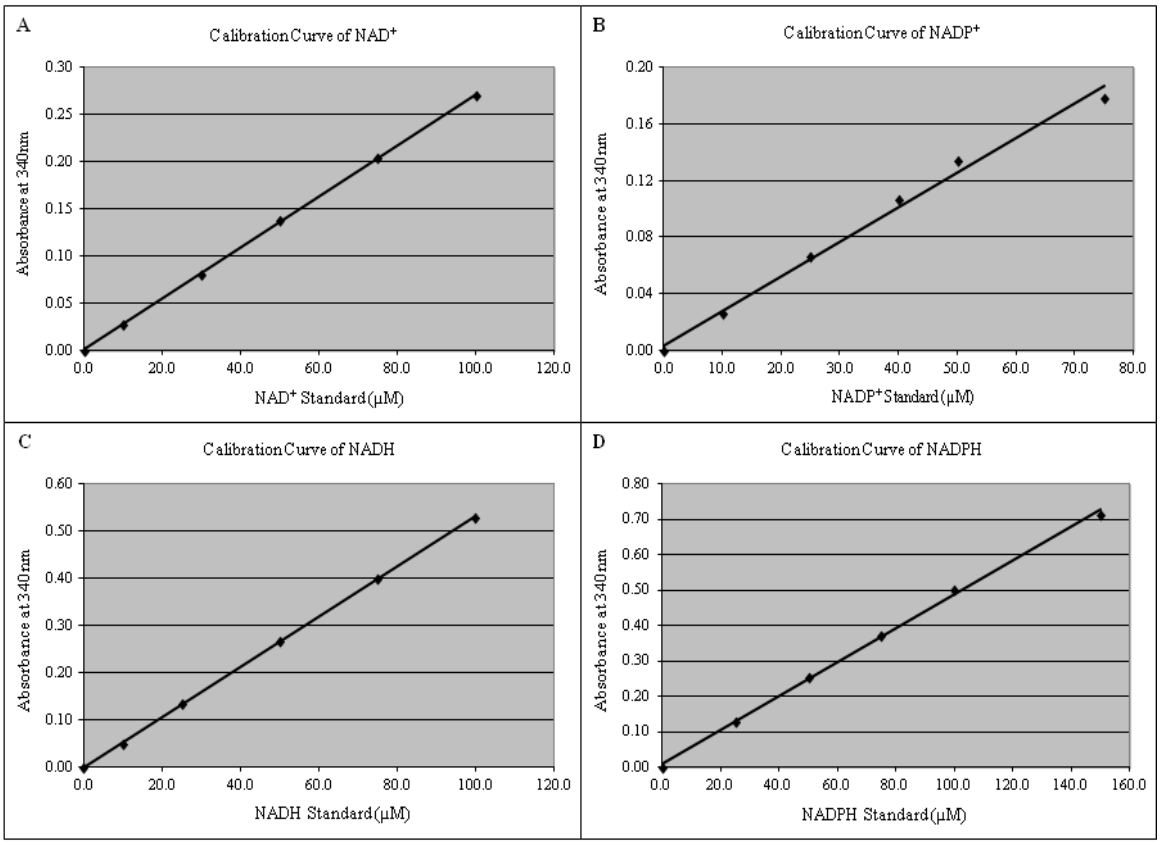


**Figure 3.2: Best-fit calibration curves for nicotinamide cofactors in cell breaking buffer.** The Y axis represents the absorbance change at 340 nm during the reactions catalyzed by alcohol dehydrogenase for the $NAD^+$ assay (A), glucose-6-phosphate dehydrogenase for the $NADP^+$ assay (B), glycerol-3-phosphate dehydrogenase for the NADH assay (C) and glutamate dehydrogenase for the NADPH assay (D). Lines represent linear least squares fits to the data. The correlation coefficient (R) and coefficient of determination ($R^2$) were calculated through regression analysis (A, R= 0.9980 and $R^2$= 0.9960; B, R= 0.9991 and $R^2$= 0.9984; C, R= of 0.9999 and $R^2$= 0.9999; D, R= 0.9992 and $R^2$= 0.9985). Standards were prepared in Buffer 2 and tested in duplicate (n = 2). The mean values (± SD) of the duplicate measurements are shown; where the error bars are not visible, they are within the symbol.

### 3.4.1.4. Measurement of nucleotide content in yeast cell lysate (without protein inhibition or removal)

Following the calibration studies, the developed assays were applied to crude cytosolic extract isolated from yeast EC-1118 cells to determine the sensitivity of each, and specifically whether the low coenzyme concentrations present in the cell extract samples could be detected and accurately quantified using the modified assays. The accuracy of the procedure was further evaluated in spike-and-recovery experiments. In the initial studies performed, the cytosolic extract was only analyzed for its $NAD^+$ and $NADP^+$ content using the respective enzyme assays as problems with the measurements immediately surfaced. For both assays, the concentration of the positive control (spike) sample was selected to be 40 µM, as this concentration was close to the middle of each calibration curve used for interpolation (Fig. 3.2A and 3.2B). However, after the assays were performed no change in absorbance ($\Delta A$) was detected in the unspiked and spiked lysate samples, thereby precluding the coenzyme concentrations from being determined.

### 3.4.1.5. Effect of protease inhibition on nucleotide determination in yeast cell lysate samples: evaluation of Complete Ultra Tablets (EDTA-free)

A cocktail manufactured by Roche Applied Science (Complete Ultra Tablets, EDTA-free, glass vials, catalogue no. 05892953001) was investigated for use as a protease inhibitor in yeast cell lysate. Calibration curves using pure coenzymes were first constructed, meeting all requirements for linearity, precision and accuracy (Appendix II, Fig. 3A and 3B), and spike-and-recovery experiments were performed using the modified assay that included Buffer 2 for $NAD^+$ and $NADP^+$ determination in yeast cell lysate samples. Recovery values of the 40 µM $NAD^+$ and 50 µM $NADP^+$ matrix spikes, and the coenzyme content in the unspiked samples could not be determined as no signal was again detected. Based on these results, the protease inhibitor cocktail did not improve the recovery of the standard concentration in the spiked samples, or the measurement of the coenzyme content in the unspiked extract samples, thereby failing to resolve the protein interference issue.

### 3.4.1.6. Effect of deproteinization on nucleotide determination in yeast cell lysate samples: evaluation of 10 kDa spin filter

A 10 kDa spin filter manufactured by Pall Life Sciences (Microsep™ Centrifugal Device; catalogue no. OD010C46) was investigated for its ability to deproteinize yeast cell lysate samples. Previously established calibration curves for $NAD^+$, $NADP^+$, NADH and NADPH were used for the coenzyme determinations (Fig. 3.2A-D), and spike-and-recovery experiments were performed to assay the nucleotide content in the deproteinized cytosolic extract using the modified assay methods. Table 3.2 shows the recoveries of the coenzymes from the standard addition experiments performed on cell lysate after correction for the contribution from yeast to the $NAD(P)^+$ or NAD(P)H content. Clarification of the extract samples was found to greatly improve the recovery of the standard concentration in the spiked samples, with recoveries ranging from 88.0% to 97.2%, depending on the coenzyme assay. However, the coenzyme content in the unspiked extract samples remained low or unmeasurable. Of all the assays, $\Delta A$ values for only the $NAD^+$ and $NADP^+$ assays were obtained, but following interpolation of the concentration from the standard curve, the respective values were lower than the LLOQ.

Table 3.2. Percent recoveries of authentic standard solutions spiked into yeast cell extract samples deproteinized using a 10 kDa spin filter (n =1).

| Standard Contents | Sample Concentration (µM) | Spiking Concentration (µM) | Measured Concentration (µM) | Percent Recovered (%) |
|---|---|---|---|---|
| 250 µM $NAD^+$ spiked extract | 0 | 250.0 | 243.0 | 97.2 |
| 50 µM $NADP^+$ spiked extract | 0 | 50.0 | 48.0 | 96.0 |
| 50 µM $NAD^+$ spiked extract | 0 | 50.0 | 44.0 | 88.0 |
| 50 µM $NADP^+$ spiked extract | 0 | 50.0 | 48.6 | 96.9 |

### 3.4.1.7. Measurement of nucleotide content in yeast cell lysate samples: investigation of the use of spin filters and membrane pre-treatment

Prior to nucleotide analyses, spike-and-recovery experiments were performed using crude cytosolic extract spiked with 40 µM $NAD^+$. A previously established calibration curve was used for coenzyme determination (Fig. 3.1A), and spike-and-recovery experiments were performed to assay the nucleotide content in the deproteinized cytosolic extract using the modified assay method. To determine the effect of the membrane pre-treatment on sample recovery, cytosolic extract samples were first spiked and subsequently deproteinized using 10 kDa and 30 kDa spin filters manufactured by Pall Life Sciences (Microsep™ Advance spin filter; catalogue no. OD010C33, 10 kDa and OD030C33, 30 kDa). Table 3.3 shows the recoveries of the coenzymes from the standard addition experiments performed on cell lysate after correction for the contribution from yeast to the $NAD^+$ content (Table 3.4). Presoaking the 10 kDa and 30 kDa membranes overnight with cell breaking buffer greatly improved the recovery of the standard concentration in the spiked samples over that determined using a dry membrane or one soaked in glycerine (10%). Recovery of a 40 µM $NAD^+$ matrix spike was 76.7% using the 10 kDa membrane filter, while recovery of a 40 µM $NAD^+$ matrix spike using the 30 kDa membrane filter was 85.6% (Table 3.3).

Table 3.3. Percent recoveries of authentic standard solutions spiked into yeast cell extract samples prior to centrifugation (n =1).

| **Sample** | **Recovery (%)** |
|---|---|
| 10 kDa device (dry) | 11.5 |
| 30 kDa device (dry) | 34.7 |
| 10 kDa device<br>(presoaked overnight in 10% glycerine) | 19.6 |
| 10 kDa device<br>(presoaked overnight in cell breaking buffer) | 76.7 |
| 30 kDa device<br>(presoaked overnight in cell breaking buffer) | 85.6 |

Table 3.4. Concentration of coenzyme determined in yeast cell extract sample (deproteinized using a 10 kDa filter).

| Sample | $NAD^+$ (µM) | LLOQ (µM) |
|---|---|---|
| Unspiked extract ($NAD^+$ assay) | <LLOQ | 10 |

## 3.5. Discussion

### 3.5.1. Method for preparing yeast cell extracts for enzymatic analyses

The $NAD^+$, NADH, $NADP^+$ and NADPH assays were developed with the objective of measuring the redox status of the cell by measuring the concentration of these coenzymes in yeast cytosolic extract isolated from *S. cerevisiae* strain EC-1118 cells. Establishment of such assays was very much dependent on the application of cytosolic extract as both $NAD^+$-dependent Ald2/ 3p and $NADP^+$-dependent Ald6p are localized in the cytosol (Navarro-Avino *et al*. 1999). The remaining aldehyde dehydrogenases, Ald4p and Ald5p, are mitochondrial and were not of interest in this study. To obtain a yeast cytosolic extract, subcellular fractionation was used and was preceded by an extraction protocol to produce a cruden yeast cell lysate. Fractionation was important for avoiding cross-contamination of the cytosol with the mitochondria as $NAD(P)^+$ and NAD(P)H are present in both, which could affect coenzyme measurements, although no additional studies were conducted to verify sample purity.

### 3.5.2. Method development of enzyme assays

The work of Klingenberg (1974; 1985) served as the conceptual basis for the development of the coenzyme assays for measuring $NAD^+$, $NADP^+$, NADH and NADPH content in yeast cytosolic extract. This work was developed for measuring the redox state of free nicotinamide cofactors in animal tissue, blood and mitochondria. Although literature indicated the work to have baseline potential for achieving our research objectives, refinement of the existing protocol was still required. To enable robust, reliable measurement of the coenzymes in yeast, it was necessary to develop a different cell lysis method for isolating the cytosolic fraction from cells, as detailed in Section 3.3.6. The cell lysis component of this protocol necessitated the inclusion of a homogenization buffer to

facilitate cell lysis, whose composition needed to be optimized for this study. Since certain buffer characteristics can either have advantages or disadvantages, depending on the goals of the experiment, it was important to ensure that the buffer composition not only created an environment conducive to cell lysis, but was also compatible with the subsequent enzymatic assays used for cofactor analyses (Hartford and Bonifacino 2009).

The first assay experiment conducted verified the enzymatic method described in Bergmeyer (1974) could be successfully repeated and performed under our laboratory conditions. For both assays assessed ($NAD^+$ and $NADP^+$), the protocols were strictly followed resulting in high linearity, accuracy and precision of the analytical procedure. With a working assay method in hand, the next step was to assess the calibration of the assay and the influence of differences between the standard and spiked sample matrices prepared in lysis buffer (Buffer 1). Recovery experiments performed on spiked $NADP^+$ samples revealed low recovery of the standard concentrations in the buffer containing 0.6 M sorbitol, 10 mM Tris-HCl (pH 7.4), 1 mM EDTA, 1 mM PMSF and 0.1% (w/ v) BSA (Table 3.1), questioning the appropriateness of this buffer for use in this study.

Standard buffers most often consist of several components including: (1) a suitable organic buffer to maintain physiological pH, (2) sorbitol or mannitol (or another osmotic balancer) to stabilize organelle membranes, (3) salts to provide the appropriate ionic strength, (4) protease inhibitors to minimize the damage caused by hydrolytic enzymes (Hartford and Bonifacino 2009), (5) and BSA, a globular protein with self-buffering capacity (Curvale 2009). Lysis buffers also commonly include EDTA or EGTA, both of which can bind to metal cations thereby making them unavailable for other reactions such as those catalyzed by proteases (Hartford and Bonifacino 2009). Since protein degradation

can be problematic in extract samples due to the exposure of subcellular components to proteases upon cell lysis, protein inhibitors, ideally those with broad enzyme specificity, are important components of lysis buffers (Hartford and Bonifacino 2009).

In this study, the presence of EDTA in the cell lysis buffer (Buffer 1) was initially thought to be interfering with the $NADP^+$ assay as the mechanism for catalysis requires the presence of $Mg^{2+}$, added in the form of $MgSO_4$, to activate glucose-6-phosphate, the substrate for glucose-6-phosphate dehydrogenase. Since only one homogenization buffer would ultimately be used for cell lysis, this result was concerning as all assays needed to be compatible with the same buffer system. The exclusion of EDTA from Buffer 1 still resulted in low recovery of the standard sample, suggesting possible interference from another component. In response to this result, a variety of buffers derived from Buffer 1 were prepared that either eliminated or substituted certain components of the original buffer recipe. Similarly, very low standard recoveries were determined in the spiked buffer samples. However, when a buffer recipe containing 0.6 M mannitol, 20 mM HEPES-KOH (pH 7.4), 1mM PMSF and 0.1% (w/ v) BSA (Buffer 2) was evaluated, lower interference was observed as a much higher standard recovery was obtained (92.0%). For the remaining assays ($NAD^+$, NADH and NADPH), the respective protocols were strictly followed only this time using standards prepared in Buffer 2 rather than Buffer 1. The results showed high linearity, accuracy and precision of the analytical procedure, suggesting good compatibility of Buffer 2 with all coenzyme assays.

Following the calibration studies, spike-and-recovery experiments were performed using yeast cell extract samples to give an estimation of the precision and accuracy of the method, and specifically whether the low coenzyme concentrations present in the extract

samples could be detected and quantified using the modified assays. The results indicated no standard recovery in the spiked yeast extract sample or measurable coenzyme concentration in the unspiked extract sample, suggesting a possible issue with the sample as all assays were previously determined to be functional. Suggested reasons for low cofactor recovery were put forward and subsequently investigated. These included: (1) the presence of proteases in the sample extract resulting from cell lysis and homogenization which could be rapidly degrading the enzymes specifically added to each reaction mixture, (2) the high turbidity of the sample extract due to proteins and the large sample volumes required for each assay (which accounted for 50-99% of the total volume of the reaction mixture) which could be interfering with the absorbance measurements taken via spectrophotometry, (3) and/ or the presence of nicotinamide coenzyme-dependent enzymes in the cell extract sample which could be rapidly consuming the coenzymes of interest.

During the development of the assays reported here, we found that protease inhibition through the addition of the Complete Ultra Tablet (EDTA-free) did not improve the standard $NAD^+$ and $NADP^+$ recoveries in the spiked yeast cell extract samples or the measurable coenzyme concentration in the unspiked cell extract samples. The results of the enzymatic analyses suggest the tablet was unable to resolve this protein issue, appearing to only heighten it by increasing the turbidity of the sample extract and the ambiguity of absorbance measurements for the higher concentrated standards due to the increase in background noise. The Complete Ultra Tablet (EDTA-free) contains 4-(2-Aminoethyl)benzenesulfonyl-fluoride hydrochloride which, due to the presence of an aromatic hydrocarbon, is also able to absorb UV light at 340 nm, along with other unidentified components of the biological sample.

The initial rational for replacing PSMF with the tablet was based on the difference in enzyme specificity between the compounds. While PMSF is specific only for the inhibition of serine proteases, the Complete Ultra Tablet has a broad specificity range, containing both irreversible and reversible serine, cysteine and aspartic protease inhibitors (Roche Applied Science 2012). Of the tablets available, the EDTA-free version was selected to avoid any assay interference EDTA may cause due to its role as a chelating agent, which prevented metalloproteases in the sample from being inhibited. Based on the experimental results, PMSF was included in the final EDTA-free buffer (Buffer 2) to function as a protease inhibitor during yeast cell lysis.

The centrifugal devices effectively clarified the sample, resulting in a clear, much less turbid sample extract. It appeared unwanted proteases or nicotinamide coenzyme-dependent enzymes capable of interfering with the assay measurements were removed as recovery values from the standard addition tests were high. The results of the initial filtration experiments using a Pall 10 kDa centrifugal device revealed that centrifugation of the yeast cell extract greatly improved the standard recovery in the spiked extract and the measurement of coenzyme concentration in the unspiked extract. However, discontinuation of this particular product demanded alternative filters be evaluated for deproteinizing the sample extract. Two Pall devices constructed of polyethersulfone to minimize protein binding were selected with molecular weight cut-offs of 10 kDa or 30 kDa. Initial results using dry filters revealed low standard recovery in the spiked cell extract, suggesting a possible issue with the filter membrane and non-specific adsorption. After pre-treatment with Buffer 2 or 10% glycerine solutions, Buffer 2 was found to greatly improve the standard recovery after filtration with both the 10 kDa and 30 kDa devices.

Although these methods effectively deproteinized and clarified the lysate samples, coenzyme levels in the native extracts were below the LLOQ, indicating the assays were not sensitive enough for measuring the low coenzyme content present.

### 3.6. Conclusions

During development of the UV-endpoint method here, we report that working assays for the measurement of $NAD^+$, NADH, $NADP^+$ and NADPH were established based on a set of protocols outlined in Bergmeyer (1974). The method was optimized to include a yeast cell lysis buffer that was compatible with all assays, as well as a deproteinization step to remove interfering compounds and clarify the sample extract prior to coenzyme analysis. Although the use of the centrifugal devices demonstrated potential in resolving the protein interference issue, the results of the filtration experiments demand that more research be conducted to determine its overall suitability for coenzyme analyses.

As part of the method development, all assays underwent validation to ensure the established protocols were accurate and reproducible. Although the results obtained indicated high linearity, accuracy and precision of the analytical method, they demonstrated insufficient sensitivity as the assays were unable to accurately measure the low coenzyme concentrations present in the yeast crude extract samples, suggesting the need for further method development to increase the sensitivity of coenzyme detection and quantification.

## 3.7. Literature Cited


Agrimi, G., L. Brambilla, G. Frascotti, I. Pisano, D. Porro, M. Vai and L. Palmieri. 2011. Deletion or overexpression of mitochondrial $NAD^+$ carriers in *Saccharomyces cerevisiae* alters cellular NAD and ATP contents and affects mitochondrial metabolism and the rate of glycolysis. Appl Environ Microbiol. 77:2239-2246.

Bakker, M.B., K.M. Overkamp, A.J.A. van Maris, M.A.H. Luttik, J.P. van Dijken and J.T. Pronk. 2001. Stoichiometry and compartmentation of NADH metabolism in *Saccharomyces cerevisiae*. FEMS Microbiol Rev. 25:15-27.

Bergmeyer, H.U. 1974. Methods in enzymatic analysis, 2nd Edition vol. IV. Verlaf Chemie Weinbeim, Acadmic Press Inc, pp. 2045-2072.

Blomberg, A. and L. Alder. 1989. Roles of glycerol and glycerol-3-phosphate dehydrogenase ($NAD^+$) in acquired osmotolerance of *Saccharomyces cerevisiae*. J Bacteriol. 171:1087-1092.

Blomberg, A. 2000. Metabolic surprises in *Saccharomyces cerevisiae* during adaptation to saline conditions: questions, some answers, and a model. FEMS Microbiol Lett. 182:1-8.

Brewster, J.L., T. de Valoir, N.D. Dwyer, E. Winter and M.C. Gustin. 1993. An osmosensing signal transduction pathway in yeast. Science. 259:1760-1763.

Bro, C., B. Regenberg, G. Lagniel, J. Labarre, M. Montero-Lomeli and J. Nielsen. 2003. Transcriptional, proteonomic, and metabolic responses to lithium in galactose-grown yeast cells. J Biol Chem. 278:31141-32149.

Bruinenberg, P.M., J.P. van Dijken and W.A. Scheffers. 1983. An enzymatic analysis of NADPH production and consumption in *Candida utilis*. J Gen Microbiol. 129:965-971.

Bruinenberg, P.M., R. Jonker, J.P. van Dijken and W.A. Scheffers. 1985. Utilization of formate as an additional energy source by glucose-limited chemostat cultures of *Candida utilis* CBS 621 and *Saccharomyces cerevisiae* CBS 8066: evidence for absence of transhydrogenase activity in yeasts. Arch Microbiol. 142:302-306.

Curvale, R.A. 2009. Buffer capacity of bovine serum albumin (BSA). J of Argent Chem Soc. 97:174-180.

Eglinton, J.M., A.J. Heinrich, A.P. Pollmitz, P. Langridge, P.A. Henschke and M. de Barros Lopes. 2002. Decreasing acetic acid accumulation by a glycerol overproducing strain of *Saccharomyces cerevisiae* by deleting the *ALD6* aldehyde dehydrogenase gene. Yeast. 19:295-301.

Erasmus, D.J., G.K. van der Merwe and H.J. van Vuuren. 2003. Genome-wide expression analyses: metabolic adaptation of *Saccharomyces cerevisiae* to high sugar stress. FEMS. 34:375-399.

Erasmus, D.J. and H.J.J. van Vuuren. 2009. Genetic basis for osmosensitivity and genetic instability of the wine yeast *Saccharomyces cerevisiae* V1N7. Am J Enol Vitic. 60:145-154.

Erasmus, D.J., M. Cliff and H.J.J. van Vuuren. 2004. Impact of yeast strain on the production of acetic acid, glycerol, and the sensory attributes of Icewine. Am J Enol Vitic. 55:371-378.

Forster, J., I. Famili, P. Fu, B.O. Palsson and J. Nielsen. 2003. Genome-scale reconstruction of *Saccharomyces cerevisiae* metabolic network. Genome Res. 13:244-253.

Hartford, J.B. and J.S. Bonifacino. 2009. Subcellular fractionation and isolation of organelles 3.0-3.0.7. Current Protocols in Cell Biology. Chapter 3.

Heux. S., R. Cachon and D. Dequin. 2006. Cofactor engineering in *Saccharomyces cerevisiae*: expression of $H_2O$-forming NADH oxidase and impact on redox metabolism. Metab Eng. 8:303-314.

Kasimova, M.R., J. Grigiene, K. Krab, P.H. Hagedorn, P.E. Andersen and I.M. Moller. 2006. The free NADH concentration is kept constant in plant mitochondria under different metabolic conditions. 18:688-698.

Klingenberg, M. 1974. Nicotinamide-adenine dinucleotides ($NAD^+$, $NADP^+$, NADH, NADPH): spectrophotometric and fluorimetric methods, p. 2045-2059. *In* H.U. Bergmeyer (ed.), Methods of enzymatic analysis, 2nd ed., vol. 4. Academic Press, New York, N.Y.

Klingenberg, M. 1985. Nicotinamide-adenine dinucleotides and dinucleotide phosphate, p. 251-278 in H.U. Bergmeyer, (ed.), Methods of enzymatic analysis, 3rd ed., vol. 7. Verlag Chemie. Deerfield Beach, FL.

Kukec, A., M. Berovic, M. Wondra, S. Celan and T. Kosmerl. 2003. Influence of temperature shock on the glycerol production in cv. Sauvignon blanc fermentation. Vitis. 42:205-206.

Lagunas, R. and J.M. Ganedo. 1973. Reduced pyridine nucleotide balance growing on *Saccharomyces cerevisiae*. Eur J Biochem. 37:90-94.

Liu, L.M. and J. Chen. 2011. Cofactor engineering enhances the physiological function of an industrial strain. Progress in molecular and environmental bioengineering-from analysis

and modeling to technology applications. Edited by Capri A. In Tech Open Access Publisher, Rijeka. 427-444.

Meaden, P.G., F.M. Dickinson, A. Misfud, W. Tessier, J. Westwater, H. Bussey and M. Midgley. 1997. The *ALD6* gene of *Saccharomyces cerevisiae* encodes a cytosolic, $Mg^{2+}$-activated acetaldehyde dehydrogenase. Yeast. 13:1319-1327.

Murdza-Inglis, D.L. 1995. Structure/ function studies of rat uncoupling protein in yeast mitochondria. PhD Thesis. McMaster University, Hamilton, ON.

Navarro-Avino, J.P., R Prasad, V.J. Miralles, R.M. Benito and R. Serreno. 1999. A proposal of nomenclature of aldehyde dehydrogenases in *Saccharomyces cerevisiae* and characterization of the stress-inducible *ALD2* and *ALD3* genes. Yeast. 15:829-842.

Neviogt, E. and U. Stahl. 1997. Osmoregulation and glycerol metabolism in the yeast *Saccharomyces cerevisiae*. FEMS Microbiol Rev. 213:231-271.

Nielsen, J. 2003. It is all about metabolic fluxes. J Bacteriol. 185:7031-7035.

Nielsen, J. 2011. Transcriptional control of metabolic fluxes. Mol Syst Biol.7:1-2.

Nissen, T.L., M. Anderlund, J. Nielsen, J. Villadsen and M.C. Kielland-Brandt. 2001. Expression of cytoplasmic transhydrogenase in *S. cerevisiae* results in formation of 2-oxoglutarate due to depletion of NADPH. Yeast. 18:19-32.

Påhlman, A.K., K. Granath, R. Ansell, S. Hohmann and L. Alder. 2001. The yeast glycerol 3-phosphatases Gpp1p and Gpp2p are required for glycerol biosynthesis and differentially involved in the cellular responses to osmotic, anaerobic, and oxidative stress. Biol Chem. 276:3555-3563.

Pigeau, G.M. and D.L. Inglis. 2007. Response of wine yeast (*Saccharomyces cerevisiae)* dehydrogenase to acetaldehyde stress during Icewine fermentation. J Appl Microbiol. 103:1576-1586.

Pigeau, G.M. and D.L. Inglis. 2005. Upregulation of *ALD3* and *GPD1* in *Saccharomyces cerevisiae* during Icewine fermentation. J Appl Microbiol. 99:112-125.

Pigeau, G.M., E. Bozza, K. Kaiser and D.L. Inglis. 2007. Concentration effect of Riesling Icewine juice on yeast performance and wine acidity. J Appl Microbiol. 103:1961-1698.

Remize, F., E. Andrieu and S. Dequin. 2000. Engineering of the pyruvate dehydrogenase bypass in *Saccharomyces cerevisiae*: role of the cytosolic $Mg^{2+}$ and mitochondrial $K^{+}$ acetaldehyde dehydrogenases Ald6p and Ald4p in acetate formation during alcoholic fermentation. Appl and Environ Microbiol. 66:3151-3159.

Remize, F., J.L. Roustan, J.M. Sablayrolles, P. Barre and S. Dequin. 1999. Glycerol overproduction by engineered *Saccharomyces cerevisiae* wine yeast strains leads to substantial changes in by-product formation and to a stimulation of fermentation rate in stationary phase. Appl Environ Microbiol. 65:143-149.

Remize, F., L. Barnavon and S. Dequin. 2001. Glycerol export and glycerol-3-phosphate dehydrogenase, but not glycerol phosphatase, are rate limiting for glycerol production in *Saccharomyces cerevisiae*. Metab Eng. 3:300-312.

Roche Applied Science. 2012. Complete ultra tablets, EDTA-free glass vials. Retrieved from: https://cssportal.roche.com/LFR_PublicDocs/ras/05892953001_en_01.pdf

van Dijken, J.P. and W.A. Scheffers. 1986. Redox balances in the metabolism of sugar by yeast. FEMS Microbiol Rev. 32:139-224.

Vemuri, G.N., M.A. Eiteman, J.E. McEwan, L. Olsson and J. Nielsen. 2007. Increasing NADH oxidation reduces overflow metabolism in *Saccharomyces cerevisiae*. PNAS. 104:2401-2407.

Verduyn, C., E. Postma, W.A. Scheffers and J.P. van Dijken. 1992. Effect of benzoic acid on metabolic fluxes in yeasts: a continuous culture study on the regulation of respiration and alcoholic fermentation. Yeast. 8:501-517.

Xie, W. 2008. Determination of $NAD^+$ and NADH in a single cell under hydrogen peroxide stress by capillary electrophoresis. MSc Thesis. Iowa State Univeristy, IA.

# Chapter 4

## Evaluation of Two Commercial Assay Kits for the Colorimetric Detection of Nicotinamide Coenzymes in Wine Yeast Cell Lysate

**Heit, C.[1,2] and D.L. Inglis[1,2,3]**

1 Cool Climate Oenology and Viticulture Institute, Brock University, St. Catharines, ON, Canada
2 Centre for Biotechnology, Brock University, St. Catharines, ON, Canada
3 Department of Biological Sciences, Brock University, St. Catharines, ON, Canada

Formatted for the Journal of Applied Microbiology

### 4.1. Abstract

**Aims:** This study describes an evaluation of nicotinamide coenzyme determinations by a colorimetric enzyme cycling method developed by Sigma-Aldrich® using a commercial "NAD/ NADH Quantification Kit" and "NADP/ NADPH Quantification Kit" for use with yeast cell extract. The biochemical interest of this determination lies in assessing the redox balance of the $NAD^+$/ NADH and $NADP^+$/ NADPH system to determine their respective roles as metabolic triggers for yeast-catalyzed acetic acid production.

**Methods:** The "NAD/ NADH Quantification Kit" provides a method for the sensitive detection of intracellular nucleotides and their ratio, and is specific for only $NAD^+$ and NADH determination. Through an undefined enzyme cycling reaction, $NAD_{total}$ ($NAD^+$ and NADH) or NADH can be quantified in a colorimetric assay using a 96-well microtitre plate (450 nm). In the same way, the "NADP/ NADPH Quantification Kit" can be used to quantify $NADP_{total}$ ($NADP^+$ and NADPH) or NADPH through the detection of NADPH.

**Results and Comments:** During evaluation of the assay method here, we report that working assays for the measurement of $NAD_{total}$ and $NADPH_{total}$ were established using a colorimetric method developed by Sigma-Aldrich®. The method was optimized to include a cell lysis buffer that was compatible with all assays, a filtration step to deproteinize the lysate prior to coenzyme analysis, and ideal incubation times for the enzyme cycling reactions. As part of the method development, all assays underwent validation to ensure the established protocols were accurate and reproducible. The results obtained indicated high linearity, accuracy and precision of the analytical method for measuring NADH and NADPH, and that it was sensitive enough to accurately quantify the low coenzyme concentrations ($NAD_{total}$ and $NADP_{total}$) present in the yeast extract,

**Conclusions:** The adapted technique was demonstrated to be relatively simple, fast and inexpensive, and overall the results of the validation experiments suggest it to be a reliable

and reproducible method for measuring the coenzyme content in cell lysate. However, issues pertaining to sample deproteinization and $NAD^+$ and $NADP^+$ decomposition in cell extract for the measurement of NADH and NADPH indicate the need for additional research and experiments.

**Keywords:** Nicotinamide coenzymes, enzyme assays, cycling reaction, quantification kits, *Saccharomyces cerevisiae*.

## 4.2. Introduction

Redox homeostasis is an essential requirement for sustained metabolism and growth in all living cells (Vemuri *et al*. 2007). Two pyridine nucleotide systems, NADH/ $NAD^+$ and NADPH/ $NADP^+$, determine the intracellular redox state in cells, primarily through the NADH: $NAD^+$ ratio and to a lesser extent by the NADPH: $NADP^+$ ratio. In *Saccharomyces cerevisiae*, these cofactor pairs play important roles as electron acceptors/ donors in over 300 biochemical reactions involving syntheses and oxidation-reduction (Lui and Chen 2011; Forster *et al*. 2003), allowing them to have a critical effect on maintaining intracellular redox balance (Heux *et al.* 2006). This importance has prompted a large amount of research in this area, which is focused on determining the nucleotide content in the cells, various organelles, and tissues of different organisms, including yeast, bacteria and mammals (Xie *et al.* 2009).

Measuring the physiological levels of intracellular metabolites is of interest in the field of metabolomics (Canelas *et al*. 2008). However, accurate quantification of NADH/ $NAD^+$ and NADPH/ $NADP^+$ levels is usually difficult to achieve. Since the turnover time of many primary and secondary metabolites of microorganisms ranges from sub seconds to several tens of seconds (Weibel *et al*. 1974; Taymaz-Nikerel *et al*. 2009; Douma *et al*. 2010), rapid changes in coenzyme ratios can occur when a sample is removed from its original environment (Sporty *et al.* 2008), thereby affecting the reliability of the resulting

measurements. For this reason, sampling and quenching of metabolic activity should be rapid to prevent (inter)conversion between metabolites (de Jonge *et al*. 2012). Furthermore, only a portion of all the coenzymes present in the cell is free while the rest is bound to protein (Kasischke *et al*. 2004), which also affects the accuracy of the measurements. Since it is the free form that has a role in redox balance, measuring the total intracellular nucleotide content ($NADH + NAD^+$ or $NADPH + NADP^+$) is not useful as it provides no indication of the current redox state (Sun *et al*. 2012).

Several methods exist for measuring $NADH/NAD^+$ and $NADPH/NADP^+$ in extract samples, although not without limitations. For some methods, only whole cell extract can be assessed for its nucleotide content (Nissen *et al*. 2001; Cronwright *et al*. 2002; Cherati *et* al. 2005; Agrimi *et al*. 2011; Serrano-Bueno *et al*. 2012) rather than specific subcellular compartments such as the cytosol or mitochondria (Klingenberg 1975; Agrimi *et al*. 2011; Sliwa *et al*. 2012; Suraniti *et al*. 2013). For others, free or bound forms of the coenzymes cannot be distinguished, and often only the total amount of $NAD(P)^+$ present in the sample can be quantified. Separately quantifying these compounds is important as their concentrations provide essential information about the metabolic, bioenergetic and/ or redox status of the organism (Omachi *et al*. 1969; Marshall *et al*. 1974; Sies *et al*. 1983).

The approaches available for $NAD(P)^+$ and NAD(P)H analysis can be divided into two groups: those which are enzymatic, including both endpoint (spectrophotometric and fluorometric) and cycling, and those which utilize chromatography, including thin-layer, high performance liquid chromatography and high-pressure anion exchange chromatography (Zerez *et al*. 1987). Since the quantities of nicotinamide adenine dinucleotides in lysate samples are small, methods that allow for the determination of very

low levels are advantageous. Of the various enzymatic techniques available, the spectrophotometric method is reputed to be accurate when the nucleotide content is sufficiently high (more than 1 x $10^{-8}$ mole) (Klingenberg and Slenczka1959), while measurements at lower concentrations (down to 0.5 $10^{-11}$ mole) are possible using a fluorometric method (Heldt and Klingenberg 1967). However, greater sensitivity can be achieved using an enzymatic cycling method which allows for a sensitivity of 1 x $10^{-8}$ to 1x $10^{-13}$ mol per assay (Matsumura and Miyachi 1983; Gibon and Larher 1997).

Currently, a kit-based method is available from Sigma-Aldrich® that is able to detect either NADH and $NAD_{total}$ ($NAD^+$ and NADH) or NADPH and $NADP_{total}$ ($NADP^+$ and NADPH) using two colorimetric enzyme assays ("NAD/ NADH Quantification Kit" and "NADP/ NADPH Quantification Kit"). The enzymatic method is based on a cycling reaction, where enzymes within the reaction system recognize either $NAD^+$/ NADH or $NADP^+$/ NADPH in the sample, which increases the detection sensitivity as the reaction is specific for particular coenzymes (Sigma-Aldrich® 2012A and 2012B). Through these reactions, the concentration of $NAD_{total}$ ($NAD^+$ and NADH) or NADH can be easily quantified by comparison with the standard NADH, while $NADP_{total}$ ($NADP^+$ and NADPH) or NADPH can be determined by comparison with the standard NADPH. The assay method requires the use of a microtitre plate reader and sample absorbance to be recorded at 450 nm. This absorbance is notably higher than that used in the previous UV spectrophotometric method (described in Chapter 3), which reduces background noise and interference caused by the biological sample. Although the cycling assays allow for the quantification of the total amount of pyridine nucleotides in cells, they cannot be used to directly differentiate between reduced and oxidized forms of the cofactors (Sporty *et al*.

2008), which is an obvious limitation of the method. To indirectly measure the coenzymes, the enzyme cycling reactions require a heating step to degrade the $NAD^+$ or $NADP^+$ present, thereby allowing only NADH and NADPH to be detected and the respective ratios (NADH: $NAD^+$ or NADPH: $NADP^+$) to be determined (Sigma-Aldrich® 2012A and 2012B).

In the previous study conducted (Chapter 3), the method to measure both oxidized and reduced forms of these coenzymes was determined to lack the sensitivity required to quantify the low levels present in yeast cytosolic extract. These traditional assays were conducted using specific enzyme assays where the reactions either consumed or produced NADH and NADPH and monitoring absorption changes in the samples using a UV-Vis spectrophotometer at 340 nm. Using this method, standard curves of each coenzyme were constructed, and the LLOQ of $NAD^+$, $NADP^+$ and NADH was determined to be 10 µM, while the LLOQ for NADPH was determined to be 25 µM. In comparison, the LLOQ of the NADH and NADPH standard curves produced via the kit method are much lower at 0.4 µM. Based on the attributes of this method, the aim of our study was to critically evaluate the applicability of two commercial assay kits for improving the detection sensitivity and quantification of $NAD^+$/ NADH and $NADP^+$/ NADPH in yeast extract.

## 4.3. Materials and Methods

**4.3.1. Yeast strain.** Refer to Chapter 3, Section 3.3.1.

**4.3.2. Culture media.** Refer to Chapter 3, Section 3.3.2.

**4.3.3. Yeast inoculation procedure and growth conditions for batch cultures.** Refer to Chapter 3, Section 3.3.3.

**4.3.4. Determination of yeast wet weight.** Refer to Chapter 3, Section 3.3.4.

**4.3.5. Determination of yeast dry weight.** Refer to Chapter 3, Section 3.3.5.

**4.3.6. Preparation of yeast extracts for assays.** Refer to Chapter 3, Section 3.3.6.

**4.3.7. Deproteinization of cell extract with spin filters.** Prior to enzymatic analysis, cytosolic extract samples were deproteinized using molecular weight cut-off (MWCO) spin filters manufactured by Pall Life Sciences (Mississauga, ON, CAN). Two devices were selected based on volume, the Microsep™ Advance spin filter (0.5-5.0 ml) and the Nanosep® spin filter (<0.5 ml), with a MWCO of 10 kDa and 30 kDa. After cytosolic extraction, a measured volume of the sample was added to each centrifugation tube. Samples in the Microsep™ Advance tubes were centrifuged at 7920 rpm at 4 ºC using the Sorvall RC5C Plus ultracentrifuge (rotor model SS-34), and samples in the Nanosep® tubes were centrifuged at 10 000 rpm at 4 ºC using the Sorvall Refrigerated Micro-Centrifuge RMC-14. All samples were centrifuged until the volume of filtrate did not change, indicating no more sample was able to pass through the pore size of the filter. Prior to performing the assays, the volume of sample recovered was determined so that the nucleotide content could be normalized to sample volume.

**4.3.8. Overview: Determination of intracellular $NAD(P)^+$ and NADPH concentrations.** Intracellular nucleotide concentrations were determined colorimetrically using a microtitre plate reader (MR600 Microplate® Reader, Dynatech Laboratories, Inc.; Alexandria, VI, USA) and "NAD/ NADH Quantification Kit" (MAK037) and "NADP/ NADPH Quantification Kit" (MAK038) supplied my Sigma-Aldrich® (St. Louis, MO, USA). Calibration curves of NADH and NADPH were generated by plotting the standard concentrations against the absorbance at 450 nm. Reactions were prepared in a clear 96-well flat-bottom microtitration plate (Corning®, VWR; Mississauga, ON, CAN), and

nucleotides were detected following enzyme cycling reactions specific for the recognition of $NAD^+$/ NADH or $NADP^+$/ NADPH. The cofactor contents, $NAD_{total}$ ($NAD^+$ and NADH) and NADH or $NADP_{total}$ ($NADP^+$ and NADPH) and NADPH, in the yeast sample extract were then quantified by comparing with the standard NADH or NADPH.

**4.3.8.1. Assay procedure for $NAD^+$/ NADH and $NADP^+$/ NADPH determination.** Quantification of $NAD^+$/ NADH and $NADP^+$/ NADPH concentrations in the yeast extract and standard samples was achieved using a colorimetric enzyme cycling method developed by Sigma-Aldrich® which was eventually optimized to include the cell breaking buffer system (0.6 M mannitol; 20 mM HEPES-KOH, pH 7.4; 1 mM PMSF; 0.1% w/v fatty acid free-BSA) used in the extraction protocol (4.3.6). Prior to using each kit, various reagents were reconstituted with specified dilutents as per the kit instructions. For $NAD^+$/ NADH quantification, NADH standards were prepared from a 10 µM kit standard stock, and for $NADP^+$/ NADPH quantification, NADPH standards were prepared from a 10 µM kit standard stock. To prepare these solutions, 10 µl of the 1 mM NADH or NADPH kit standard were first diluted 100-fold with "NADH/ NAD Extraction Buffer" or "NADPH/ NADP Extraction Buffer" or cell breaking buffer to prepare a 10 µM standard solution. The standard solution was then used to perform a series of dilutions to obtain a range of calibration standards (0, 0.4, 0.8, 1.2, 1.6 and 2.0 µM NADH or NADPH) to construct a calibration curve. To prepare standard samples, 0, 2, 4, 6, 8 and 10 µl of the 10 µM stock were transferred into plate wells and brought to a final volume of 50 µl with buffer. For cell extract samples, 50 µl of the deproteinzied sample (undiluted or diluted with buffer) were transferred to a plate well. Standards and samples were tested in duplicate. To detect only NADH or NADPH in the cell extract sample, $NAD^+$ or $NADP^+$ were first decomposed

prior to initiating the enzyme cycling reaction. To achieve decomposition, 200 µl of extracted samples were aliquoted into 2 ml Eppendorf tubes and heated to 60ºC for 30 minutes in a water bath. After the heating period, samples were cooled on ice and centrifuged at 10 000 rpm for 5 min at 4ºC to remove any precipitates using the Sorvall Refrigerated Micro-Centrifuge RMC-14 (Newtown, CT, USA). These conditions facilitated the decomposition of $NAD^+$ or $NADP^+$, leaving only NADH or NADPH in the sample extract. Up to 50 µl of the decomposed sample were then transferred into a plate well and brought to 50 µl with cell breaking buffer. Following standard and sample preparation, all enzyme cycling reactions were initiated with the addition of 100 µl of the kit Master Reaction Mix, which consisted of 98 µl of "NAD Cycling Buffer" or "NADP Cycling Buffer" and 2 µl of "NAD Enzyme Cycling Mix" or "NADP Enzyme Cycling Mix". The contents in each well were mixed well by pipetting and the reactions were incubated for 5 minutes at room temperature to convert $NAD^+$ to NADH or $NADP^+$ to NADPH. Following this conversion, 10 µl of NADH or NADPH developer were added to each well and the reactions were incubated at room temperature. After a specified time (approximately 30 min), the absorbance was measured at 450 nm by the microplate reader. The reactions were then terminated by the addition of 10 µl of Stop Solution.

**4.3.9. Establishing an enzymatic assay method for nucleotide determination.** Although the assays used in this method had been previously validated by the manufacturer (Sigma-Aldrich®), they were optimized for mammalian cells and contain reagents whose formulations are proprietary. Therefore, during the validation process it was necessary to perform additional experiments to investigate certain aspects of this assay method. Firstly, it was important to ensure that the kit reagents of each assay were compatible with the cell

breaking buffer system used in the extraction protocol (Section 4.3.6), and hence that there were no interferences caused by components of the buffer, and secondly that the commercial assay systems could be adapted to yeast cells. During all validation experiments, sufficient quality control procedures were carried out to ensure that the expected performance of each assay was maintained throughout the duration of the analyses. The fundamental parameters for evaluating this included: (1) linearity and range (calibration curve), (2) precision (repeatability), (3) sensitivity (lower limit of quantification), and (4) accuracy (recovery).

**4.3.9.1. Linearity, precision, sensitivity and accuracy provided by the method.** During the initial stage of the validation process, it was necessary to first construct calibration curves that defined the relationship between the known concentrations of each coenzyme and optical density at the desired wavelength. The calibration curves for both NADH and NADPH included standards from 0-2.0 µM. The linearity was evaluated by linear regression analysis. Regression analysis was calculated using the least square method (Microsoft Excel 2013), and was utilized to determine the linear correlation coefficient (R) and coefficient of determination ($R^2$) of standard curves for each standard. An R-value of $\geq$0.985 was used as criterion of linearity, while a high $R^2$-value of $\geq$0.980 was used as criterion for goodness of fit of the regression line. The precision of the procedure was determined by analyzing duplicate samples of standard. The repeatability was expressed numerically as the coefficient of variation (CV) of the duplicate measurements, which was defined as the: (standard deviation of the analyte assay values/ mean concentration of the analyte assay values) x 100. The precision was assessed for each concentration level and did not exceed more than 20% of the CV. Assay sensitivity was evaluated on the basis of

the lower limit of quantification (LLOQ) using the concentration of the lowest detectable standard from the data set that was in the prescribed accuracy and precision of the assay. The accuracy of each assay method as based on recovery of known standards in the assay based on standard addition. When preparing standard samples, known quantities of pure analyte were added to the sample matrix (cell breaking buffer) and the increase in measured concentration was determined. A comparison of the assayed coenzyme concentration versus the predicted amount provided the recovery of the method and an estimation of its accuracy, which was expressed as the: (average measured concentration of analyte/ predicted concentration of analyte) x 100. A recovery value found within the range of 90-110% was considered acceptable.

## 4.4. Results

### 4.4.1. In-study validation of assays

#### 4.4.1.1. Evaluation of commercial test kits for nucleotide determination

To determine if the assays were running according to the manufacturer's specifications, an initial experiment using the "NAD/ NADH Quantification Kit" and "NADP/ NADPH Quantification Kit" was performed using standard solutions of the cofactors to determine if suitable linearity, precision and accuracy could be obtained. Using the respective kit reagents and standard solutions made up in the "NADH/ NAD Extraction Buffer" or "NADPH/ NADP Extraction Buffer", two linear calibration curves were obtained between final concentrations of 0 to 2.0 µM NADH and NADPH (Fig. 4.1A and 4.1B). For the NADH calibration curve, the R-value was estimated to be 0.9971 and the $R^2$-value was estimated to be 0.9943. For the NADPH calibration curve, the R-value was estimated to be 0.9907 and the $R^2$-value was estimated to be 0.9814. Both results show high linearity and good fit of the data. For duplicate measurements at each concentration level, the calculated precision did not exceed more than 20% of the CV, and the acceptance criterion for recovery was met (±10%). The results demonstrated that NADH and NADPH can be precisely and accurately quantified within the established working range using the colorimetric kits developed by Sigma-Aldrich®.

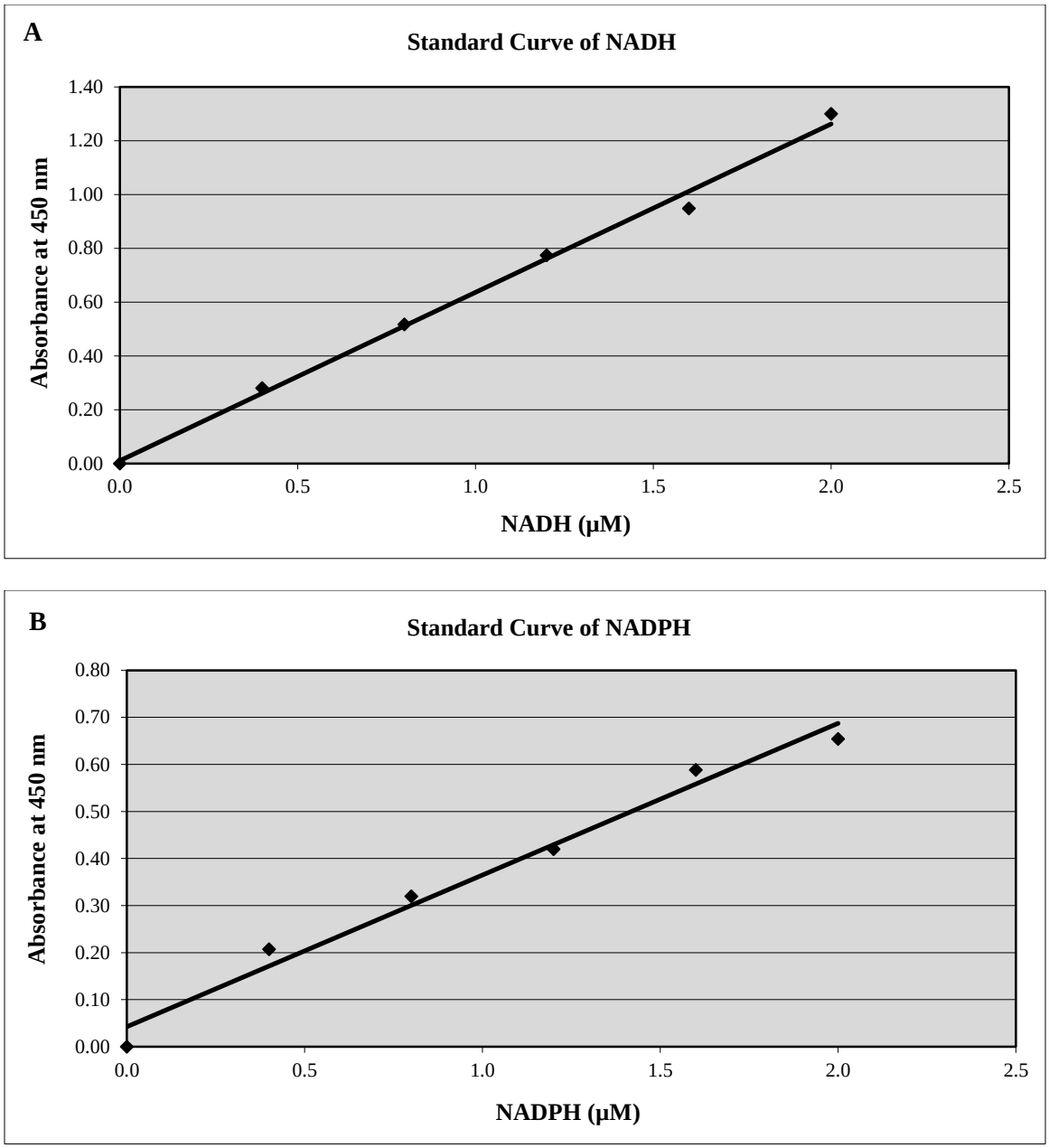


**Figure 4.1: Best-fit calibration curve of NADH and NADPH with cofactor dissolved in extraction buffer.** The Y axis represents the absorbance change at 450 nm during the enzyme cycling reactions for NADH (A) and NADPH (B). Lines represent linear least squares fits to the data. The correlation coefficient (R) and coefficient of determination ($R^2$) were calculated using linear regression analysis. For (A), an R-value of 0.9971 and $R^2$-value of 0.9943 were determined; for (B) an R-value of 0.9907 and $R^2$-value of 0.9814 were determined. Standards were prepared in kit extraction buffer and tested in duplicate (n = 2). The mean values (± SD) of the duplicate measurements are shown; where the error bars are not visible, they are within the symbol.

#### 4.4.1.2. Evaluation of commercial test kits using yeast cell breaking buffer in place of the cofactor extraction buffer

A second experiment was conducted to investigate the use of cell breaking buffer in lieu of the "NADH/ NAD Extraction Buffer" or "NADPH/ NADP Extraction Buffer" provided in the kit for preparation of the calibration standards NADH and NADPH (Fig. 4.2A and 4.2B). For the NADH calibration curve, the R-value was estimated to be 0.9974 and the $R^2$-value was estimated to be 0.9949. For the NADPH calibration curve, the R-value was estimated to be 0.9966 and the $R^2$-value was estimated to be 0.9933. Both calibration curve results show high linearity and good fit of the data. For duplicate measurement at each concentration level, the calculated precision did not exceed more than 20% of the CV, and the acceptance criterion for recovery was met (±10%). These results demonstrated that NADH and NADPH in yeast cell breaking buffer can be precisely and accurately quantified within the established working range using the colorimetric kits developed by Sigma-Aldrich®.

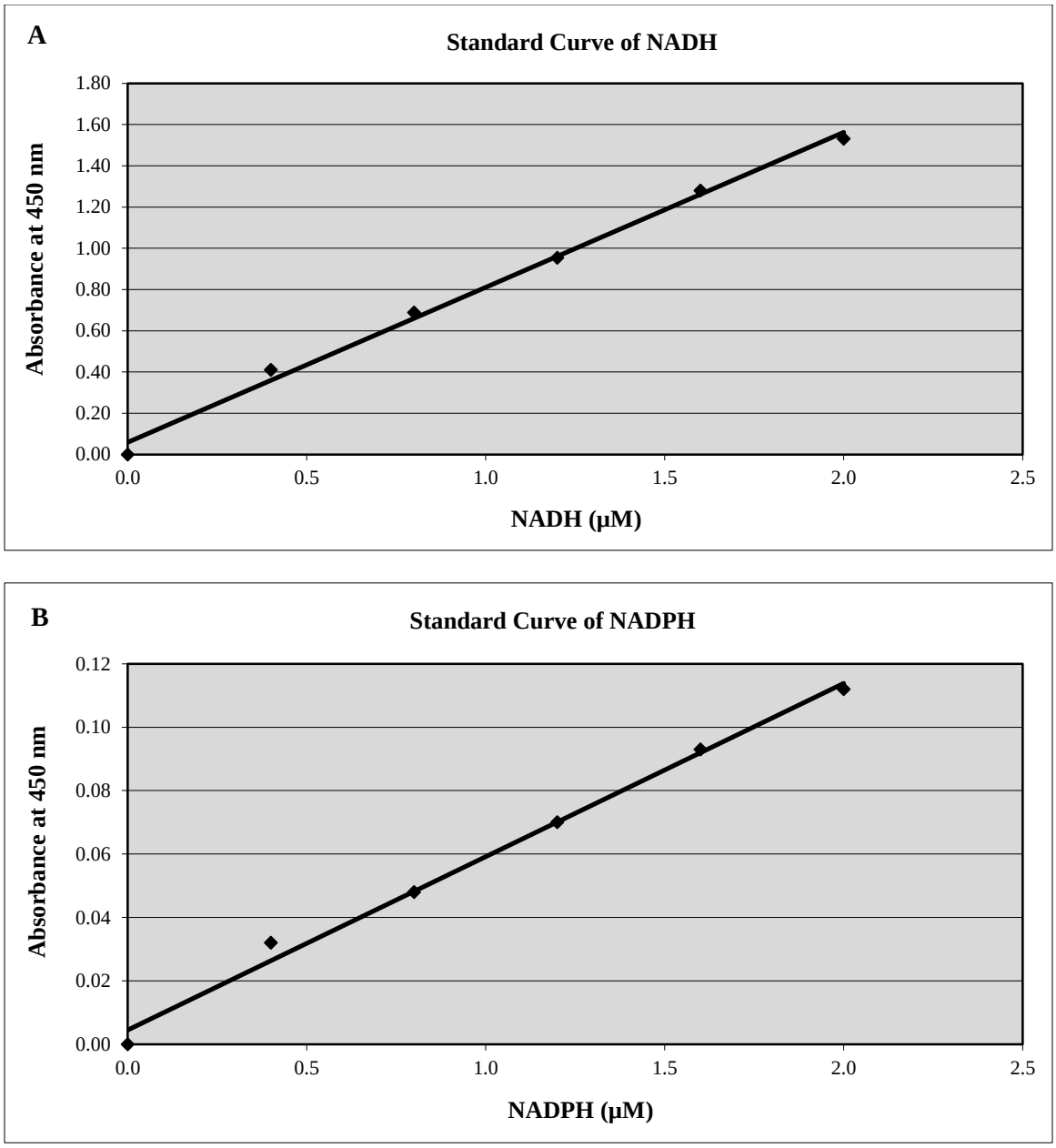


**Figure 4.2: Best-fit calibration curve of NADH and NADPH with cofactor dissolved in yeast cell breaking buffer.** The Y axis represents the absorbance change at 450 nm during the enzyme cycling reactions for NADH (A) and NADPH (B). Lines represent linear least squares fits to the data. The correlation coefficient (R) and coefficient of determination ($R^2$) were calculated using linear regression analysis. For (A), an R-value of 0.9974 and $R^2$-value of 0.9949 were determined; for (B) an R-value of 0.9966 and $R^2$-value of 0.9933were determined. Standards were prepared in cell breaking buffer and tested in duplicate (n = 2). The mean values (± SD) of the duplicate measurements are shown; where the error bars are not visible, they are within the symbol.

#### 4.4.1.3. Calibration of assay incubation times

In both manuals for the "NAD/ NADH Quantification Kit" and "NADP/ NADPH Quantification Kit", the incubation time for the cycling reaction was indicated to range between 1-4 hours. To assist in addressing this logistic and timing issue, time-course experiments were conducted to determine the range of acceptable times for the incubation step in the assay. The length of incubation time was limited by the upper threshold level of the microtitre plate reader, which was set to 1.900.

##### 4.4.1.3.1. Calibration of $NAD^+$/ NADH assay incubation times

For the NADH assay, reactions were carried out according to the kit manual and absorbance readings were taken at 10 minute intervals, beginning 10 minutes after the start of incubation and terminating after 40 minutes (Appendix III, Fig. 1). At each interval, the resulting calibration curve was assessed for its linearity and range, and for the precision and accuracy of each measurement. After 20 and 30 minutes of incubation time, the respective R and $R^2$-values of each curve were determined to be the highest and closest to one, suggesting high linearity and good fit of the data. The calculated precision for duplicate measurements at each concentration level did not exceed more than 20% of the CV, and the acceptance criterion for recovery was met (±10%). As the incubation time increased, the absorbance measurements of the higher concentrated standards began to exceed the upper absorbance limit of the plate reader resulting in no numerical values. These results demonstrated the optimal incubation time for the $NAD^+$/ NADH cycling reaction to be around 20 to 30 minutes using the colorimetric kit method.

#### 4.4.1.3.2. Calibration of $NADP^+$/ NADPH assay incubation times

For the NADPH assay, reactions were carried out according to the manual and absorbance readings were taken at 20 minute intervals, beginning 10 minutes after the start of incubation and terminating after 90 minutes (Appendix III, Fig. 1). At each interval, the resulting calibration curve was assessed for its linearity and range, as well as for the precision and accuracy of each measurement. At the 50 minute interval and thereafter, the respective R and $R^2$-values of each calibration curve were determined to be greater than 0.9990 suggesting high linearity and good fit of the data. The calculated precision for duplicate measurements at each concentration level did not exceed more than 20% of the CV, and the acceptance criterion for recovery was met (±10%). These results demonstrated the optimal incubation time for the $NADP^+$/ NADPH cycling reaction to be around 50 minutes using the colorimetric kit method.

#### 4.4.1.4. Measurement of nucleotide contents in cell lysate

Following the calibration studies, the assay method was applied to cell lysate samples isolated from *S. cerevisiae* EC-1118 to determine the sensitivity of the each assay, and specifically whether the low coenzyme concentrations present in the cytosolic extract samples could be precisely and accurately detected and quantified using the commercial assay kits. Assay sensitivity was also evaluated on the basis of the lower limit of quantification (LLOQ) using the concentration of the lowest detectable standard from the data set. As shown on the calibration curves for each assay, the LLOQ (0.4 µM) was the same for the "NAD/ NADH Quantification Kit" and "NADP/ NADPH Quantification Kit" (Fig. 4.1 and 4.2). Coenzyme concentrations below the LLOQ were considered inaccurate as the values were outside the range of the standard curve.

The accuracy of the procedure was further evaluated using spike-and-recovery experiments. A comparison of the assayed coenzyme concentration versus the theoretical amount provided the recovery of the method and an estimation of its accuracy. For a calibration curve with a range of 0 to 2.0 µM, the concentration of the positive control (spike) sample was selected to be 0.8 µM as this concentration was close to the middle of the curve. Table 4.2 shows the recoveries of the coenzymes from the standard addition experiments performed on cell lysate after correction for the contribution from yeast to the $NAD_{total}$ or $NADP_{total}$ content (Table 4.1). Recovery of a 0.8 µM NADH matrix spike was 93.8%, while recovery of a 0.8 µM NADPH matrix spike was 90.0%. In addition to the high recovery of the standard concentrations, the coenzyme content in the unspiked cell lysate was also quantifiable. The $NAD_{total}$ content was determined to be 0.74 ± 0.01 µM,

while the $NADP_{total}$ content was determined to be 0.84 ± 0.02 µM. Both values were above the LLOQ and within the range of the standard curves.

Table 4.1. Concentration of $NAD_{total}$ or $NADP_{total}$ determined in cell extract samples deproteinized using a 10 kDa spin filter, and the LLOQ of the each standard curve.

| Sample | $NAD_{total}$ or $NADP_{total}$ (µM) | LLOQ of std curve (µM) |
|---|---|---|
| Unspiked extract ($NAD^+$/ NADH assay) | 0.74 ± 0.01 | 0.40 |
| Unspiked extract ($NADP^+$/ NADPH assay) | 0.84 ± 0.02 | 0.40 |

Table 4.2. Percent recoveries of yeast cell extract samples spiked with 0.8 µM NADH or NADPH standard stock.

| Spike Contents | Background Concentration in Lysate (µM) | Standard Addition Concentration (µM) | Difference in Concentration (µM) | Percent Recovered (%) |
|---|---|---|---|---|
| 0.8 µM NADH spiked yeast extract | 0.74 ± 0.01 | 1.49 ± 0.06 | 0.75 ± 0.06 | 93.8 |
| 0.8 µM NADPH spiked yeast extract | 0.84 ± 0.02 | 1.56 ± 0.04 | 0.72 ± 0.04 | 90.0 |

## 4.5. Discussion

### 4.5.1. Method for preparing yeast cell extracts for enzymatic analyses

The coenzyme assays were developed with the objective of measuring the redox status of the cell by measuring the concentration of $NAD^+$, NADH, $NADP^+$ and NADPH in yeast cytosolic extract isolated from *S. cerevisiae* strain EC-1118 cells. Establishment of such assays was dependent on the application of cytosolic extract as both $NAD^+$-dependent Ald2/ 3p and $NADP^+$-dependent Ald6p are localized in the cytosol (Navarro-Avino *et al*. 1999). The remaining aldehyde dehydrogenases, Ald4p and Ald5p, are mitochondrial and were not of interest in this study. To obtain a cytosolic extract, subcellular fractionation was used and was preceded by an extraction protocol to produce a crude cytosolic extract. This method was established in the previous study (Chapter 3) evaluating the use of a UV-endpoint method for measuring the nicotinamide coenzymes in yeast cell lysate (Bergmeyer 1974, Chapter 3).

### 4.5.2. Method development of enzyme assays

Assay kits developed by Sigma-Aldrich® formed the basis for the establishment of coenzyme assays for measuring the nucleotide content in yeast cytosolic extract. Although background information on the kits indicated this method to have baseline potential for achieving our research objectives, refinement of the existing protocol was still required. To enable robust, reliable measurement of the coenzymes in yeast, it was initially necessary to develop a cell lysis method for isolating the cytosolic fraction from yeast cells, as detailed in Section 4.3.6, different from that described in the technical bulletins of the "NAD/ NADH Quantification Kit" and "NADP/ NADPH Quantification Kit" (Sigma-Aldrich® 2012A and 2012B). In these bulletins, the protocol for cell sample preparation is

based on whole cell extract, which would preclude us from achieving our research objectives as our interest is only in the cytosolic fraction of the yeast cell.

Furthermore, as part of the kit protocol "NAD/ NADH Extraction Buffer" and "NADP/ NADPH Extraction Buffer" are required for nucleotide extraction from whole cells whose formulations are proprietary. However, the cell lysis component of our protocol necessitated the inclusion of a homogenization buffer to facilitate cell lysis, which was previously determined to be suitable for coenzyme analysis using a UV-endpoint enzymatic method (Chapter 3). This buffer was to be used in lieu of the kit extraction buffers, making it essential that the kit reagents of each assay were compatible with the components of the buffer system used in the extraction protocol (Section 4.3.6). The contents of the buffer included 0.6 M mannitol, 20 mM HEPES-KOH (pH 7.4), 1mM PMSF and 0.1% (w/ v) fatty-acid free-BSA.

The initial assay experiment conducted verified the enzymatic method established by Sigma-Aldrich® could be successfully repeated and performed under our laboratory conditions. For both assays assessed ($NAD^+$/ NADH and $NADP^+$/ NADPH), the protocols were strictly followed using standards made up in extraction buffer resulting in high linearity, accuracy and precision of the analytical procedure. With a working assay method in hand, the next experiment conducted investigated the use of the cell breaking buffer in lieu of the kit extraction buffer for preparation of the calibration standards. The results of the method validation demonstrated compatibility of the cell breaking buffer with the kit reagents as the acceptance criterion for accuracy, precision and linearity were met, indicating that NADH and NADPH can be quantified within the established working range of the standard curves using the modified colorimetric method. As no interference was

detected, further optimization of the lysis buffer was unnecessary, allowing the method to be further refined to determine the optimal incubation time for each assay.

Following the calibration studies, spike-and-recovery experiments were performed using deproteinized cell extract to give an estimation of the accuracy of the method, and specifically whether the low coenzyme concentrations present in the cytosolic extract could be precisely and accurately detected and quantified using the established assay protocols. The results indicated standard recovery in the spiked extract to be high, and the measured $NAD_{total}$ and $NADP_{total}$ concentrations in the unspiked extract to be above the LLOQ and within the established working range of each standard curve, suggesting no issues with the yeast lysate sample.

However, issues with the detection of only NADH and NADPH did surface following analysis of the decomposed samples. The results indicated the content of NADH and NADPH to be the same or higher than that of $NAD_{total}$ and $NADP_{total}$, suggesting a potential issue with the decomposition procedure used to obtain only the reduced cofactors in the yeast extract sample. Although a heating step to detect only NADH or NADPH is typical for enzymatic cycling reactions, redox reactions may continue during this time, thereby altering the redox state of the cell (Sporty *et al*. 2008). It is also possible that the heat treatment performed on the sample (60˚C water bath for 30 min) was insufficient to properly degrade the $NAD^+$ and $NADP^+$ present, necessitating the need for additional work to be done on this in the future. Since the individual coenzymes could not be quantified, the ratios of $NAD^+$/ NADH and $NADP^+$/ NADPH were unable to be determined, consequently limiting the application of this method.

## 4.6. Conclusions

During development of the assay here, we report that working assays for the measurement of $NAD_{total}$ and $NADP_{total}$ were established based on two colorimetric kits manufactured by Sigma-Aldrich®. The method was optimized to include a yeast cell lysis buffer that was compatible with all assays, a deproteinization step to remove interfering compounds and clarify the sample extract prior to coenzyme analysis, and ideal incubation times for the enzyme cycling reactions. As part of the method development, all assays underwent validation to ensure the established protocols were reliable and reproducible. The results obtained indicated high linearity, accuracy and precision of the analytical method, and that it was sensitive enough to accurately quantify the low coenzyme concentrations present in the extract samples. However, issues pertaining to sample deproteinization and $NAD^+$ and $NADP^+$ decomposition in cell extract for the measurement of only NADH and NADPH suggest the need for additional research and experiments.

## 4.7. Literature Cited


Agrimi, G., L. Brambilla, G. Frascotti, I. Pisano, D. Porro, M. Vai and L. Palmieri. 2011. Deletion or overexpression of mitochondrial $NAD^+$ carriers in *Saccharomyces cerevisiae* alters cellular NAD and ATP contents and affects mitochondrial metabolism and the rate of glycolysis. Appl Environ Microbiol. 77:2239-2246.

Bergmeyer, H.U. 1974. Methods in enzymatic analysis, 2nd ed, vol. IV. Verlag Chemie Weinbeim, Acadmic Press Inc, pp. 2045-2072.

Canelas, A.B., C. Ras, A. ten Pierick, J.C. van Dam, J.J. Heijen and W.M. van Gulik. 2008. Leakage-free rapid quenching technique for yeast metabolomics. Metabolomics. 4:226-239.

Cherati, N., S. Guezenec and J.M. Salmon. 2005. Redox interactions between *Saccharomyces cerevisiae* and *Saccharomyces uvarum*. Appl Enviro Microbiol. 71:255-260.

Cronwright, G.R., J.M. Rohwer and B.A. Prior. 2002. Metabolic control analysis of glycerol synthesis in *Saccharomyces cerevisiae*. Appl Enviro Microbiol. 68:4448-4456.

de Jonge, J.J., R.D. Douma, J.J. Heijnen and W.M. van Gulik. 2012. Optimization of cold methanol quenching for quantitative metabolomics of *Penicillium chrysogenum*. Metabolomics. 4:727-735.

Douma, R. D., L.P. de Jonge, C.T.H. Jonker, R.M. Seifar, J.J. Heijnen and W.M. van Gulik. 2010. Intracellular metabolite determination in the presence of extracellular abundance: application to the penicillin biosynthesis pathway in *Penicillium chrysogenum*. Biotechnol Bioeng. 107:105-115.

Forster, J., I. Famili, P. Fu, B.O. Palsson and J. Nielsen. 2003. Genome-scale reconstruction of *Saccharomyces cerevisiae* metabolic network. Genome Res. 13:244-253.

Gibon, Y. and F. Larher. 1997. Cycling assay for nicotinamide adenine dinucleotides: NaCl precipitation and ethanol solubilization of the reduced tetrazolium. Anal Biochem. 251:153-157.

Heldt, H.W. and M. Klingenberg in S.P. Colowick and N.O. Kaplan: Methods in enzymology, Vol. X, p. 3, Academic press, New York/ London 1967.

Heux. S., R. Cachon and D. Dequin. 2006. Cofactor engineering in *Saccharomyces cerevisiae*: expression of $H_2O$-forming NADH oxidase and impact on redox metabolism. Metab Eng. 8:303-314.

Kasischke, K.A., H.D. Vishwasra, P.J. Fisher, W.R. Zipfel and W.W. Webb. 2004. Neural activity triggers neuronal oxidative metabolism followed by astrocytic glycolysis. Science. 305: 99–103.

Klingenberg, M. 1974. Nicotinamide-adenine dinucleotides ($NAD^+$, $NADP^+$, NADH, NADPH): spectrophotometric and fluorimetric methods, p. 2045-2059. *In* H.U. Bergmeyer (ed.), Methods of enzymatic analysis, 2nd ed., vol. 4. Academic Press, NY, NY.

Klingenberg, M. and W. Slenczka. 1959. Pyridynnucleotide in leber-mitochondrien. Eine analyse ihrer redox-beziehungen. Biochem Z. 331:486-517.

Liu, L.M. and J. Chen. 2011. Cofactor engineering enhances the physiological function of an industrial strain. Progress in molecular and environmental bioengineering-from analysis and modeling to technology applications. Edited by Capri A. In Tech Open Access Publisher, Rijeka. 427-444.

Navarro-Avino, J.P., R Prasad, V.J. Miralles, R.M. Benito and R. Serreno. 1999. A proposal of nomenclature of aldehyde dehydrogenases in *Saccharomyces cerevisiae* and characterization of the stress-inducible *ALD2* and *ALD3* genes. Yeast. 15:829-842.

Marshall, W.E. and A. Omachi. Measured and calculated $NAD^+$/NADH ratios in human erythrocytes. 1974. Biochim Biophys Acta. 354:1-10.

Matsumura, H. and S. Miyachi. 1983. Cycling assay for nicotinamide adenine dinucleotides. p. 465-470 in Method in enzymology. Vol. 69, San Pietro, A., Ed. NY, NY.

Nissen, T.L., 2001. Expression of cytoplasmic transhydrogenase in *S. cerevisiae* results in formation of 2-oxoglutarate due to depletion of the NADPH. Yeast. 18:19-32.

Omachi, A., C.B. Scott and H. Hegarty. 1969. Pyridine nucleotides in human erythrocytes in different metabolic states. Biochim Biophys Act. 184:139-147.

Serrano-Bueno, G., A. Hernandez, G. Lopez-Lluch, J. R. Perez-Castineira, P. Navas and A. Serrano. 2012. Inorganic pyrophosphatase defects lead to cell cycle arrest and autophagic cell death through NAD depletion in fermenting yeast. J Biol Chem. 288:13082-13092.

Sies, H., R. Brigelius, H. Wefers, A. Müller and E. Cadenas. 1983. Cellular redox changes and response to drugs and toxic agents. Fundam Appl Toxicol. 3:200-208.

Sigma-Aldrich®. 2012A. Complete product information- NAD/ NADH Quantification Kits. Retrieved from:

http://www.sigmaaldrich.com/content/dam/sigmaaldrich/docs/Sigma/Bulletin/1/mak037bul.pdf

Sigma-Aldrich®. 2012B. Complete product information- NADP/ NADPH Quantification Kits. Retrieved from: http://www.sigmaaldrich.com/content/dam/sigmaaldrich/docs/Sigma/Bulletin/1/mak038bul.pdf

Sliwa, D., J. Dairou, J.M. Camadro and R. Santos. 2012. Inactivation of mitochondrial aspartate aminotransferase contributes to the respiratory deficit of yeast frataxin-deficient cells. Biochem J. 441:945-953.

Sporty, J.L., M.M. Kabir, K.W. Turteltaub, T. Ognibene, S.J. Lin and G. Bench. 2008. Single sample extraction protocol for the quantification of NAD and NADH redox states in *Saccharomyces cerevisiae*. J Sep Sci. 31:3202-3211.

Sun, F., C. Dai, J. Xie and X. Hu. 2012. Biochemical issues in estimation of cytosolic free NAD/ NADH ratio. Plos One. 7:1-10.

Suraniti, E., V.S. Vajrala, B. Goudeau, S.P. Bottari and M. Rigoulet. 2013. Monitoring metabolic responses of single mitochondria within poly(dimethylsiloxane) wells: study of their endogenous reduced nicotinamide adenine dinucleotide evolution. Anal Chem. 85: 5146-5152.

Taymaz-Nikerel, H., M. De Mey, C. Ras, C., A. ten Pierick, R.M. Seifar, J. C. van Dam, J.J. Heijen and W.M. van Gulik. 2009. Development and application of a differential method for reliable metabolome analysis in *Escherichia coli*. Anal Biochem. 386:9-19.

Vemuri, G.N., M.A. Eiteman, J.E. McEwan, L. Olsson and J. Nielsen. 2007. Increasing NADH oxidation reduces overflow metabolism in *Saccharomyces cerevisiae*. PNAS. 104:2401-2407.

Weibel, K. E., J.R. Mor and A. Fiechter. 1974. Rapid sampling of yeast-cells and automated assays of adenylate, citrate, pyruvate and glucose-6-phosphate pools. Anal Biochem. 58:208-216.

Xie, W., A. Xu and E.S. Yeung. 2009. Determination of $NAD^+$ and NADH in a single cell under hydrogen peroxide stress by capillary electrophoresis. Anal Chem. 81:1289-1284.

Zerez, C.R., S.J. Lee and K.R. Tanaka. 1987. Spectrophotometric determination of oxidized and reduced pyridine nucleotides in erythrocytes using a single extraction procedure. Anal Biol. 164:367-373.

## 5. Discussion and Conclusions

### 5.1. Overall discussion and future research directions

Wines produced from high sugar musts, including Icewine and appassimento-style wines, represent a considerable investment for growers and winemakers. Allowing grapes to dry off-vine postharvest using different drying techniques until the desired sugar content is reached exposes berries to potential mold and bacteria formation and the risk of spoilage. Once these shrivelled, dehydrated berries have been obtained, the winemaker may then be confronted with slower fermentation rates due to the higher sugar content of the resulting must, risk of lower alcohol levels being achieved in the final wines, and the production of off-flavours.

Acetic acid and ethyl acetate are important components of wine because of their association with spoilage and their abilities to negatively impact wine composition and quality. When present in sufficient concentrations, these metabolites affect the organoleptic properties of wine and may cause the volatile acidity (VA) levels to exceed legal limits. At high levels, acetic acid imparts a vinegar aroma to the sensory profile of a wine while ethyl acetate contributes a nail polish remover or solvent-like aroma. In Canada, Vintners Quality Alliance (VQA) defines the maximum allowable limit of VA in Icewine and table wine to be 2.1 g $l^{-1}$ and 1.3 g $l^{-1}$ acetic acid, respectfully (VQA 2013). Although usually present in lower concentrations, the low detection threshold of ethyl acetate makes it easier to perceive in Icewine than acetic acid, and consequently a problematic compound for producers desiring their wines to be VQA-approved. Cliff and Pickering (2006) determined the sensory threshold for acetic acid in Icewine to be 3.185 g $l^{-1}$, while its reported concentration range was between 0.49 to 2.29 g $l^{-1}$ (Nurgel *et al.* 2004). On the other hand,

the sensory threshold of ethyl acetate was determined to be 0.198 g $l^{-1}$ (Nurgel *et al.* 2004), thereby falling within the range produced in Canadian Icewines currently on the market (0.086 to 0.369 g $l^{-1}$) (Cliff and Pickering 2006).

Due to prevalent concerns within the wine industry regarding volatile acidity production in high sugar wines, as well as the desire of our lab group to advance knowledge on this topic, a main goal of this project was to gain a better understanding of the adapted response of wine yeast to sugar-induced osmotic stress and factors controlling acetic acid and ethyl acetate production during high sugar fermentations. The second goal of this project was to establish a method for measuring pyridine nucleotides ($NAD^+$, NADH, $NADP^+$, NADPH) in yeast cytosolic extract that can be used in future research experiments to understand how these stress responses relate to the intracellular redox balance of fermenting wine yeast for controlling metabolic pathways.

### 5.1.1. Osmostress induced by appasssimento-type must reduced the fermentation capacity of wine yeast and increased glycerol and acetic acid formation by *S. cerevisiae*

In this study, the high osmotic stress experienced by commercial *S. cerevisiae* EC-1118 and the natural isolate of *S. bayanus* throughout the course of fermentation in appassimento-type must induced changes in yeast metabolism which correlated to several fermentation challenges including slower fermentation rates and increased production of metabolites involved in the yeast's stress response, including glycerol and acetic acid. Two fermentation conditions were examined in this study and included an 18˚Brix must and a 27˚Brix must, which was produced from grapes that were harvested at 18˚Brix and subsequently kiln-dried to 27˚Brix.

In agreement with Caridi *et al*. (1999), a positive relationship between the increasing initial sugar concentration of juice and elevated acetic acid production has been demonstrated in this study, specifically in the 27°Brix must fermented by EC-1118. This increase in acetic acid was preceded and eventually accompanied by an increase in glycerol production. Past studies have concluded that *S. cerevisiae* cells produce glycerol to serve as a compatible solute when placed under osmotic stress (Blomberg and Alder 1989; Nevoigt and Stahl 1997; Blomberg 2000). The osmotic stress induced by Icewine juice in particular was found to increase *GPD1* expression and glycerol production (Pigeau and Inglis 2005), where NADH is used as a cofactor to catalyze the reduction of DHAP to glyceraldehyde-3-phosphate by glyceraldehyde-3-phosphate dehydrogenase. The biosynthesis of acetic acid by an $NAD^+$-dependent aldehyde dehydrogenase can regenerate the NADH required by yeast to maintain intracellular redox balance and thus homeostasis, which is supported by the positive correlation observed between glycerol and acetic acid following normalization to sugar consumed (Pigeau *et al*. 2007). However, the role that each Aldp plays in *S. cerevisiae* is not clear as yeast lack trans-

hydrogenase to convert between reducing equivalents (van Dijken and Scheffers 1986).

### 5.1.2. Acetic acid formation in *S. cerevisiae* during high sugar fermentations and relationship to acetylCoA

The reason for elevated acetic acid production by wine yeast under hyperosmotic stress is still unresolved, but may be due to a combination of metabolic and transcriptional factors resulting in a build-up of acetic acid due to a lack of further conversion to acetylCoA (Pigeau and Inglis 2005; 2007; Martin 2008). Several aldehyde dehydrogenases are involved in acetic acid production during table wine fermentation, but the elevated levels observed in high sugar wines appear to be due to the activity of Ald3p or Ald6p. Erasmus

*et al*. (2003) reported *ALD2*, *ALD3*, *ALD4* and *ALD6* to be up-regulated following brief exposure to increased osmotic stress, which corresponded to an increase in acetic acid production during fermentation. However, it is unknown whether these initial expressions were transient or sustained throughout the fermentation as levels were not monitored for the entire duration. Of the isogenes up-regulated, *ALD6* was expressed at the highest level and has been reported to be responsible for the majority of acetic acid generated in a laboratory *S. cerevisiae* strain grown under aerobic conditions exposed to 40% (w/ v) glucose (Erasmus and van Vuuren 2009). This study linked acetic acid generation under osmotic stress to NADPH production, possibly as a way to compensate for the down-regulation of NADPH generated through the pentose phosphate pathway (Bro *et al*. 2003; Erasmus and van Vuuren 2009).

In contrast, the work of Pigeau and Inglis (2005; 2007) indicated a larger role for Ald3p as *ALD3* was shown to be differentially up-regulated in Icewine juice compared to table wine juice, which corresponded to an increase in acetaldehyde and acetic acid production during Icewine fermentation. The results showed *ALD3* displayed a 6.2-fold up-regulation on day 4 of fermentation compared to the table wine juice, which could account for the elevated level of acetic acid found in Icewine. *ALD3* was also found to be the only *ALD* further up-regulated by acetaldehyde stress, while the expression of the remaining *ALD* genes was determined to be unaffected (Pigeau and Inglis 2007). Based on these findings, the increased expression of *ALD3* was proposed to be necessary but not sufficient to cause elevated acetic acid during the high sugar fermentation, suggesting additional hyperosmotic stress responses may be required.

During alcoholic fermentation, acetic acid can be converted to acetylCoA in an ATP-dependent reaction catalyzed by an acetylCoA synthetase encoded by *ACS1* and *ACS2*. Within the yeast cell, acetylCoA is required for the biosynthesis of lipids, sterols and amino acids during growth. Since only *ACS2* is present in the cytosol under anaerobic conditions and is required for growth on glucose (van den Berg and Steenma 1995), it is likely responsible for catalyzing the conversion of acetic acid to acetylCoA during alcoholic fermentation. Under high sugar stress, Martin (2008) reported both *ACS* isoforms to be strongly down-regulated in yeast fermenting Icewine juice compared to table wine juice, and therefore may be a contributing factor to the high acetic acid levels released in Icewine. Down-regulation of these genes would reduce the need for acetate as a substrate for acetylCoA synthetase, thereby reducing the formation of acetylCoA and resulting in a build-up in acetic acid.

Although the contribution of acetaldehyde to increased acetic acid production during Icewine fermentation has been investigated (Pigeau and Inglis 2007), the substrate availability of $NAD^+$ or $NADP^+$ to aldehyde dehydrogenase has not. Thus, an essential part of the research lies in understanding the altered redox state of the yeast cells during fermentation and determining its impact on the metabolic regulation of acetic acid production under hyperosmotic stress. For these determinations to be made, the ratio of $NAD^+$/ NADH versus $NADP^+$/ NADPH in yeast during fermentation in high versus low sugar juice will be measured, which will allow the redox status of both coenzyme systems to be assessed and its influence on acetic acid and glycerol production to be determined. The concentration of the oxidized nicotinamide cofactors, $NAD^+$ and $NADP^+$, will also be

compared to the rate of acetic acid production to determine if substrate availability is a controlling factor in increased acetic acid production.

To date, factors controlling the metabolic regulation of elevated acetic acid production have only been examined partially at the substrate level in Icewine and appassimento-style wine, and at the transcriptional level in Icewine. Future projects will include using enzyme assays to analyze the activity levels of yeast cytosolic and mitochondrial aldehyde dehydrogenases and acetylCoA synthetases to ascertain their contributions to acetic acid production. Completion of these experiments will also enable the respective activity levels to be compared to the previously measured gene expression levels (Pigeau and Inglis 2005; 2007; Martin and Inglis 2006; Martin 2008) to determine whether up- or down-regulation of gene expression translates to an increase or decrease in enzyme activity. These results will confirm whether enzyme activity is, at least partially, under transcriptional control and its role in acetic acid production.

### 5.1.3. Ethyl acetate formation in *S. cerevisiae* during high sugar fermentations and relationship to acetylCoA

A second consequence of low *ACS* expression may be the formation of low ethyl acetate levels during high sugar fermentations. Since acetylCoA is a substrate for alcohol acetyltransferases, low acetylCoA levels would reduce the amount of substrate available to acetyltransferases, thereby reducing the amount of ethyl acetate formed during fermentation. In a previous study, two-fold lower ethyl acetate levels were determined to be produced in Icewine by a commercial *S. cerevisiae* strain compared to that found in the table wine, whereby acetylCoA is required for catalysis (Heit 2011; Heit and Inglis 2012). This same production trend was observed in the appassimento study as higher levels of ethyl acetate were measured in table wine compared to appassimento-style wine.

Since ethanol is unlikely a limiting substrate contributing to low ethyl acetate formation due to its high levels in wine, future research will involve measuring acetylCoA production by wine yeast fermenting under high and low sugar stress to determine differences in substrate availability between the two sugar conditions. While limited substrate availability reduces ester synthesis, reduced enzyme activity also decreases the amount of product formed. Unfortunately, the activity levels of enzymes indirectly involved in ester synthesis, including aldehyde dehydrogenases and acetylCoA synthestases, and those directly involved in ester synthesis, including alcohol acetyltransferases, were not measured, and therefore differences in enzyme activity levels within strains fermenting under high and low sugar stress were not determined. Due to this limitation, the contribution of the relevant enzymes to increased ethyl acetate formation under low sugar stress could not be ascertained from this study. This would be important to investigate in the future to gain a more comprehensive understanding of the factors influencing ethyl acetate formation during high sugar fermentations.

### 5.1.4. Strain-related differences in acetic acid and ethyl acetate formation

Two wines yeasts, commercial *S. cerevisiae* strain EC-1118 and a natural isolate of *S. bayanus*, were investigated to evaluate their differences in acetic acid and ethyl acetate production in appassimento-type must produced using kiln drying. The *S. bayanus* strain produced significantly less acetic acid per gram of sugar metabolized than EC-1118 during fermentation in the high sugar must, which is consistent with past studies demonstrating acetic acid production is yeast-strain dependent (Patel and Shibamoto 2002; Torrens *et al*. 2008; Erasmus *et al*. 2004). *S. bayanus* also demonstrated trends consistent with lower ethyl acetate production compared to *S. cerevisiae* (Heit and Inglis 2013), a result

consistent with previous studies conducted in Icewine juice (Heit 2011; Heit and Inglis 2012). However, although acetic acid and ethyl acetate play important roles as (off) flavours in wine, little is known about the factors controlling their production during alcoholic fermentation, as previously discussed, and strain-related differences that exist that may contribute to higher or lower formation.

Acetic acid production is complex process in wine yeast. During alcoholic fermentation, acetate is produced as an intermediate of the cytosolic pyruvate dehydrogenase (PDH) bypass, an alternative route to the PDH reaction for the direct conversion of pyruvate to acetylCoA (Remize *et al*. 2000). This pathway involves the conversion of pyruvate to acetaldehyde, which is subsequently oxidized to acetate by aldehyde dehydrogenase. Through the action of acetylCoA synthetase, acetate is then converted into acetylCoA, ensuring its availability for lipid and sterol biosynthesis. Therefore, acetate production by fermenting yeast represents the balance between aldehyde dehydrogenase and acetylCoA synthetase activity (Cordente *et al*. 2013); yeast with the lowest aldehyde dehydrogenase activity and highest acetylCoA synthetase activity produce the least amount of acetic acid (Verduyn *et al*. 1990), although substrate availability may also exert a controlling influence. This is also true for ethyl acetate, which can be formed enzymatically via an alcohol acetyltransferase through the condensation of acetylCoA and ethanol (Plata *et al*. 2003). Due to the relationship of these compounds to acetaldehyde and ethanol, yeast strains used in this study were evaluated for their production of other metabolites involved in the stress response leading to acetic acid and ethyl acetate formation. Analysis of these metabolites allowed for a better understanding of ethyl acetate

formation during fermentation, and evaluation of its relationship to acetic acid formation and increased osmotic stress in fermenting wine yeast (Heit 2011; Heit and Inglis 2013).

However, the contribution of the various enzymes and substrates to lower acetic acid and ethyl acetate formation by *S. bayanus* and higher formation of both metabolites by EC-1118 could not be ascertained from this study as enzyme activity levels and all substrates involved in catalysis were not measured. This would valuable to investigate in the future to gain a more comprehensive understanding of the factors influencing metabolite formation during high sugar fermentations and to elucidate differences between wine yeast strains. Future experiments will be conducted to determine if acetic acid and ethyl acetate production differences between strains fermenting under increased osmotic stress are due to differences in aldehyde dehydrogenase, acetylCoA synthetase and/ or alcohol acetyltransferase activity, substrate availability or a combination of both.

## 5.2. Conclusions

This future work, along with studies contained herein, will contribute to the understanding of the metabolic responses of *S. cerevisiae* during high sugar fermentations. Once we understand why and how certain metabolites are formed during the hyperosmotic stress response, steps can be taken to minimize or eliminate unwanted compounds such as acetic acid and ethyl acetate through the selection or development of yeast strains best suited for Icewine and wine styles based on high sugar juice, including appassimento-style wine. To our enthusiasm, the reported findings of our yeast trial research do offer a potential strategy for managing VA levels for appassimento-style wine production, making *S. bayanus* a potential candidate for commercialization. Furthering our research in the aforementioned areas will assist in producing higher quality wine as this information is

applicable to winemakers, aiding them in maintaining Canada's powerful influence in the global Icewine market, and supporting their needs as they expand into new wine styles involving high sugar juices.

### 5.3. Literature Cited


Bro, C., B. Regenberg, G. Lagniel, J. Labarre, M. Montero-Lomeli and J. Nielsen. 2003. Transcriptional, proteonomic, and metabolic responses to lithium in galactose-grown yeast cells. J Biol Chem. 278:31141-32149.

Blomberg, A. 2000. Metabolic surprises in *Saccharomyces cerevisiae* during adaptation to saline conditions: questions, some answers, and a model. FEMS Microbiol Lett. 182:1-8.

Blomberg, A. and L. Alder. 1989. Roles of glycerol and glycerol-3-phosphate dehydrogenase ($NAD^+$) in acquired osmotolerance of *Saccharomyces cerevisiae*. J Bacteriol. 171:1087-1092.

Brewster, J.L., T. de Valoir, N.D. Dwyer, E. Winter, and M.C. Gustin. 1993. An osmosensing signal transduction pathway in yeast. Science. 259:1760-1763.

Caridi, A., P. Crucitti and D. Ramondino. 1999. Winemaking of musts at high osmotic strength by thermotolerant yeasts. Biotech Lett. 21:617-620.

Cliff, M.A. and G.J. Pickering. 2006. Determination of odor detection thresholds for acetic acid and ethyl acetate in ice wine. Aust J Wine Res. 17:45-52.

Cordente, A.G., G. Cordero-Bueso, I.S. Pretorius and C.D. Curtin. 2013. Novel wine yeast with mutations in *YAP1* that produces less acetic acid during fermentation. FEMS Yeast Res. 13:62-73.

Erasmus, D.J., G.K. van der Merwe and H.J. van Vuuren. 2003. Genome-wide expression analyses: metabolic adaptation of *Saccharomyces cerevisiae* to high sugar stress. FEMS. 34:375-399.

Erasmus, D.J. and H.J.J. van Vuuren. 2009. Genetic basis for osmosensitivity and genetic instability of the wine yeast *Saccharomyces cerevisiae* V1N7. Am J Enol Vitic. 60:145-154.

Erasmus, D.J., M. Cliff and H.J.J. van Vuuren. 2004. Impact of yeast strain on the production of acetic acid, glycerol, and the sensory attributes of Icewine. Am J Enol Vitic. 55:371-378.

Heit, C. and D. Inglis. 2013. Acetic acid and ethyl acetate production during high brix fermentations: effect of yeast strain. Am J Enol Vitic. 64:4.

Heit, C. and D. Inglis. 2012. An investigation of the relationship between ethyl acetate production and osmotic stress in *Saccharomyces cerevisiae* K1-V1116 during high brix fermentations. Am J Enol Vitic. 63:4.

Heit, C. 2011. Effect of yeast strain and sugar concentration on ethyl acetate production in Icewine juice. BSc Hons Thesis. Brock University, ON.

Martin, S.J. 2008. The osmoadaptive response of the wine yeast *S. cerevisiae* K1-V1116 during Icewine fermentation. PhD Thesis. Brock University, ON.

Martin, S.J. and D. Inglis. 2006. Yeast osmoadaptive response response during Icewine fermentation. Am J Enol Vit. 57:527A.

Neviogt, E. and U. Stahl. 1997. Osmoregulation and glycerol metabolism in the yeast *Saccharomyces cerevisiae*. FEMS Microbiol Rev. 213:231-271.

Nurgel, C., G.J. Pickering and D.L. Inglis. 2004. Sensory and chemical characteristics of Canadian ice wines. J Sci Food Agric. 84:1675-1684.

Patel, S. and S. Shibamoto. 2002. Effect of different strains of *Saccharomyces cerevisiae* on production of volatiles in Napa Gamay wine and Petit sirah wine. J Agric Food Chem. 50:5649-5653.

Pigeau, G.M. and D.L. Inglis. 2007. Response of wine yeast (*Saccharomyces cerevisiae)* aldehyde dehydrogenase to acetaldehyde stress during Icewine fermentation. J Appl Microbiol. 103:1576-1586.

Pigeau, G.M. and D.L. Inglis. 2005. Upregulation of *ALD3* and *GPD1* in *Saccharomyces cerevisiae* during Icewine fermentation. J Appl Microbiol. 99:112-125.

Pigeau, G.M., E. Bozza, K. Kaiser and D.L. Inglis. 2007. Concentration effect of Riesling Icewine juice on yeast performance and wine acidity. J Appl Microbiol. 103:1961-1698.

Plata, C., C. Millán, J.C. Mauricio and J.M. Ortega. 2003. Formation of ethyl acetate and isoamyl acetate by various species of wine yeasts. Food Microbiol. 20:217- 224.

Remize, F., E. Andrieu and S. Dequin. 2000. Engineering of the pyruvate dehydrogenase bypass in *Saccharomyces cerevisiae*: role of the cytosolic $Mg^{2+}$ and mitochondrial $K^{+}$ acetaldehyde dehydrogenases Ald6p and Ald4p in acetate formation during alcoholic fermentation. Appl and Environ Microbiol. 66:3151-3159.

Torrens, J., P. Urpi, M. Riu-Aumatell, S. Vichi, E. Lopez-Tamanes and S. Buxaderas. 2008. Different commercial yeast strains affecting volatile and sensory profile of cava base wine. Int J Food Microbiol. 124:48-57.

van den Berg, M.A. and H.Y. Steensma. 1995. *ACS2*, a *Saccharomyces cerevisiae* gene encoding acetyl-coenzyme A synthetase, essential for growth on glucose. Eur J Biochem. 231:704-713.

van Dijken, J. and W. Sheffers. 1986. Redox balances in the metabolism of sugars by yeasts. FEMS Microbiol Rev. 32:199-224.

Verduyn, C., E. Postma, A. Scheffers and J.P. van Dijken. 1990. Physiology of *Saccharomyces cerevisiae* in anaerobic glucose-limited chemostat culture. J Gen Microbiol. 136:395-403.

VQA Ontario. 2013. Wine standards. Retrieved from: http://www.vqaontario.com/Regulations/Standards

# Appendix I: Data from Appassimento Study

## 1. Physical and chemical changes in grape berries during tobacco kiln drying

### 1.1. Soluble solids and reducing sugars concentrations during kiln drying

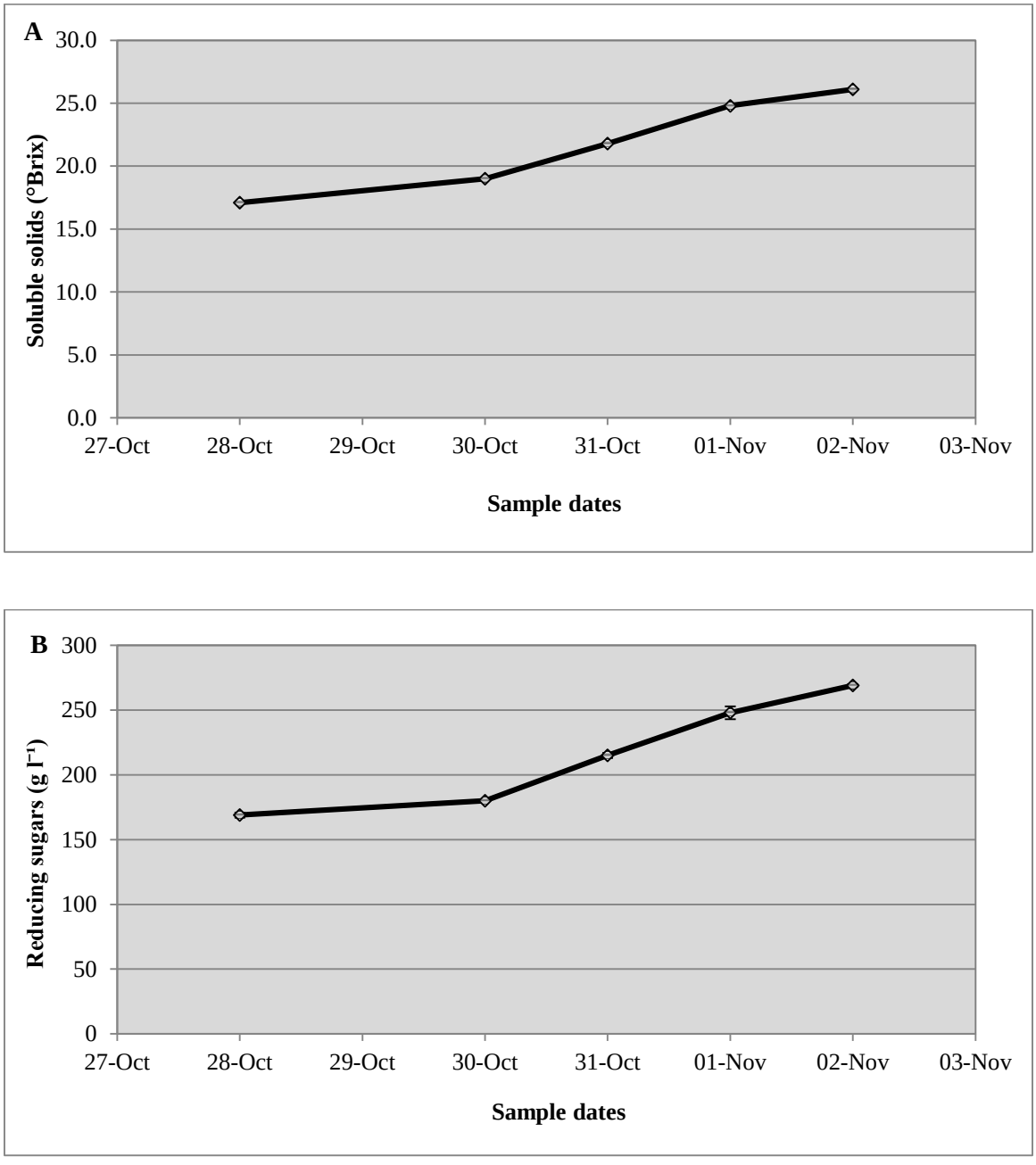


**Figure 1: Soluble solids and reducing sugar concentrations during kiln drying.** Soluble solids (A) and reducing sugars (B) were measured during the drying process. The mean values (± SD) of the duplicate measurements are shown (n = 2); where the error bars are not visible, they are within the symbol.

## 1.2. Berry weight and acidity (titratable acidity and pH) during kiln drying

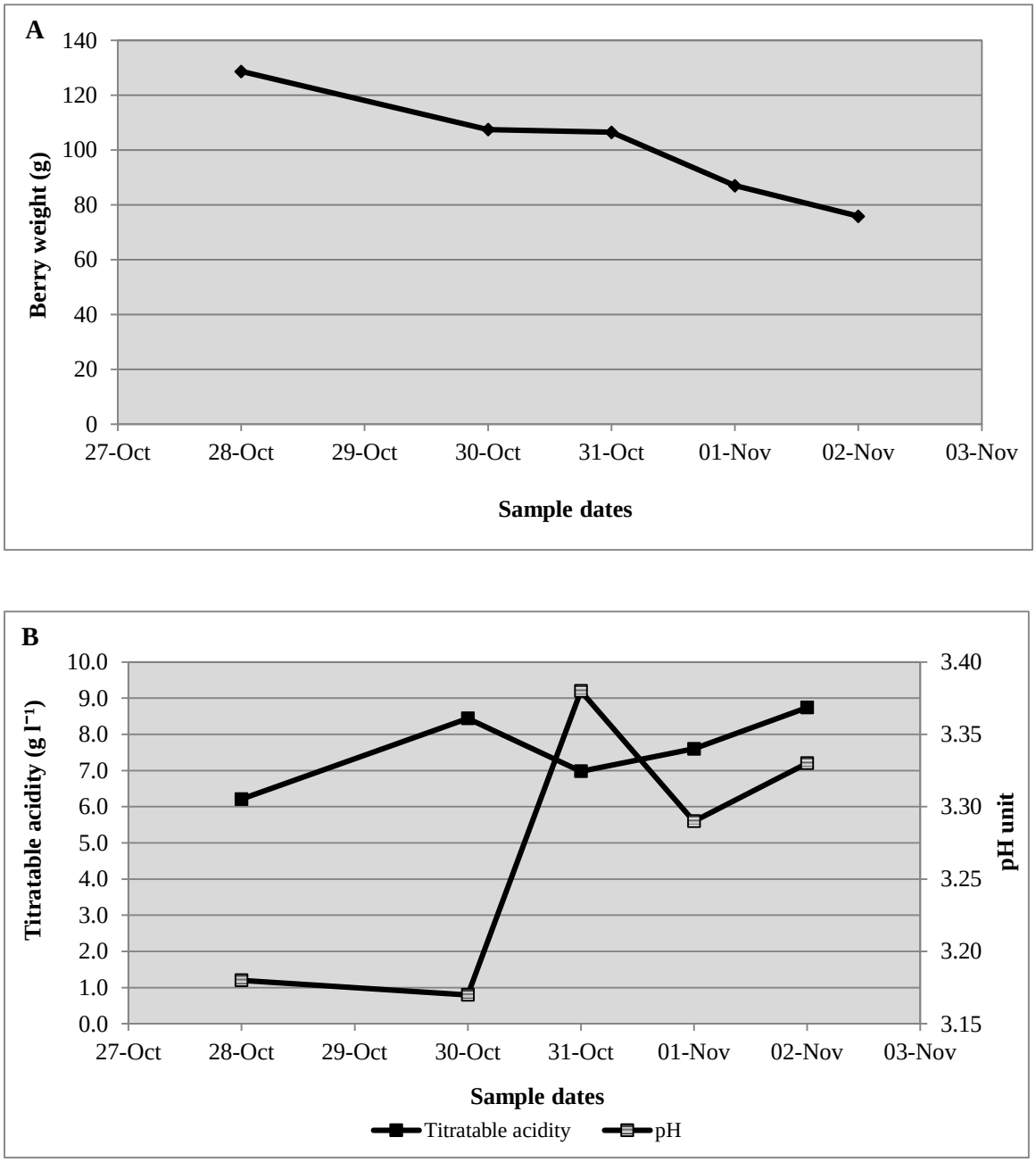


**Figure 2: Berrry weight and acidity during kiln drying.** Berrry weight (A) and acidity (titratable acidity and pH) (B) were measured throughout the drying process. The mean values (± SD) of the duplicate measurements are shown (n = 2); where the error bars are not visible, they are within the symbol.

## 1.3. Metabolite concentrations during kiln drying

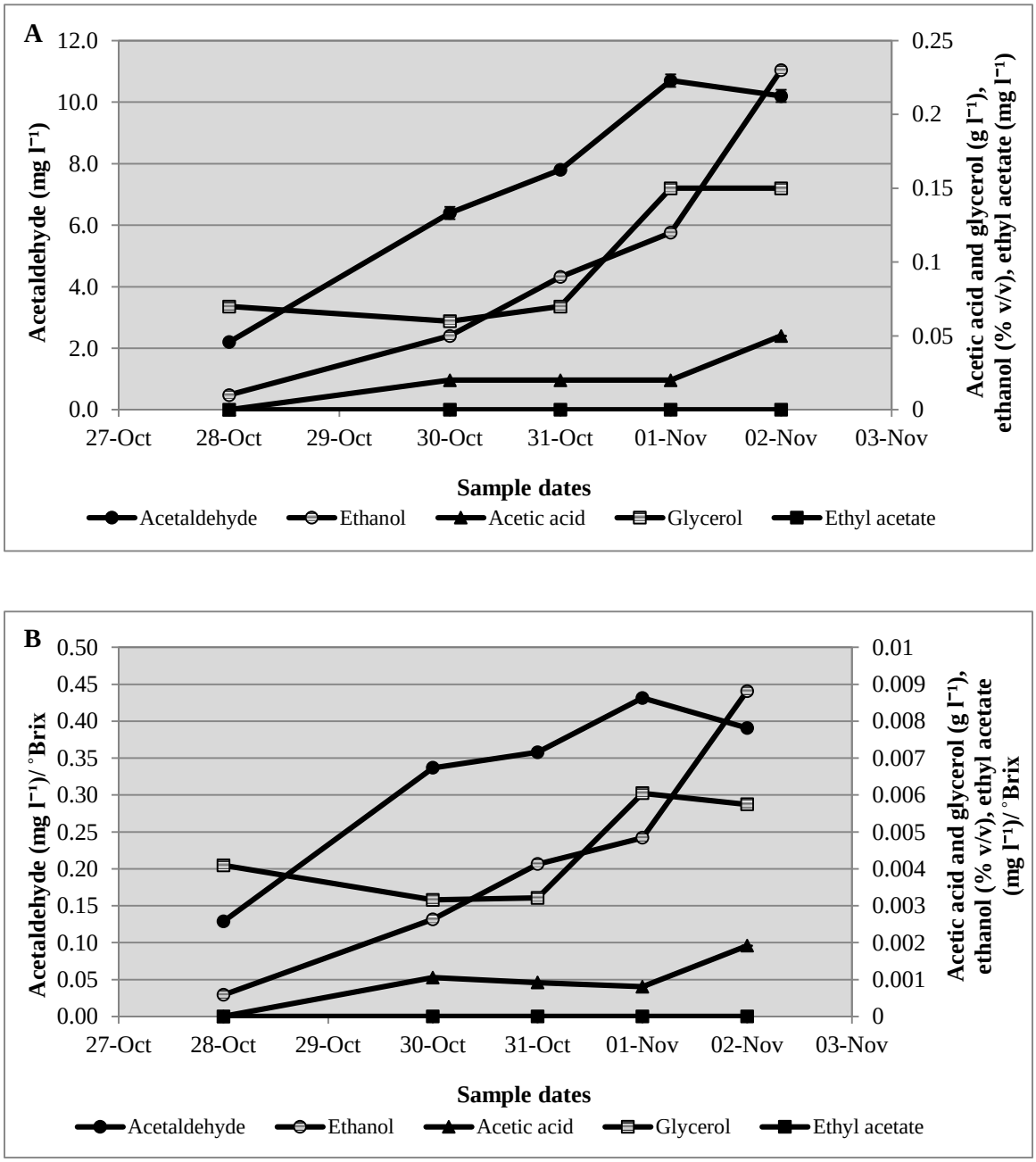


**Figure 3: Metabolite concentrations (glycerol, acetaldehyde, ethanol, acetic acid and ethyl acetate) during kiln drying.** Metabolite concentration was measured throughout the drying course (A) and normalized to soluble solids (˚Brix). The mean values (± SD) of the duplicate measurements are shown (n = 2); where the error bars are not visible, they are within the symbol.

## 2. Formation of other yeast metabolites during fermentation

### 2.1. Glycerol formation during fermentation

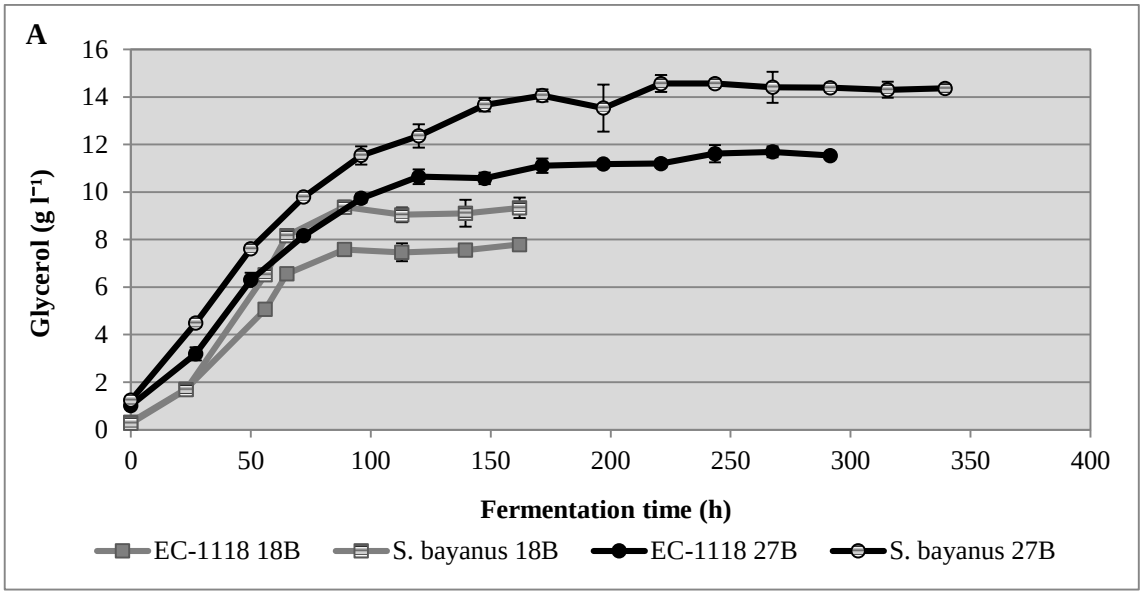


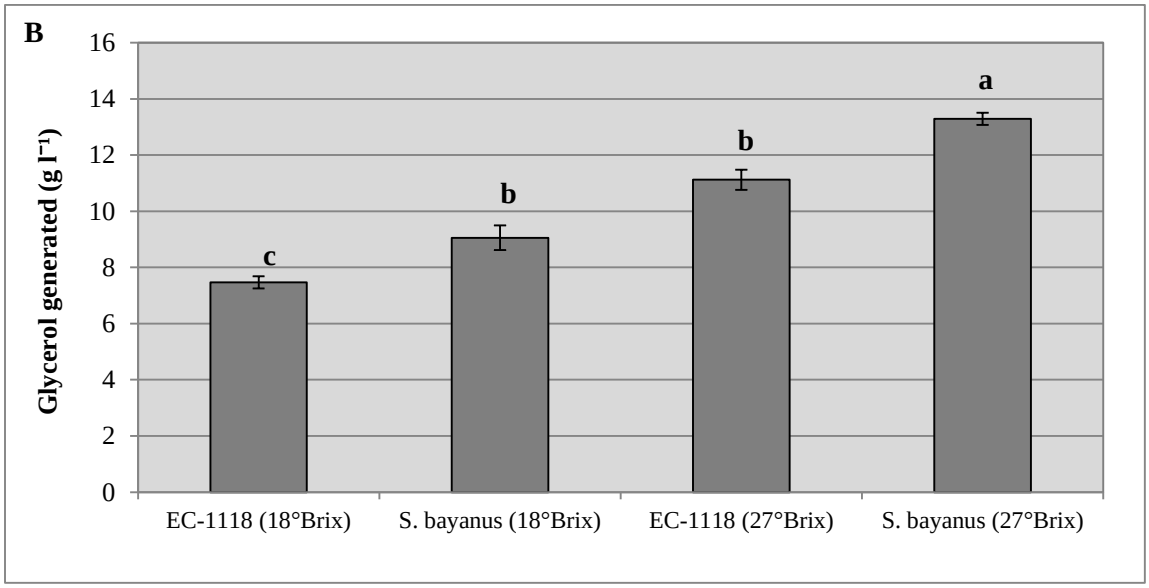


**Figure 4: Glycerol production during fermentation of red table wine must and appassimento-type must.** Glycerol was measured throughout the course of the fermentations (A) and the total glycerol production was compared between yeast strains in high and low sugar environments (B). Fermentations were performed in triplicate and samples from each treatment were analyzed in duplicate, for an n = 6 for each measurement. The mean values (± SD) of the triplicate fermentations are shown; where the error bars are not visible, they are within the symbol. Treatments were compared to each other and analyzed statistically using analysis of variance (ANOVA) with mean separation by Fisher's Least Significant Difference (LSD) test ($p < 0.05$). In descending order, lowercase letters indicate a unique group based on statistical difference using Fisher's $LSD_{0.05}$.

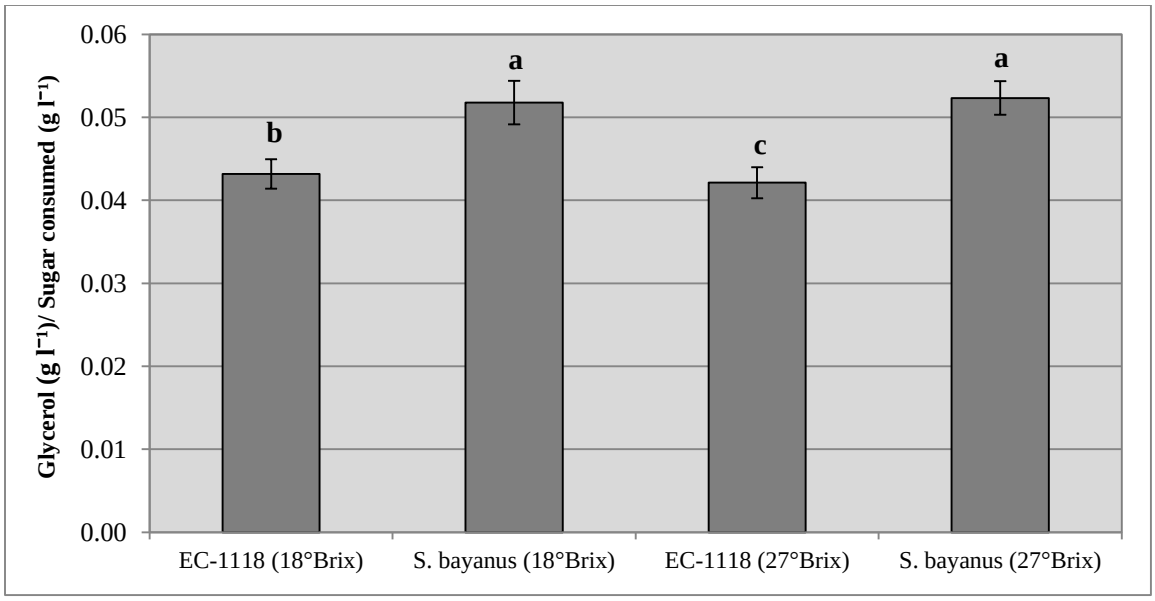


**Figure 5: Glycerol produced/sugar consumed during fermentation of red table wine must and appassimento-type must.** Total glycerol production was normalized to the amount of sugar consumed during the course of the fermentations, and compared between yeast strains. Fermentations were performed in triplicate and samples from each treatment were analyzed in duplicate, for an n = 6 for each measurement. The mean values (± SD) of the triplicate fermentations are shown. Treatments were compared to each other and analyzed statistically using analysis of variance (ANOVA) with mean separation by Fisher's Least Significant Difference (LSD) test ($p < 0.05$). In descending order, lowercase letters indicate a unique group based on statistical difference using Fisher's $LSD_{0.05}$.

## 2.2 Acetaldehyde formation during fermentation

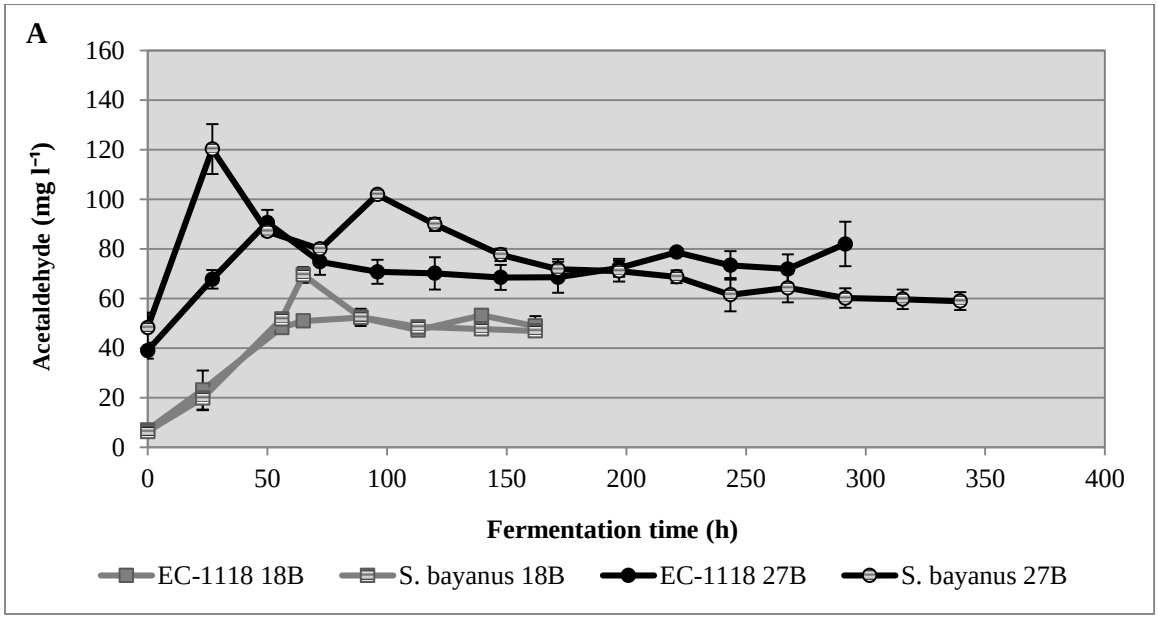


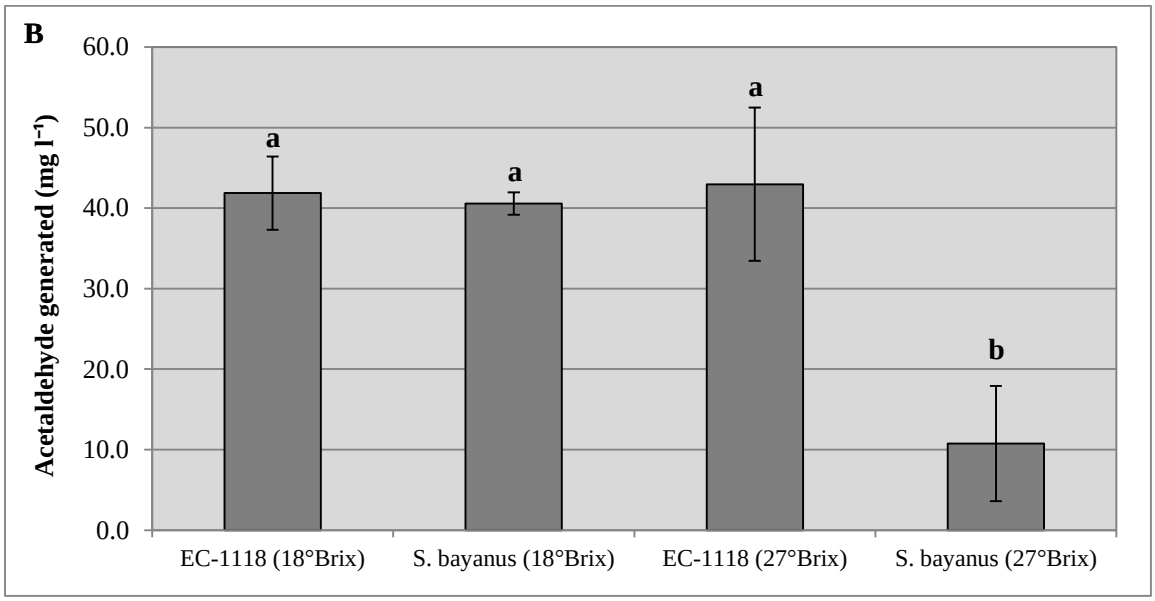


**Figure 6: Acetaldehyde production during fermentation of red table wine must and appassimento-type must.** Acetaldehyde was measured throughout the course of the fermentations (A) and the total acetaldehyde production was compared between yeast strains in high versus low sugar environments (B). Fermentations were performed in triplicate and samples from each treatment were analyzed in duplicate, for an n = 6 for each measurement. The mean values (± SD) of the triplicate fermentations are shown; where the error bars are not visible, they are within the symbol. Treatments were compared to each other and analyzed statistically using analysis of variance (ANOVA) with mean separation by Fisher's Least Significant Difference (LSD) test ($p < 0.05$). In descending order, lowercase letters indicate a unique group based on statistical difference using Fisher's $LSD_{0.05}$.

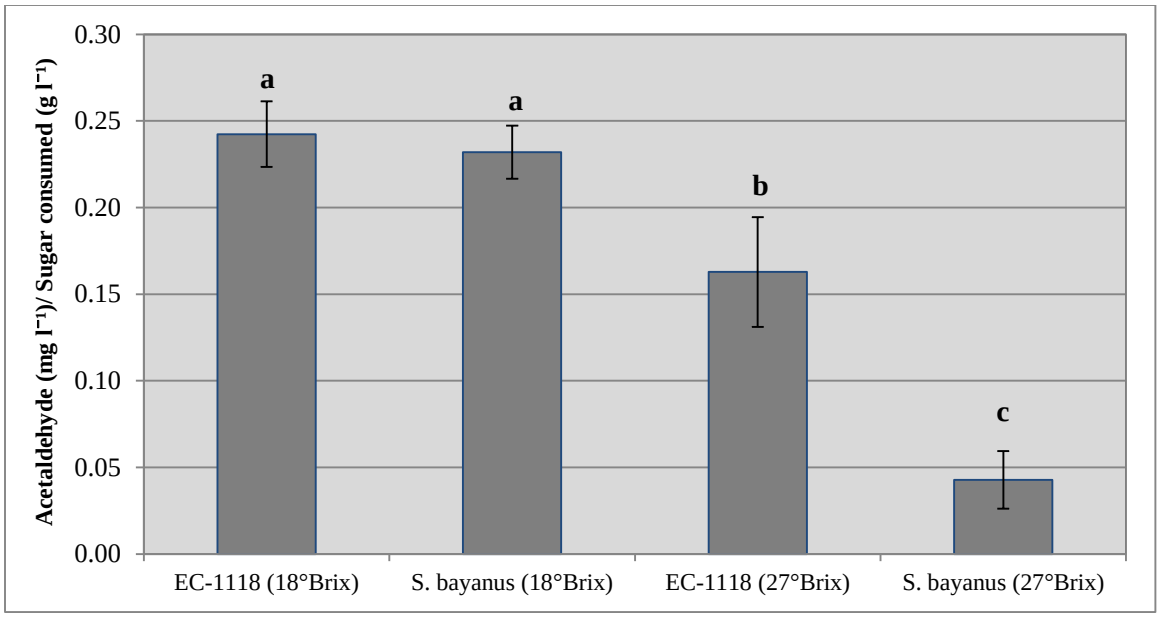


**Figure 7: Acetaldehyde produced/sugar consumed during fermentation of red table wine must and appassimento-type must.** Total acetaldehyde production was normalized to the amount of sugar consumed during the course of the fermentations, and compared between yeast strains. Fermentations were performed in triplicate and samples from each treatment were analyzed in duplicate, for an n = 6 for each measurement. The mean values (± SD) of the triplicate fermentations are shown. Treatments were compared to each other and analyzed statistically using analysis of variance (ANOVA) with mean separation by Fisher's Least Significant Difference (LSD) test ($p < 0.05$). In descending order, lowercase letters indicate a unique group based on statistical difference using Fisher's $LSD_{0.05}$.

## 2.3 Metabolomics analysis between strains

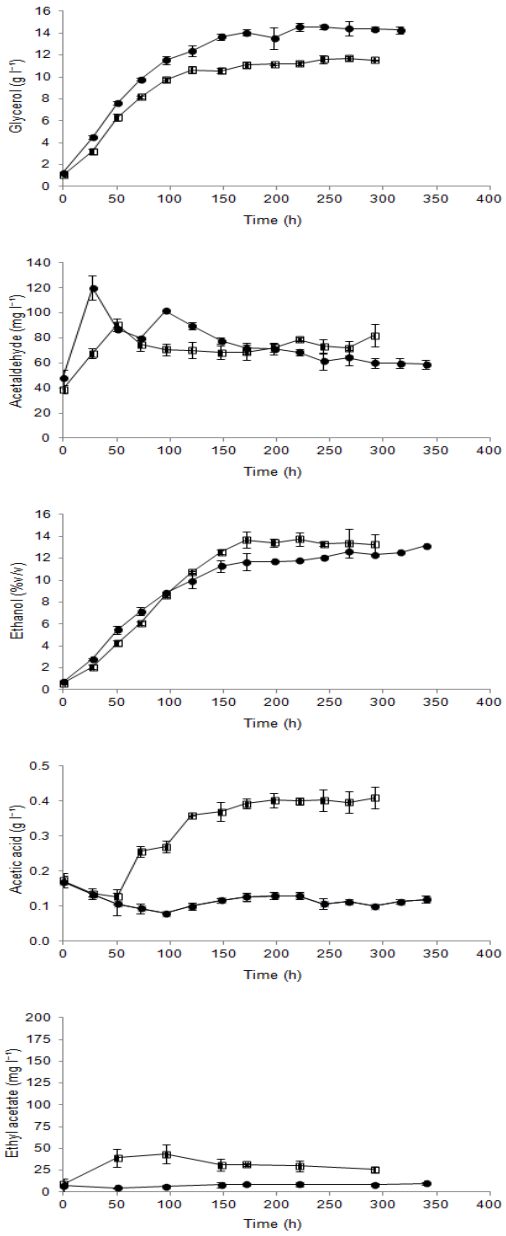


**Figure 8: Metabolite production during fermentation by *S. cerevisiae* and *S. bayanus*.** Fermentations of appassimento-type must were monitored for (a) glycerol, (b) acetaldehyde, (c) ethanol, (d) acetic acid and (e) ethyl acetate formation during fermentation, and compared between wine yeast strains, *S. cerevisiae* EC-1118 (□) and *S. bayanus* (●). Metabolite production was determined by substracting the concentration measured on day 0 of fermentation (inoculation day) from the level determined on the final day of fermentation. Fermentations were performed in triplicate and samples from each treatment were analyzed in duplicate, for an n = 6 for each measurement. The mean values (± SD) of the triplicate fermentations are shown; where the error bars are not visible, they are within the symbol.

### 3. Conversion of other metabolites during fermentation.

**Table 1:** Chemical composition of the finished table and appassimento wines (mean ± SD).

| | ***S. cerevisiae* EC-1118** | | ***S. bayanus*** | |
|---|---|---|---|---|
| | 18°Brix | 27°Brix | 18°Brix | 27°Brix |
| **Residual sugar ($g\ l^{-1}$)** | 0 ± 0 **a** | 0 ± 0 **a** | 1 ± 0 **b** | 1 ± 0 **b** |
| **Titratable Acidity ($g\ l^{-1}$)** | 6.9 ± 0.1 **c** | 7.8 ± 0.3 **b** | 7.9 ± 0.1 **b** | 9.6 ± 0.2 **a** |
| **pH** | 3.48 ± 0.08 | 3.87 ± 0.03 | 3.43 ± 0.04 | 3.72 ± 0.05 |
| **Ammonia ($mg\ N\ l^{-1}$)** | 4 ± 0 **b, c** | 1 ± 1 **c** | 5 ± 0 **a, b** | 7 ± 3 **a** |
| **PAN ($mg\ N\ l^{-1}$)** | 15 ± 2 **c** | 25 ± 1 **b** | 21 ± 7 **b** | 38 ± 2 **a** |
| **Glycerol ($g\ l^{-1}$)** | 7.79 ± 0.22 **d** | 9.33 ± 0.43 **b** | 12.14 ± 0.34 **b** | 14.53 ± 0.16 **a** |
| **Acetaldehyde ($mg\ l^{-1}$)** | 48.8 ± 4.0 **c** | 81.9 ± 8.9 **a** | 46.9 ± 0.93 **c** | 58.9 ± 3.7 **b** |
| **Ethanol (% v/v)** | 9.6 ± 0.5 **b** | 13.3 ± 0.9 **a** | 8.8 ± 0.8 **b** | 13.2 ± 0.6 **a** |
| **Acetic acid ($g\ l^{-1}$)** | 0.20 ± 0.04 **b** | 0.41 ± 0.03 **a** | 0.09 ± 0.01 **c** | 0.12 ± 0.01 **c** |
| **Ethyl acetate ($mg\ l^{-1}$)** | 147 ± 31 **a** | 30 ± 6 **c** | 63 ± 6 **b** | 16 ± 2 **d** |

Lowercase letters indicate statistical difference between treatments for a given parameter using Fisher's $LSD_{0.05}$.

**Table 2:** Metabolite conversions during table wine juice and appassimento juice fermentations (mean ± SD).

| | ***S. cerevisiae* EC-1118** | | ***S. bayanus*** | |
|---|---|---|---|---|
| | 18°Brix | 27°Brix | 18°Brix | 27°Brix |
| **Sugar consumed (g $l^{-1}$)** | 173 ± 5 **b** | 264 ± 8 **a** | 175 ± 3 **b** | 253 ± 9 **a** |
| **Glycerol (mg $l^{-1}$)** | 7.47 ± 0.22 **c** | 11.12 ± 0.36 **b** | 9.06 ± 0.43 **b** | 13.29 ± 0.21 **a** |
| **Acetaldehyde (mg $l^{-1}$)** | 41.9 ± 4.6 **a** | 43.0 ± 9.5 **a** | 40.6 ± 1.4 **a** | 10.8 ± 7.2 **b** |
| **Ethanol (% v/v)** | 9.4 ± 0.5 **b** | 12.7 ± 0.9 **a** | 8.7 ± 0.8 **b** | 12.5 ± 0.7 **a** |
| **Acetic acid (g $l^{-1}$)** | 0.17 ± 0.04 **b** | 0.24 ± 0.04 **a** | 0.07 ± 0.01 **c** | 0.00 ± 0.00 **d** |
| **Ethyl acetate (mg $l^{-1}$)** | 88 ± 8 **a** | 17 ± 3 **c** | 75 ± 7 **b** | 3 ± 9 **d** |

Lowercase letters indicate statistical difference between treatments for a given parameter using Fisher's $LSD_{0.05.}$

**Table 3:** Normalized production of metabolites during table wine juice and appassimento juice (mean ± SD).

| | ***S. cerevisiae* EC-1118** | | ***S. bayanus*** | |
|---|---|---|---|---|
| | 18°Brix | 27°Brix | 18°Brix | 27°Brix |
| **Glycerol (g $l^{-1}$)/ Sugar consumed (g $l^{-1}$)** | 0.043 ± 0.002 **b** | 0.035 ± 0.001 **c** | 0.030 ± 0.001 **a** | 0.052 ± 0.003 **a** |
| **Acetaldehyde (mg $l^{-1}$)/ Sugar consumed (g $l^{-1}$)** | 0.24 ± 0.02 **a** | 0.16 ± 0.01 **b** | 0.23 ± 0.02 **a** | 0.07 ± 0.04 **c** |
| **Ethanol (% v/v)/ Sugar consumed (g $l^{-1}$)** | 0.05 ± 0.00 | 0.05 ± 0.00 | 0.05 ± 0.01 | 0.05 ± 0.00 |
| **Acetic acid (g $l^{-1}$)/ Sugar consumed (g $l^{-1}$)** | 1.00 ± 0.28 **a** | 0.90 ± 0.12 **a** | 0.38 ± 0.12 **b** | 0.00 ± 0.00 **c** |
| **Ethyl acetate (mg $l^{-1}$)/ Sugar consumed (g $l^{-1}$)** | 0.51 ± 0.05 **a** | 0.06 ± 0. **c** | 0.43 ± 0.04 **b** | 0.01 ± 0.03 **c** |

Lowercase letters indicate statistical difference between treatments for a given parameter using Fisher's $LSD_{0.05}$

## Appendix II: Data from Bergmeyer (1974) method development

### 1. Evaluation of Bergmeyer (1974) assay using standards in water

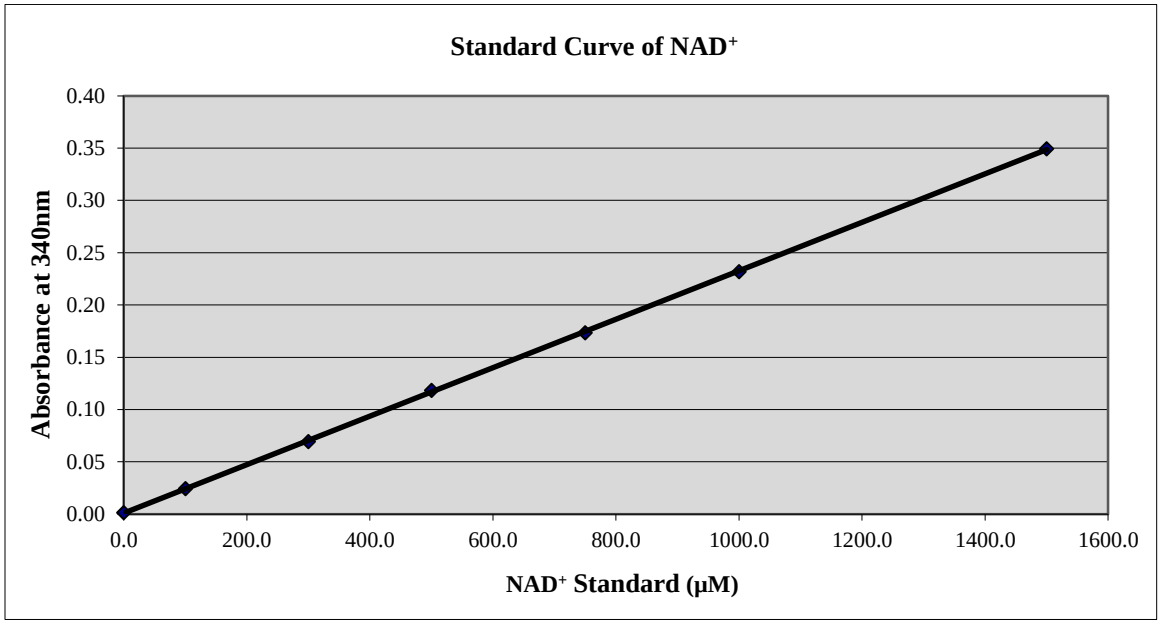


**Figure 1: Best-fit calibration curve of $NAD^+$ with cofactor dissolved in water (0 to 1500 µM).** The Y axis represents the absorbance change at 340 nm during the reaction catalyzed by alcohol dehydrogenase. Lines represent linear least squares fits to the data. Through regression analysis, the correlation coefficient (R) and coefficient of determination were ($R^2$) were calculated (R-value of 0.9999; $R^2$-value of 0.9999). Calibration standards were prepared in water and tested in duplicate (n = 2). The mean values (± SD) of the duplicate measurements are shown; where the error bars are not visible, they are within the symbol.

## 2. $NAD^+$ assay in Buffer 2

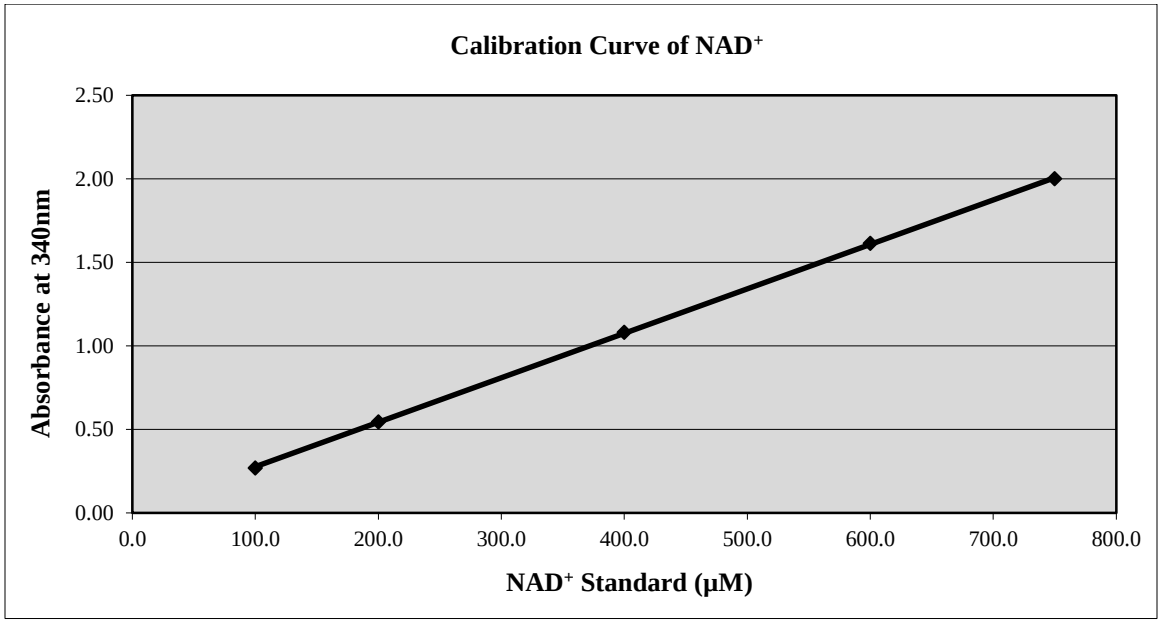


**Figure 2: Best-fit calibration curve of $NAD^+$ with cofactor dissolved in yeast cell breaking buffer (100 to 750 µM).** The Y axis represents the absorbance change at 340 nm during the reaction catalyzed by alcohol dehydrogenase. Lines represent linear least squares fits to the data. Through regression analysis, the correlation coefficient (R) and coefficient of determination were ($R^2$) were calculated (R-value of 0.9999; $R^2$-value of 0.9999). Calibration standards were prepared in cell breaking buffer and tested in duplicate (n = 2). The mean values (± SD) of the duplicate measurements are shown; where the error bars are not visible, they are within the symbol.

### 3. Effect of protease inhibition on nucleotide determination in cell lysate samples: evaluation of Complete Ultra Tablets (EDTA-free)

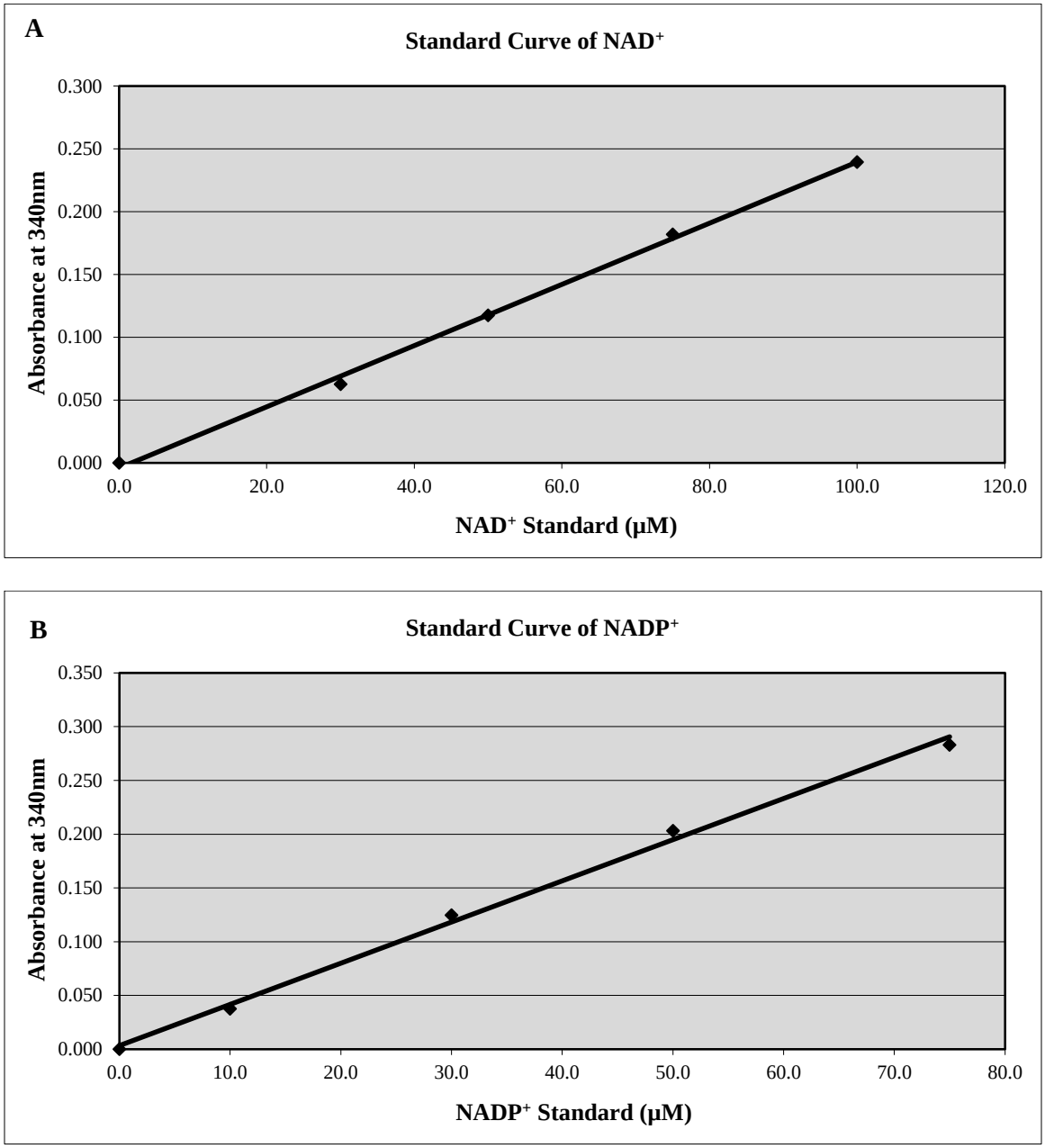


**Figure 3: Best-fit calibration curve of $NAD^+$ and $NADP^+$ with cofactor dissolved in yeast cell breaking buffer**. The Y axis represents the absorbance change at 340 nm during the reactions catalyzed by alcohol dehydrogenase in the $NAD^+$ assay (A) and glucose-6-phosphate dehydrogenase in the $NADP^+$ assay (B). Lines represent linear least squares fits to the data. For (A), an R-value of 0.9990 and $R^2$-value of 0.9980 were determined; for (B) an R-value of 0.9982 and $R^2$-value of 0.9965 were determined. Standards were prepared in cell breaking buffer with one Complete Ultra Tablet, EDTA-free and tested in duplicate (n = 2). The mean values (± SD) of the duplicate measurements are shown; where the error bars are not visible, they are within the symbol.

## Appendix III: Data from method development using Sigma-Aldrich® kits

### 1. Calibration of assay incubation times

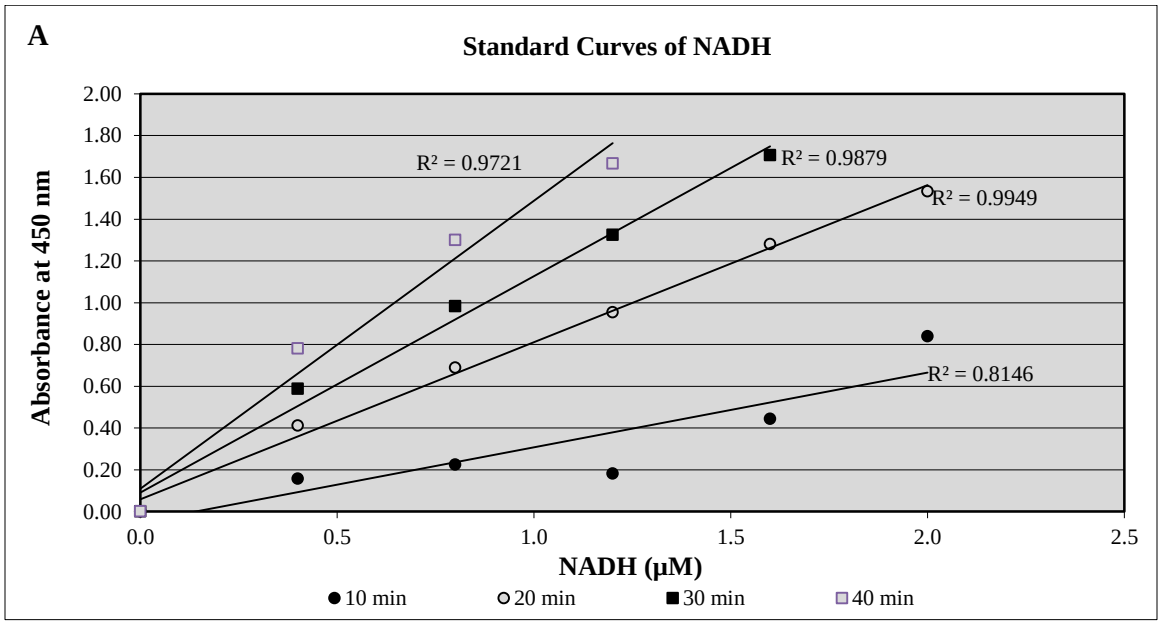


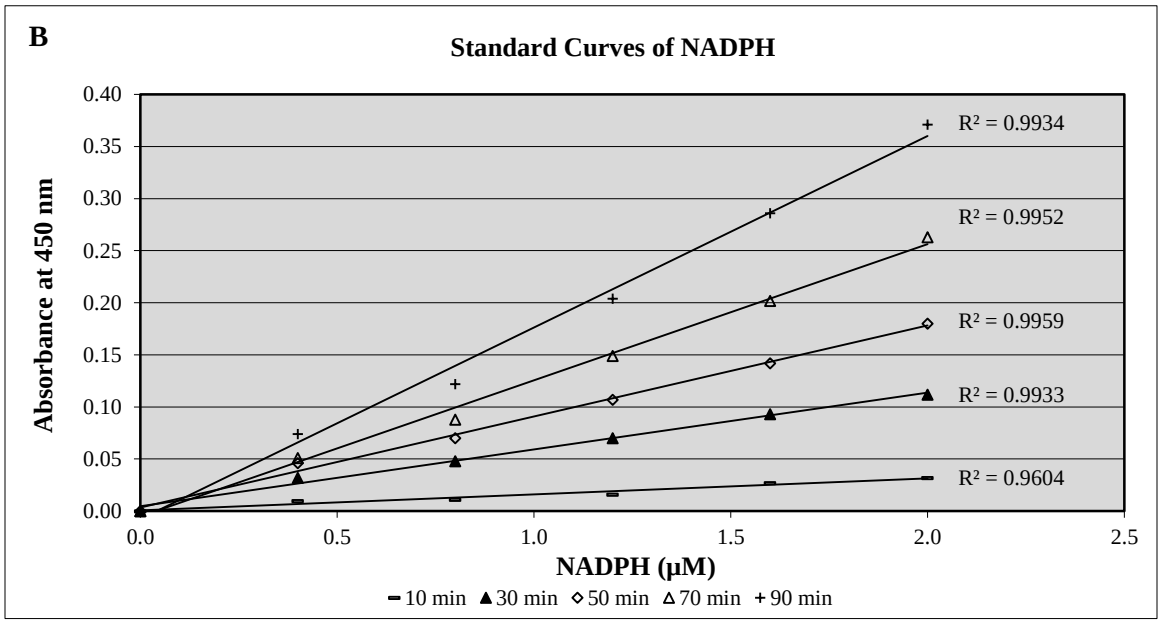


**Figure 1: Best-fit calibration curve of NADH and NADPH with cofactor dissolved in yeast cell breaking buffer.** The Y axis represents the absorbance change at 450 nm during the enzyme cycling reactions for the NADH assay (A) and NADPH assay (B) at various incubation times. Lines represent linear least squares fits to the data. The correlation coefficient (R) and coefficient of determination ($R^2$) were calculated using linear regression analysis. Standards were prepared in cell breaking buffer and tested in singlet (n = 1).